

*From intracellular recording to structural
analysis – new approaches on the mode of action
of anthropogenic chemicals*

DISSERTATION

to attain the academic degree of
Doctor of Natural Science (Dr. rer. nat)
of the Faculty of Biology, Chemistry and Earth Sciences
of the University of Bayreuth

presented by

Elisabeth Schirmer

born in Prenzlau

Bayreuth, 2021

This doctoral thesis was prepared at the Department of Animal Physiology at the University of Bayreuth from 01/2017 until 04/2021 and was supervised by Prof. Dr. Stefan Schuster.

This is a full reprint of the dissertation submitted to obtain the academic degree of Doctor of Natural Sciences (Dr. rer. nat.) and approved by the Faculty of Biology, Chemistry and Geosciences of the University of Bayreuth.

Date of submission: 09.04.2021

Date of defence: 17.12.2021

Acting dean: Prof. Dr. Benedikt Westermann

Doctoral committee:

Prof. Dr. Stefan Schuster (reviewer)

Prof. Dr. Heike Feldhaar (reviewer)

Prof. Dr. Christian Laforsch (chairman)

Prof. Dr. Birgitta Wöhrl

Table of contents

1. Summary	1
2. Zusammenfassung	3
3. Introduction	6
3.1 The Mauthner neuron as a new model to assay the effect of anthropogenic chemicals on the vertebrate nervous system	6
3.2 Recording in the Mauthner neuron provides urgently needed information for targeted application of anaesthetics in fish	11
3.3 Bisphenols affect the adult brain	13
3.4 MALDI mass spectrometry imaging workflow reveals histology-linked lipid pattern in aquatic model organisms	15
3.5 References	18
4. Synopsis	27
5. Publications	30
6. Own contribution in joined publications and manuscripts	31
7. Chapter 1	32
7.1 Recordings in an integrating central neuron provide a quick way for identifying appropriate anaesthetic use in fish	32
8. Chapter 2	54
8.1 Bisphenols exert detrimental effects on neuronal signaling in mature vertebrate brains.....	54
9. Chapter 3	81
9.1 Histology-linked MALDI mass spectrometry imaging workflow for <i>Danio rerio</i> and <i>Daphnia magna</i>	81
10. Conference participations	103
11. Acknowledgements	104
12. (Eidesstattliche) Versicherungen und Erklärungen	105

1. Summary

Despite their many benefits, anthropogenic chemicals also pose potential threats to human and animal health. They can potentially act on various levels of organization – from molecular level, affecting the lipid composition to neuronal key functions, affecting synaptic information transmission and circuit function. However, methods providing comprehensive and, in particular, quick information about the mode of action of anthropogenic chemicals are rare. In this thesis I first focus on functional effects of anthropogenic chemicals on neuronal function. I present the goldfish's Mauthner neuron, a giant central command neuron, which is individually identifiable from one animal to the next and accessible for intracellular *in vivo* recording, as a new model to obtain quick and comprehensive information on key aspects of neuronal and circuit function.

In this context, I initially present how recording in the Mauthner cell can quickly and systematically help filling the gap that currently exists between the legislation of many countries and informed decision-making on anaesthetic use in ectothermic vertebrates. The pair of Mauthner cells has a crucial role in triggering one of the most studied behavioural responses, the vital escape start in teleost fish. To fulfil this role, the Mauthner neurons need to integrate and process information from all sensory systems. This allows to directly and efficiently assay specific effects of anaesthetic agents on central processing and sensory information transmission. Concentration-effect curves further enable the informed decision-making if and at which concentration a given anaesthetic affects neuronal function. I applied the method to four chemicals commonly used as equivalently anaesthetics in fish. I demonstrate that this approach allows to rapidly obtain comprehensive and reliable information with a small number of animals, emphasizing these experiments also from an ethical point of view. These findings provide the basis for an equally informed decision-making on the anaesthetic use in fish, comparable to what is standard since the last 50 years in higher vertebrates. This is the first step in fulfilling the demands by present legislation, which demands the application of anaesthetic agents for any intervention that could be stressful for all vertebrates.

I further present the unique opportunity to use the Mauthner neuron as a new model to assay the impact of anthropogenic chemicals on neuronal function, by revealing the alarming and uncompensated impact of one month of exposure to two plasticizers (bisphenol A and its substitute bisphenol S) on basically every neuronal property. Due to the broad range of application of these plasticizers they are annually released at rates of hundreds of tons into the

biosphere, which makes them already ubiquitously present in the environment. Beside their proven effect to act as xeno-estrogens, recent studies also demonstrate effects on juvenile developing brains. However, for both bisphenols, the impact on the intact adult brain, whose powerful homeostatic mechanisms could potentially compensate any effects bisphenols might have on isolated neurons, is completely unknown. Using recording in the Mauthner neuron, I could reveal similar effects of both bisphenols, which strongly affect all basic aspects of neuronal function, and additionally show that these effects occur even at low, environmentally relevant concentrations. Comparable effects on neuronal function observed after exposure of EE2 (ethinyl estradiol), indicate that the examined effects after bisphenol exposition could at least partly occur due to the activation of estrogen receptors. The observed dramatic impact on the mature brain is not only worrying for aquatic organisms, but also for human health. It has been shown that offsetting balance in the brain might be the basis of severe neurological disorders. Hence, I call for the rapid replacement of both plasticizers and recommend this assay, due to its speed and resolution, to be part of early testing phases for new developed plasticizers.

In the third chapter of this thesis, I address the lipid composition within two aquatic model organisms (zebrafish and water flea). I demonstrate the capacity of MALDI MSI, an analytical imaging technique being able to identify lipids and visualise their spatial distribution within thin tissue sections, by providing highly resolved histology-linked lipid pattern even down to subcellular resolution. This could serve as a basis for future studies assaying molecular changes caused by anthropogenic chemicals. Using this analytical approach, I could not only visualise the anatomical arrangement of different organs due to their lipid content in the analysed tissue section, but, in the case of zebrafish, additionally provide a deeper insight into characteristic features like different eye layers, brain regions and neuronal structures (e.g. axon of the Mauthner neuron).

In summary, I present groundbreaking findings by assaying the impact of anthropogenic chemicals on neuronal and molecular level. Those approaches open up new possibilities for the risk assessment of anthropogenic chemicals.

2. Zusammenfassung

Trotz ihrer vielen Vorteile stellen anthropogene Chemikalien auch eine potenzielle Bedrohung für die Gesundheit von Menschen und Tieren dar. Sie können potenziell auf verschiedenen Organisationsebenen wirken – von der molekularen Ebene, durch Beeinträchtigung der Lipidzusammensetzung, bis hin zu zentralen neuronalen Funktionen, durch den Einfluss auf die synaptische Übertragung von Information und die neuronale Interaktion in funktionellen neuronalen Netzwerken. Methoden, die umfassend und vor allem schnell Informationen über die Wirkungsweise anthropogener Chemikalien geben, sind jedoch selten. In dieser Arbeit konzentriere ich mich zunächst auf funktionelle Effekte hervorgerufen durch anthropogene Chemikalien auf die neuronale Funktionalität. Dabei stelle ich die Mauthner-Zelle des Goldfisches, ein riesiges zentrales Kommandoneuron, welches individuell von einem Tier zum nächsten identifizierbar und für intrazelluläre *in vivo*-Ableitungen zugänglich ist, als ein neues Modell vor. Dieses ermöglicht schnell umfassende Informationen bezüglich zentraler neuronaler Funktionalität und Netzwerkfunktion zu erhalten.

In diesem Zusammenhang stelle ich zunächst vor, wie Ableitungen in der Mauthner-Zelle schnell und systematisch dazu beitragen können, die Lücke zu schließen, die derzeit zwischen dem tatsächlichen Einsatz von Anästhetika bei ektothermen Wirbeltieren und den Vorgaben des Tierschutzgesetzes vieler Länder besteht. Das Mauthner-Zell-Paar ist entscheidend für die Ausführung einer der am besten untersuchtesten Verhaltensreaktionen, dem lebensrettenden Fluchtstart der Knochenfische. Um diese Aufgabe zu erfüllen, müssen die Mauthner-Neurone Informationen aus allen sensorischen Systemen integrieren und verarbeiten. Dies ermöglicht die direkte und effiziente Untersuchung spezifischer Effekte von Anästhetika auf die zentrale Verarbeitung sensorischer Information und die sensorische Informationsübertragung. Konzentrations-Wirkungskurven ermöglichen darüber hinaus die fundierte Entscheidung, ob und bei welcher Konzentration ein bestimmtes Anästhetikum neuronale Funktionen beeinflusst. Ich habe die Methode auf vier Chemikalien angewandt, die üblicherweise als gleichwertige Anästhetika bei Fischen eingesetzt werden und zeige, dass mein Versuchsdesign schnell eine umfassende und zuverlässige Informationsgewinnung anhand einer kleinen Versuchstieranzahl ermöglicht, was diese Experimente auch unter ethischen Gesichtspunkten interessant macht. Die Ergebnisse dieser Studie bilden die Grundlage für einen Einsatz von Anästhetika bei Fischen, der vergleichbar ist mit dem, was bei höheren Wirbeltieren seit über 50 Jahren Standard ist. Dies ist ein erster Schritt zur Erfüllung der Forderungen der gegenwärtigen

Gesetzgebung, die den auf den jeweiligen Eingriff abgestimmten Einsatz von Narkosemitteln für alle Wirbeltiere verlangt.

Darüber hinaus präsentiere ich hier die Möglichkeit, das Mauthner-Neuron als Modell zur Bestimmung von Effekten anthropogener Chemikalien auf die neuronale Funktionalität zu verwenden, indem ich die alarmierenden und nicht kompensierten Auswirkungen einer einmonatigen Exposition gegenüber zwei Weichmachern (Bisphenol A und sein Ersatzstoff Bisphenol S) auf praktisch alle neuronalen Eigenschaften aufzeige. Weichmacher werden aufgrund des breiten Anwendungsspektrums jährlich in Mengen von Hunderten von Tonnen in die Biosphäre freigesetzt, wodurch sie bereits ubiquitär in der Umwelt vorhanden sind. Neben der nachgewiesenen Wirkung von Bisphenolen als Xeno-Östrogene, zeigen Studien auch Effekte auf sich entwickelnde Gehirne. Wirkungen auf das adulte Gehirn, dessen leistungsfähige homöostatische Mechanismen potenziell alle Effekte, die Bisphenole auf isolierte Neurone ausüben, kompensieren könnten, waren jedoch für beide Bisphenole bisher nicht bekannt. Durch Ableitungen im Mauthner-Neuron konnte ich ähnliche Effekte beider Bisphenole auf die neuronale Funktionalität aufzeigen. Zusätzlich konnte ich zeigen, dass diese Effekte schon bei niedrigen, umweltrelevanten Konzentrationen auftreten. Vergleichbare Effekte auf die neuronale Funktionalität nach Exposition mit EE2 (Ethinylestradiol) deuten darauf hin, dass die nach Bisphenol-Exposition beobachteten Effekte zumindest teilweise durch Aktivierung von Östrogen-Rezeptoren auftreten könnten. Die beobachteten dramatischen Auswirkungen auf das adulte Gehirn sind jedoch nicht nur für aquatische Organismen besorgniserregend, sondern betreffen auch die menschliche Gesundheit. Eine Störung der Homöostase im Gehirn kann die Grundlage für schwere neurologische Erkrankungen sein. Daher plädiere ich für das schnelle Ersetzen beider Weichmacher und empfehle die hier verwendete Methode aufgrund ihrer Schnelligkeit und der detaillierten Informationen, die diese in der Lage ist zu liefern, in der frühen Testphase für neu entwickelte Weichmacher einzusetzen.

Im dritten Kapitel dieser Arbeit beschäftige ich mich mit der Lipidzusammensetzung in zwei aquatischen Modellorganismen (Zebrafisch und Wasserfloh). Ich demonstriere die Fähigkeit von MALDI MSI, einem analytischen Bildgebungsverfahren, das die Identifizierung von Lipiden und ihre räumliche Verteilung in dünnen Gewebeschnitten ermöglicht, anhand hochaufgelöster Histologie-bezogener Lipidmuster, die sich bis hin zu subzellulärer Auflösung erstreckt. Dies könnte als Grundlage für zukünftige Studien dienen, in denen molekulare Veränderungen, hervorgerufen durch anthropogene Chemikalien, untersucht werden. Mit diesem analytischen Ansatz konnte ich nicht nur die anatomische Anordnung verschiedener Organe aufgrund ihres Lipidgehalts im analysierten Gewebeschnitt sichtbar machen, sondern

im Falle des Zebrafisches zusätzlich einen tieferen Einblick in charakteristische Merkmale wie verschiedene Augenschichten, Hirnregionen und Bestandteile einzelner Neurone (z.B. Axon und Soma des Mauthner-Neurons) geben.

Zusammenfassend stelle ich bahnbrechende Erkenntnisse über die Effekte von anthropogenen Chemikalien auf neuronaler und molekularer Ebene vor. Die hier vorgestellten Ansätze eröffnen darüber hinaus neue Möglichkeiten in der Risikobewertung anthropogener Chemikalien.

3. Introduction

3.1 The Mauthner neuron as a new model to assay the effect of anthropogenic chemicals on the vertebrate nervous system

The potential impact of anthropogenic chemicals on the nervous system has attracted particular attention in public and legislation. Today, there are 120,000 chemicals in use in the European Union¹. Some of them are listed to be of very high concern, like bisphenol A and are therefore replaced by substitutes that are considered to be safe, while others continue to be used even without comprehensive knowledge about their actual mode of action on animal and human health. Here, I focus on how to determine the impact of specific chemicals on the vertebrate central nervous system. This is challenging, because these chemicals can potentially act on various levels of neuronal function – from the generation of resting and action potentials, to synaptic transmission and central processing of sensory information – and methods providing rapidly comprehensive and comparable information are rare. I show here, that characteristics of the so-called Mauthner neuron, a giant central command neuron within the *medulla oblongata* of fish (Fig. 1) and some amphibians^{2,3} provide the opportunity to address this challenge.

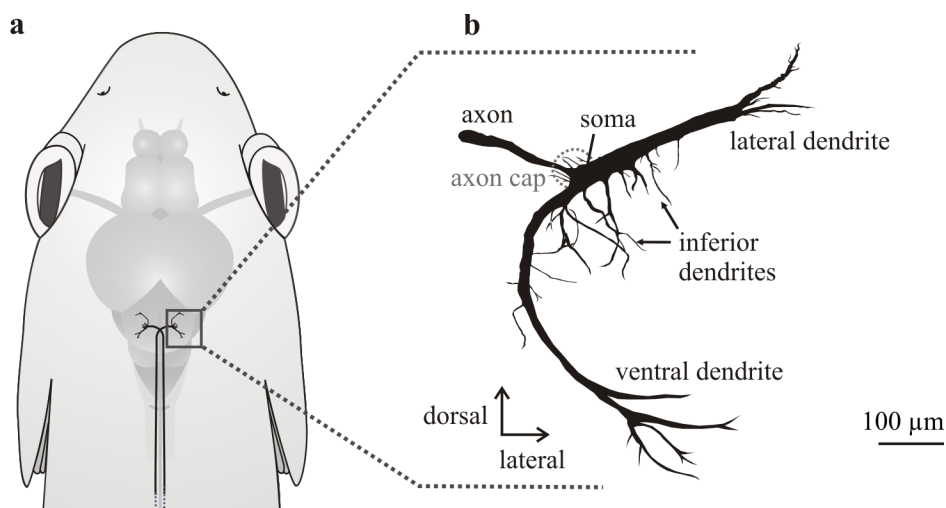


Figure 1 **Morphological structure of the goldfish Mauthner neuron.** **a.** Schematic view of both Mauthner neurons (black) as seen from above, which are located on the left and right side within the *medulla oblongata* in a goldfish (*Carassius auratus*) brain. Mauthner axons cross the midline and extend contralaterally down the entire spinal cord. **b.** Two-dimensional reconstruction of the Mauthner neuron after neurobiotin/streptavidin-Cy3 staining (from serial 70 μm sections) in coronal view (as seen looking along the longitudinal axis of the fish). The soma is up to 100 μm in cross-sectional diameter and the main dendrites extend dorsolateral (lateral dendrite) and ventrorostral (ventral dendrite). The axon cap (dotted light grey semicircle) surrounds the unmyelinated part of the axon and the axon hillock.

Mauthner neurons always occur as a pair, one on the left and one on the right side. The Mauthner neuron is one of the very few neurons in the vertebrate central nervous system that can be morphologically and physiologically individually identified from one animal to the next^{3,4}. This fact and its enormous size (soma, main dendrites and axons), which exceeds those of other neurons within the vertebrate nervous system, are the basis for identifiability. Identifiability is defined by consistent characteristics, through which a neuron can be clearly distinguished from others in a normal individual². Individually identifiable neurons of invertebrates had already been central for research. Studies of A. L. Hodgkin and A. F. Huxley on the large axons of the squid provided fundamental insights into nerve cell excitability, contributing on the understanding of the interaction of voltage-gated ion channels and the generation of an action potential, which was honoured with a Nobel prize in 1963^{5,6}. Evidence for individually identifiable neurons within the vertebrate nervous system is confirmed since the discovery of the Mauthner axon in 1859⁷, too. Studies on the Mauthner cell not only questioned previous assumptions, such as that protein synthesis is not restricted to the soma but that the Mauthner axon also contains ribosomal RNA indicating axoplasmatic ribosomes, but also provided many initial studies for the vertebrate neuroscience⁸. In this context, the accessibility, morphologically and electrophysiologically, of the Mauthner neuron enabled major insights into fundamental mechanisms of synaptic communication, neuronal and circuit function⁹ in the vertebrate central nervous system. For example, the question if synaptic transmission in the vertebrate central nervous system is solely chemical or also electrical could be revealed by the identification of gap junctions at the distal part of the large and electrophysiologically accessible lateral dendrite of the Mauthner neuron. Those gap junctions are proof for electrical synapses and pre- and postsynaptic recordings further demonstrated that the electrotonic flow of current occurs in both directions¹⁰. Moreover, the gap junctions are part of a mixed-synapse, the so-called large myelinated club ending, enabling not only electrotonic but also chemical (via transmitter release) transmission¹¹. The strength of those synapses can further undergo activity-dependant changes, which can influence the probability of the Mauthner neuron to elicit an action potential for triggering the vital fast start behaviour⁸. This correlation, caused by long-term depression of the gap junctions in the myelinated club endings was surprising, because for a long time only chemical but not electrical synapses were considered to be modifiable by experience⁹.

Moreover, the Mauthner neuron not only enabled insights into synaptic communication within the vertebrate nervous system, but additionally demonstrated the correlation of the activity of a single cell with a defined response, the vital fast-start escape response of teleost fish^{2,12}. This

behaviour is one of the most studied behavioural responses and the Mauthner neuron as central true-decision making neuron deciding whether to induce an escape response or not, requires multisensory integration. Sensory information is thereby integrated to specific local postsynaptic domains making the Mauthner neuron also a reliable tool assaying targeted integration of inputs. Sensory information is thereby mainly integrated at one of the two main dendrites of the Mauthner neuron, extending laterally (lateral dendrite) or ventrally (ventral dendrite)⁷ (Fig. 2a) and as I show in chapter 1 and 2 of this thesis, the postsynaptic potentials resulting from visual or acoustic stimulation (orthodromic stimulation) (Fig. 2c) can further be used to evaluate the effects of anthropogenic chemicals on sensory systems and central processing of sensory information. Visual information is forwarded from the retina via the *optic tectum* to the ventral dendrite¹³ (Fig. 2a). In contrast, the lateral dendrite integrates auditory information, which is forwarded from the acoustic hair cells to the 8th cranial nerve and further projected to large myelinated club endings located at its distal part^{14,15} (Fig. 2a,b).

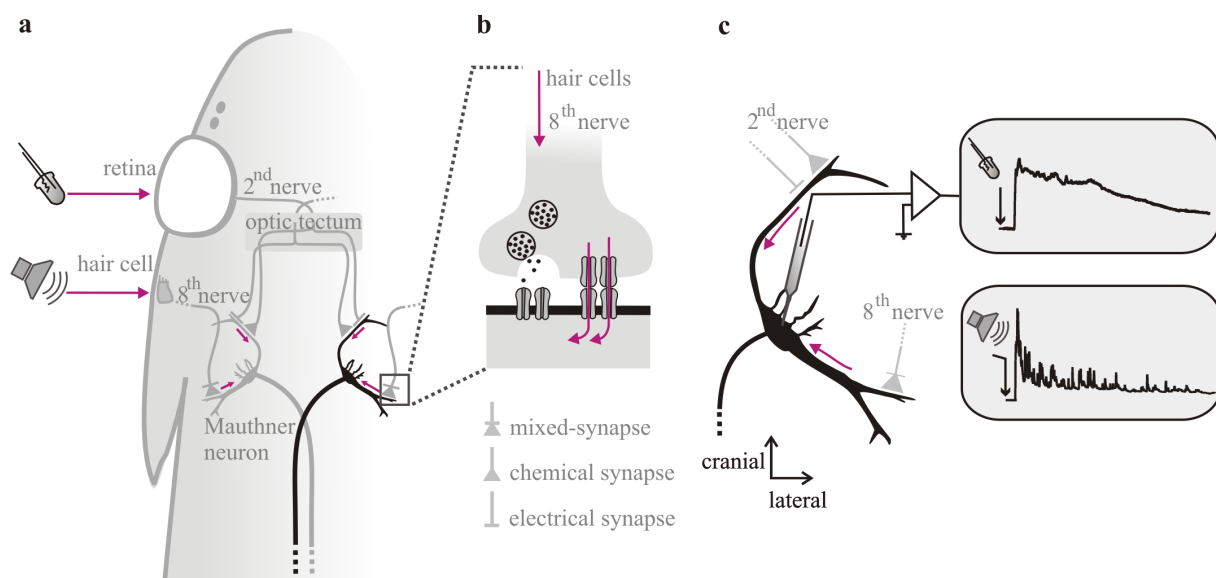


Figure 2 Integration of auditory and visual inputs in the goldfish Mauthner neuron. **a.** Illustrated goldfish (*Carassius auratus*) presenting a magnified view of both Mauthner neurons. Visual input (indicated by the LED) is forwarded from the retina via the 2nd nerve and integrated at chemical or electrical synapses located at the ventral dendrite of the Mauthner neuron. Auditory information (indicated by the loudspeaker) is forwarded from the acoustic hair cells via the 8th cranial nerve and integrated at mixed-synapses, the so-called myelinated club endings, localized at the distal part of the lateral dendrite. **b.** Large-myelinated club ending with the afferent's origin at the 8th cranial nerve and integrate acoustic information forwarded from the acoustic hair cells. Club endings transmit information through chemical synapses via transmitter release (presented on the left side of the synapse) and electrotonic via gap junctions (presented on the right side of the synapse). Pink arrows indicate the direction of the current electrotonic flow. **c.** Postsynaptic potentials resulting from visual or acoustic input can be recorded intracellular in the Mauthner neuron (orientation as seen from above).

As mentioned above, the club endings are mixed-synapses, providing both gap junction mediated potentials (electrical synapse)¹¹ followed by transmitter mediated potentials (chemical synapse) and contribute in the fast transmission of sensory information (Fig. 2b). The combination of electrotonic and chemical information transmission thereby enabled the study of interesting effects. In this context, electrical stimulation of the Mauthner axon (antidromic activation) evokes action potentials at the axon hillock, the only active spike-generating region of the Mauthner neuron⁷ (Fig. 3). Simultaneously, the generated currents spread towards the presynaptic site of the large-myelinated club endings via the gap junctions and cause a depolarization. This process, also called backfiring, then results once again in a presynaptic transmitter release (glutamate) giving rise to a delayed postsynaptic potential (longer lasting component) following the action potential (early fast component)^{16,17}, which can also backfire (causing a second delayed potential) (Fig. 3). In my thesis, I could demonstrate that the occurrence of those delayed potentials due to backfiring is a valuable tool to assess the impact of anthropogenic chemicals like bisphenols on synaptic transmission and presynaptic transmitter release (for details see chapter 2). This, again, clearly emphasizes the Mauthner neuron as a new model to obtain comprehensive information about the impact of anthropogenic substances on the vertebrate nervous system.

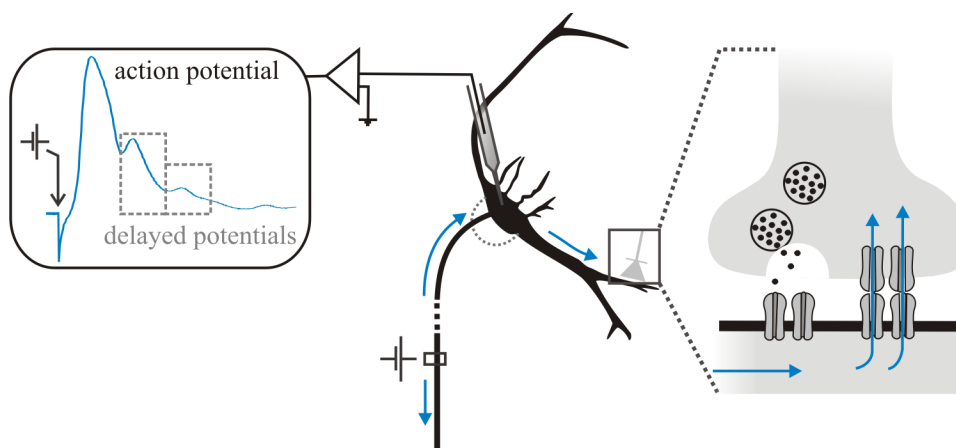


Figure 3 **Backfiring from the Mauthner axon hillock to presynaptic sites.** Schematic presentation of the Mauthner neuron. Blue arrows indicate direction of the current flow after electrical stimulation of the Mauthner axon (antidromic stimulation). After electrical stimulation an action potential is generated at the axon hillock and can be recorded intracellularly in the Mauthner soma. The axon hillock is the only active spike-generating site of the Mauthner neuron and surrounded by the axon cap (presented as a dotted light grey semicircle). The generated current further depolarizes the presynaptic site of the mixed-synapses localized at the distal part of the lateral dendrite. This causes once again a transmitter release, which gives rise to a delayed potential following the action potential. If this also backfires a second delayed potential occurs.

Since the discovery of the Mauthner axon, this neuron became one of the best studied neurons due to the number of breakthroughs it has enabled because of its giant size and accessibility^{7,8}. Here, I used the Mauthner system for the first time as a new model to determine the impact of different anthropogenic substances on the mature vertebrate brain. First, as legislation demanded the equal treatment of all vertebrates and therefore declared the use of anaesthetic agents for all interventions that could be stressful, the lack of information for the targeted application of anaesthetic agents in fish can no longer be tolerated. In this context I introduce recording in the Mauthner neuron to quickly obtain effects of different anaesthetic agents, in particular, on sensory information processing, offering a first guide for both aquaculture industry and research facilities to provide a basis for informed decisions, which anaesthetic to use. Second, the use of bisphenols and the replacement of bisphenol A by presumably safe substitutes such as bisphenol S is critically discussed, because of accumulating evidence of similar problematic effects. By using recording in the Mauthner neuron, I demonstrate new and alarming effects of bisphenols, originally thought to only act as endocrine disrupting chemicals, on the adult brain and recommend using *in vivo* recording in the Mauthner neuron to be part of test series contributing in the early risk assessment of new developed substances, before they also become ubiquitous in the environment.

3.2 Recording in the Mauthner neuron provides urgently needed information for targeted application of anaesthetics in fish

Fish gained increasing interest not only in different fields of research, as model organism for neurobiological, developmental or environmental studies, but also in other branches such as nutritional sciences and in aquaculture industries. According to the FAO, the global fish production, actually, reached an annual volume of more than 170 million tonnes with 47 % represented by aquaculture¹⁸. Numbers of fish in use during experimental procedures reached a value of 350.000 in 2019 in Germany¹⁹ and a value of 276.800 in the United Kingdom²⁰. Beyond that, the exact number of fish used in the United States has not to be recorded as prescribed by law, but even exceeds those obtained in the European union with the estimated values of 3.5 – 7 million, annually²¹. However, in conjunction with the growing numbers of fish in use, studies revealed accumulating evidence on the higher cognitive function of fish²²⁻²⁸. This pointed towards their capability to suffer, which therefore highly demanded for action, to contribute on the wellbeing of those animals. Hence, the European Union legislative decided the equal treatment for all vertebrates and therefore declared the mandatory use of anaesthetic agents for all interventions that could be stressful in the Directive 2010/63/EU^{25,29-32}. Although legislation no longer distinguishes between higher (e.g. birds and mammals) and lower vertebrates (e.g. fish, amphibians), information needed for the targeted application of anaesthetic agents in fish is highly insufficient, whereas data obtained over years for mammals and birds already allow to adapt a careful mix of anaesthetic agents to the underlying research question³³⁻³⁶. In fish, MS-222 is the most common used anaesthetic agent in both research facilities and aquaculture industry^{37,38}. However, its mode of action is still not fully investigated and this ambiguity is also reflected in the guidelines and legislation, which differ between the countries³⁹⁻⁴¹. In Canada, MS-222 is used for all food fish⁴², while in the United Kingdom the number of applications of the drug in food fish is limited⁴³. In the United States, MS-222 application is not only limited to selected fish species, but in addition it is the only market authorized drug⁴⁴. In Norway, MS-222 is now substituted by a new anaesthetic agent, Aqui-S, for the use in aquaculture and transportation³². However, apart from its potential to make handling easier, information about the effects on various sensory systems and sensory processing in fish and other ectothermic vertebrates as well as concentration-dependant differences is still lacking. Moreover, licensing new drugs is time consuming and costly^{32,45} and we have to be aware of the fact that anaesthetic quantities used for the high amount of fish in use and regardless of their responsible application, are nevertheless steadily increasing due to the lack of sufficient information and alternatives. In consequence, there is a serious conflict

between legislative demands, comprehensive information to fulfil them and the time needed to develop and evaluate new anaesthetic agents.

It is therefore important to establish ways in which useful and reliable information can be obtained quickly both on potential novel anaesthetics and on the anaesthetics that are presently in use to obtain an equal data basis as it is available for the so-called higher vertebrates. In chapter 1, I therefore demonstrate how intracellular recording in the Mauthner neuron contributes in obtaining urgently needed information for the targeted application of anaesthetics in ectothermic vertebrates. The Mauthner neuron in the hindbrain of most fish and some amphibians^{2,3}, functions as a central command neuron for triggering the fast-start escape response^{2,12} in teleost fish, for which it requires multisensory integration. I used this fact and further characteristics of the Mauthner neuron to address several questions in chapter 1: can this system detect differential effects of given anaesthetics by the example of four given anaesthetics – MS-222 (CAS Registry No. 886-86-2), benzocaine (CAS Registry No. 94-09-7), Aqui-S (CAS Registry No. 97-53-0) and 2-phenoxyethanol (CAS Registry No. 122-99-6) (Fig. 4)? Is it possible to even narrow down their site of action? Are there concentration-dependant differences? How many animals are needed to obtain quick reliable and comprehensive results? Results obtained on neuronal function, sensory information integration and processing can further function as a first guide to scientists, veterinarians and aquaculture specialists.

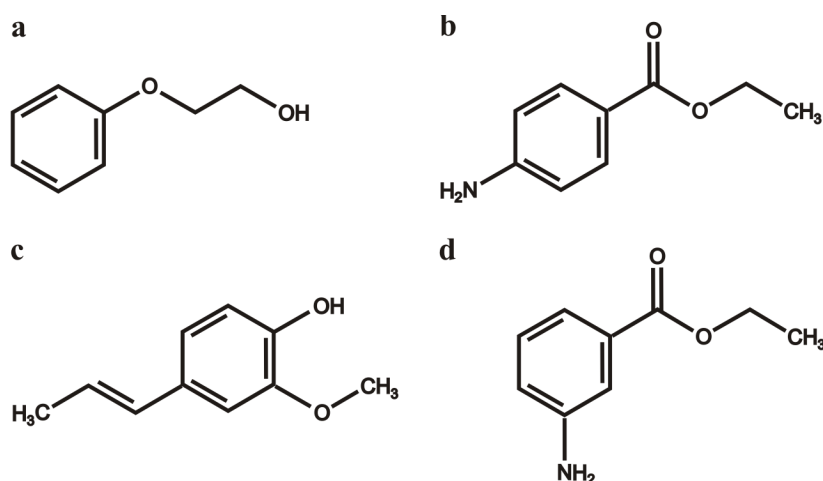


Figure 4 **Chemical structures of anaesthetic agents commonly used in fish.** a. 2-phenoxyethanol. b. benzocaine. c. Aqui-S. d. MS-222.

3.3 Bisphenols affect the adult brain

The use of chemical substances in consumer goods provides an everyday risk for our health and nature. Adverse effects of these substances can only become visible over time and the risk assessment e.g. in registration processes is therefore challenging for both manufacturing industries and approving authorities. In this context, one of today's mainly discussed issues is the composition of plastic. Due to its favourable properties and despite today's legitimate concerns, plastic is still the material of choice for a wide range of applications and products. Plastics are considered to be versatile, durable, lightweight and inexpensive in production^{46,47}. But plastic polymers – as the underlying structure of plastic – are not inherently stable under natural condition. They are brittle and tend to break. To overcome this undesirable characteristic in the final product, plasticizers are generally added⁴⁸⁻⁵¹. Chemical and natural processes like solar radiation, biological degradation and wash out then lead to a release of these additives from their original compound into the environment, which makes plasticizer contamination nowadays ubiquitously a serious environmental issue⁵³⁻⁵⁴.

One of the most frequently used plasticizers is bisphenol A (BPA; 2,2-bis-(4-hydroxyphenyl)-propane; CAS Registry No. 80-05-7) (Fig. 5). Its global production has a volume of about 8 million tons per year and is accompanied by an annual release of 100 tons into biosphere⁵⁵⁻⁵⁷. Nowadays, it can be detected ubiquitously in environment from surface water to breast milk^{53,55,58}. Started as an additive assumed to be relatively harmless, BPA was reported to act as an endocrine disrupting chemical by binding to the estrogen receptors ER α and ER β ⁵⁸. It affects hormonal balance and reproduction potential and alters neuronal development and metabolic processes both in humans and in so-called lower vertebrates^{52,59,60}. Since 2018, BPA is officially classified as a substance of very high concern by the European Chemical Agency and, in consequence, has been replaced from many products, which are now labelled as BPA free. However, this does not mean that these products do not contain alternative plasticizers instead.

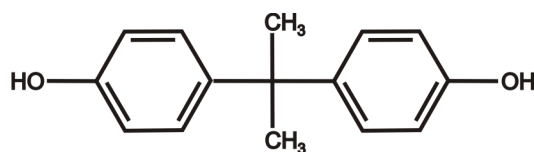


Figure 5 **Chemical structure of bisphenol A** (BPA; 2,2-bis-(4-hydroxyphenyl)-propane).

The main substitute of BPA in products labelled to be BPA-free is bisphenol S (BPS; 4,4'-sulfonyldiphenol; CAS Registry No. 80-09-1) (Fig. 6)⁶¹, which is similar to BPA in chemical structure, but has been proclaimed as a safer alternative for the usage in consumer goods⁶². The question, if this point of view is really justified is critically discussed^{53,63-65}. Since the annually manufactured or imported rate of BPS is up to 10,000 tons in the European economic area⁵⁷, it is no surprise that BPS can already be detected ubiquitously in the environment, too^{54,57}. Due to its sulfonyl group, BPS is less vulnerable to heat and light exposure. However, its water solubility is more than 10-times higher than that of BPA (1,774 mg L⁻¹ : 146 mg L⁻¹). Therefore, BPS is nevertheless and especially present in aqueous milieus and environments^{66,67}.

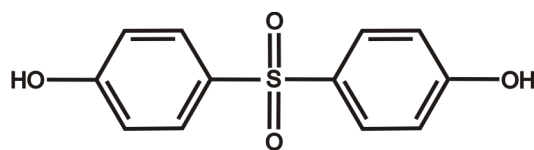


Figure 6 **Chemical structure of bisphenol S (BPS; 4,4'-sulfonyldiphenol)**

Replacing one toxic chemical by another cannot be the method of choice, especially if there are studies indicating harmful effects of BPS^{53,68,69} and some effects potentially similar to BPA⁶⁹⁻⁷³. Furthermore, considering the proven adverse effects of the endocrine disrupting chemicals (EDC), we cannot spend another 10 years figuring out if further substitutes with similar chemical structure act the same way and are therefore also a risk for our health and environment. Bisphenols are able to pass the blood-brain barrier⁷⁴ and it has been shown that – besides acting as EDC – BPA especially interferes with brain development of juvenile vertebrates^{70,71,75}.

Motivated particularly by the varied effects of estrogens on neuronal circuits, in chapter 2 I addressed whether this is restricted only to juvenile developing brains or if similar effects might also exist in mature brains. *In vivo* recording from the Mauthner neuron allows to compare most directly the impact of BPS with that of BPA in the mature vertebrate brain. Unique properties make the Mauthner neuron an ideal neurobiological model for efficiently obtaining the differential effects agents have on neuronal key functions, including action potential generation, neuronal backfiring (giving insights of how electrical synapses and presynaptic transmitter release are affected), synaptic transmission and circuit function. Thereby, I demonstrate that recording from the Mauthner neuron provide a suitable, sensitive and reliable method for taking a first step in risk assessment and question the use of both BPA and BPS in plastic products in general.

3.4 MALDI mass spectrometry imaging workflow reveals histology-linked lipid pattern in aquatic model organisms

The pollution of freshwater and marine ecosystems due to the increasing amount of chemicals in use today causes growing concern regarding their effect on aquatic organisms⁷⁶. Pollution by plastic products is thereby a major concern with 70,000 to 270,000 tons of marine plastic⁷⁶⁻⁷⁹. Besides the plastic particles, causing physical tissue damage after ingestion, the chemicals released from the original plastic product can interact with the molecular content of the tissue. Bisphenols are one of the chemicals released from plastic products due to chemical and physical processes and are proven to disrupt the lipid distribution and content in animal tissue⁸⁰. This is alarming, since lipids play various essential roles in animals. As the main components of cellular membranes, they maintain the structural integrity and, in particular within the nervous system, participate in neuronal information transmission^{81,82}. They are also involved in further fundamental processes such as energy storage or hormone regulation and it could be demonstrated, that changes in the lipid pattern can correlate with the development of diseases⁸³⁻⁸⁵. Hence, in regard to the growing pollution and the related health risk for aquatic animals, it is crucial to understand to which extent animals can stabilize their lipid composition in the presence of anthropogenic chemicals in general. Considering the various functions of lipids, commonly used analytical methods like LC-MS (liquid chromatography mass spectrometry) to analyze the lipid content in extracted tissue homogenates are not sufficient, as they do not provide spatial information. Structural methods are rather required to visualize the lipid signatures and link them to histological features at various scales – from more extended structures like different organs even down to subcellular resolution.

Matrix-assisted laser desorption/ionization (MALDI) mass spectrometry imaging (MSI) is a molecular imaging technique enabling both the identification of compounds and the visualization of the compound distribution in thin tissue sections of the sample⁸⁶⁻⁸⁸. The use of MALDI, a soft ionization method, thereby allows the ionization of intact lipids, which is crucial for structural elucidation not only for identifying simple fatty acids but in particular for more complex lipids such as glycerophospholipids^{89,90}. Moreover, technological improvements, including increased spatial resolution and high-resolution mass spectrometers^{91,92}, already forwarded lipid analysis from whole body sections even down to single cells⁹³, emphasizing MALDI MSI as a powerful analytical technique putting common histological analysis on a higher level⁹⁴. In MALDI MSI experiments, the sample is scanned pixel-wise by a laser and a mass spectrum is recorded at every pixel with the signals measured as m/z (mass to charge

ratio). The generated image represents a plot of the abundance of a detected analyte against the respective x/y coordinate of each pixel (Figure 7).

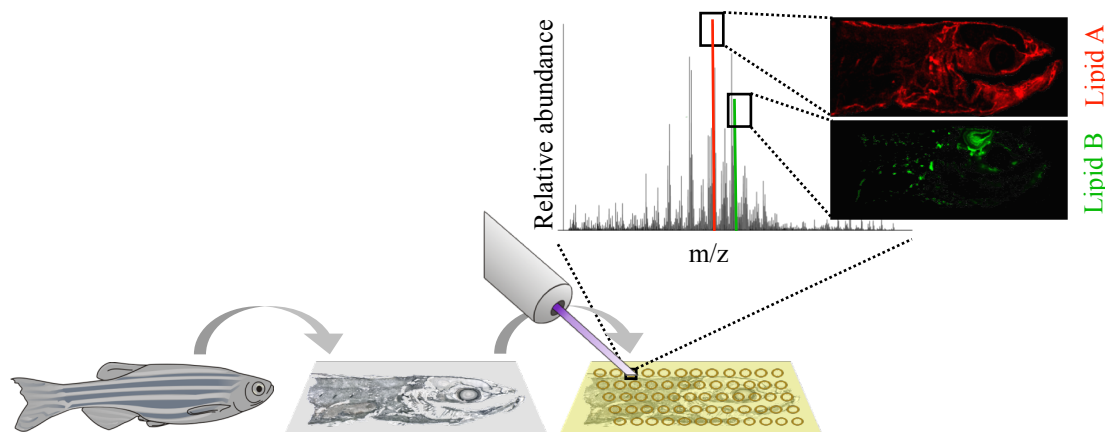


Figure 7 **Basic MALDI MSI workflow.** A biological sample (e.g. zebrafish) is sectioned into thin tissue-sections, which are then coated with a MALDI matrix (indicated in yellow). A laser scans the sample pixel-wise. Each ablation point represents a mass spectrum presenting the measured signals (e.g. lipid signals) as m/z values relative to their abundance. The final generated image presents a distribution map of one measured m/z value (e.g. lipid A) across the whole measured region of the sample. The lipid pattern of lipid A and B can be linked to histological features.

Here, I show, that the obtained anatomical structure-linked lipid pattern can serve as a histological map, which can further be used to monitor potent molecular changes under the exposure of anthropogenic chemicals, evaluating the physiological state of biological tissue. Initial MALDI MSI experiments in aquatic organisms took advantage of the zebrafish (*Danio rerio*), as it is small in size, enabling the analysis of whole-body tissue sections⁹⁵. Furthermore, there is a first study monitoring changes in phospholipid pattern in the eye of zebrafish after the exposure to fipronil, a common insecticide and biocide⁸³. However, urgently needed detailed spatial information is still missing, and therefore I addressed different questions in chapter 3: Is it possible to overcome present limits of solely localizing different organs due to their lipid composition by linking the molecular pattern with highly-resolved histology and visualize different anatomical compartments with clear borders? In addition, I asked whether it is possible to even visualize single neuronal structures? Here, the Mauthner neuron localized in the *medulla oblongata* of zebrafish (as well as in other vertebrates and some amphibians) is a suitable target, as it exceeds in size compared to other neurons in the vertebrate nervous system and I used its morphological characteristics (large soma up to 100 μm in diameter, contralateral

arranged of the large axons) to individually identify this neuron in brain sections. I could already demonstrate, that intracellular recording in the Mauthner neuron revealed its potential to evaluate the impact of anthropogenic chemicals on the nervous system (in particular see chapter 2). Spatial localization of those chemicals within or next to this neuron could provide an additional aspect of their already proven adverse effects by simultaneously investigating potent changes in lipid pattern. Beside the zebrafish, *Daphnia magna* provides a biological system, which was successfully used to evaluate effects caused by chemical stressors on the lipidome⁹⁶. However, it is unclear to which extent the lipid composition and spatial distribution of lipids in tissue sections are affected by chemical substances, because maintaining tissue integrity during cryosectioning remained a tough challenge. Therefore, in chapter 3, I present a novel way to maintain tissue integrity in non-preserved samples during cryosectioning, while lipid signals can still be detected with high signal intensities during MALDI MSI analysis.

Obtained lipid signatures within highly-resolved histological structures of both organisms – zebrafish and *Daphnia magna* – are not only an ideal basis analyzing changes caused by anthropogenic chemicals or further pollutants, but additionally will shed light towards early risk assessment strategies for aquatic organisms. Lipids are essential in maintaining tissue integrity and function and early observed changes could help not only to evaluate the animal's health but also to evaluate the intended safety of new developed substances before they can become a real health hazard.

3.5 References

1. European Chemical Agency (ECHA). Know more about the effects of the chemicals we use in Europe (ECHA/PR/16/01). Available on <https://echa.europa.eu/de/-/know-more-about-the-effects-of-the-chemicals-we-use-in-europe> (Accessed 21 March 2021) (2016).
2. Sillar, K. T., Picton, L. D. & Heitler, W. J. Fish Escape: the Mauthner System in *The Neuroethology of Predation and Escape* (eds. Sillar, K. T., Picton, L. D. & Heitler, W. J.), 212–243 (Wiley Blackwell, 2016).
3. Zottoli, S. J. Comparative morphology of the Mauthner cell in fish and amphibians in *Neurobiology of the Mauthner cell* (eds. Faber, D. S. & Korn, H.), 13-45 (Raven Press, 1978).
4. Furshpan, E. J. & Furukawa, T. Intracellular and extracellular responses of the several regions of the Mauthner cell of goldfish. *J. Neurophysiol.* **25**, 732–771 (1962).
5. Hodgkin, A. L. & Huxley, A. F. Action Potentials Recorded from Inside a Nerve Fibre. *Nature* **144**, 710-711 (1939).
6. Hodgkin, A. L., Huxley, A. F. & Katz, B. Measurements of current-voltage relations in the membrane of the giant axon of *Loligo*. *J. Physiol.* **116**, 424-448 (1952).
7. Faber, D. S. & Korn, H. *Neurobiology of the Mauthner Cell* (Raven Press, 1978).
8. Zottoli, S. J. & Faber, D. S. The Mauthner Cell: What Has it Taught us? *Neuroscientist* **6**, 26-38 (2000).
9. Korn, H. & Faber, D. S. The Mauthner Cell Half a Century Later: A Neurobiological Model for Decision-Making? *Neuron* **47**, 13–28 (2005).
10. Furshpan, E. J. “Electrical Transmission” at an Excitatory Synapse in a Vertebrate Brain. *Science* **144**, 878–880 (1964).
11. Nakajima, Y. Fine structure of the Mauthner cell: synaptic topography and comparative study in *Neurobiology of the Mauthner Cell* (eds. Faber, D. S. & Korn, H.), 133-166 (Raven Press, 1978).
12. Hecker, A., Schulze, W., Oster, J., Richter, D. O. & Schuster, S. Removing a single neuron in a vertebrate brain forever abolishes an essential behavior. *PNAS* **117**, 3254–3260 (2020).
13. Zottoli, S. J., Hordes, A. R. & Faber, D. S. Localization of optic tectal input to the ventral dendrite of the goldfish Mauthner cell. *Brain Res.* **401**, 113-121 (1987).

14. Zottoli, S. J. & Faber, D. S. Properties and distribution of anterior VIIIth nerve excitatory inputs to the goldfish Mauthner cell. *Brain Res.* **174**, 319-323 (1979).
15. Mirjany, M. & Faber, D. S. Characteristics of the anterior lateral line nerve input to the Mauthner cell. *J. Exp. Biol.* **214**, 3368-3377 (2011).
16. Curti, S. & Pereda, A. E. Functional specializations of primary auditory afferents on the Mauthner cells: Interactions between membrane and synaptic properties. *J. Physiol.* **104**, 203-214 (2010).
17. Pereda, A. E., Bell, T. D. & Faber, D. S. Retrograde synaptic communication via gap junctions coupling auditory afferents to the Mauthner cell. *J. Neurosci.* **15**, 5943–5955 (1995).
18. FAO. The State of World Fisheries and Aquaculture 2018 – Meeting the sustainable development goals, Available on <http://www.fao.org/3/i9540en/i9540en.pdf> (Accessed 21 March 2021) (2018).
19. Bundesministerium für Ernährung und Landwirtschaft. Versuchstierzahlen 2019 (Pressemitteilung Nr 246/2020), Available on [https://www.bmel.de/SharedDocs/Pressemitteilungen/DE/2020/246-versuchstierzahlen-2019.html#:~:text=2019%20wurden%20in%20Tierversuchen%20347.543,192.040\)%20gestiegen](https://www.bmel.de/SharedDocs/Pressemitteilungen/DE/2020/246-versuchstierzahlen-2019.html#:~:text=2019%20wurden%20in%20Tierversuchen%20347.543,192.040)%20gestiegen) (Accessed 21 March 2021) (2019).
20. Home Office. Annual Statistics of Scientific Procedures on Living Animals, Great Britain 2019, Available on https://assets.publishing.service.gov.uk/government/uploads/system/uploads/attachment_data/file/901224/annual-statistics-scientific-procedures-living-animals-2019.pdf (Accessed 21 March 2021) (2020).
21. The American Anti-Vivisection Society. Fish. Available on <https://aavs.org/animals-science/animals-used/fish/#:~:text=It%20is%20estimated%2C%20however%2C%20that,the%20study%20of%20complex%20processes> (Accessed 21 March 2021) (2021).
22. Bshary, R., Wickler, W. & Fricke, H. Fish cognition: a primate's eye view. *Anim. Cogn.* **5**, 1-13 (2002).
23. Sneddon, L. U. The Evidence for Pain in Fish: The Use of Morphine as an Analgesic. *Appl. Anim. Behav. Sci.* **83**, 153–162 (2003).
24. Sneddon, L. U. Pain in aquatic animals. *J. Exp. Biol.* **218**, 967–976 (2015).

25. Brown, C., Laland, K. & Krause, J. *Fish Cognition and Behavior* (Wiley-Blackwell, 2011).
26. Bshary, R. & Brown, C. *Fish Cognition. Curr. Biol.* **24**, R947–R950 (2014).
27. Sneddon, L. U., Elwood, R. W., Adamo, S. A. & Leach, M. C. Defining and assessing animal pain. *Anim. Behav.* **97**, 201–212 (2014).
28. Sneddon, L. U. et al. Fish sentience denial: Muddying the waters. *Anim. Sent.* **115** (2018).
29. European Commission. Animals used for scientific purposes, Available on https://ec.europa.eu/environment/chemicals/lab_animals/index_en.htm (Accessed 21 March 2021).
30. Treves-Brown, K. M. *Applied Fish Pharmacology*, (Kluwer Academic Publishers, 2000).
31. Browman, H. I., Cooke, S. J., Cowx, I. G., Derbyshire, S. W. G., Kasumyan, A., Key, B., Rose, J. D., Schwab, A., Skiftesvik, A. B., Don Stevens, E., Watson, C. A. & Arlinghaus, R. Welfare of aquatic animals: where things are, where they are going, and what it means for research, aquaculture, recreational angling, and commercial fishing. *ICES J. Mar. Sci.* **76**, 82-92 (2019).
32. Ross, L. G. & Ross, B. *Anaesthetic and Sedative Techniques for Aquatic Animals*, (Wiley-VCH, 2008).
33. Vogler, G. A. Chapter 19 - Anesthesia and Analgesia in *The Laboratory Rat* (eds. Suckow, M. A., Weisbroth, S. H., Franklin, C. L.), 627-664 (Academic Press, 2006).
34. Otto, K. Chapter 34 - Anesthesia, Analgesia and Euthanasia in *The Laboratory Mouse* (eds. Hedrich, H. J., Gillian Bullock, G.), 555-569 (Academic Press, 2004).
35. Fish, R., Danneman, P., Brown, M., Karas, A. *Anesthesia and Analgesia in Laboratory Animals* (Academic Press, 2008).
36. Katzung, B. G., Masters, S. B. & Trevor, A. J. *Basic & Clinical Pharmacology*, 12th edition (McGraw-Hill, 2012).
37. Zahl, I. H., Samuelsen, O. & Kiessling, A. Anaesthesia of farmed fish: implications for welfare. *Fish Physiol. Biochem.* **38**, 201–218 (2012).
38. Ackerman, P. A., Morgan, J. D. & Iwama, G. K. *Anaesthetics*, Available on http://www.ccac.ca/Documents/Standards/Guidelines/Add_PDFs/Fish_Anesthetics.pdf. Accessed (Accessed 21 March 2021) (2007).

39. Bernstein, P. S., Digre, K. B. & Creel, D. J. Retinal Toxicity Associated with Occupational Exposure to the Fish Anaesthetic MS-222. *Am. J. Ophthalmol.* **124**, 843-4 (1997).
40. Frazier, D. T. & Narahashi, T. Tricaine (MS-222): Effects on ionic conductances of squid axon membranes. *Eur. J. Pharmacol.* **33**, 313–317 (1975).
41. Sneddon, L. U. Clinical Anesthesia and Analgesia in Fish. *J. Exot. Pet Med.* **21**, 32–43 (2012).
42. Health Canada. List of veterinary drugs that are authorized for sale by health Canada for use in food-producing aquatic animals, Available on http://www.hc-sc.gc.ca/dhp-mps/vet/legislation/pol/aquaculture_anim-eng.php, (Accessed 21 March 2021) (2010).
43. Veterinary Medicines Directorate. Product Information Database, Available on <http://www.vmd.gov.uk/ProductInformationDatabase/Search.aspx>. (Accessed 21 March 2021) (2010).
44. U.S. Food and Drug Administration (FDA) Database of approved animal drug products. U.S. Department of Health and Human Services, Food and Drug Administration, Center for Veterinary Medicine. VMRCVM Drug Information Laboratory, Available on <http://www.accessdata.fda.gov/scripts/AnimalDrugsAtFDA/> (Accessed 21 March 2021) (2006).
45. Coyle, S. D., Durborow, R. M. & Tidwell, J. H. Anesthetics in aquaculture. *Southern Regional Aquaculture Center (SRAC)* **3900**, 1–6 (2004).
46. Andrady, A. L. & Neal, M. A. Applications and societal benefits of plastics. *Philos. Trans. R. Soc. B Biol. Sci.* **364**, 1977–1984 (2009).
47. Thompson, R. C., Swan, S. H., Moore, C. J. & vom Saal, F. S. Our plastic age. *Philos. Trans. R. Soc. B Biol. Sci.* **364**, 1973–1976 (2009).
48. Daniels, P. H. A brief overview of theories of PVC plasticization and methods used to evaluate PVC-plasticizer interaction. *J. Vinyl Addit. Technol.* **15**, 219–223 (2009).
49. Koelmans, A. A., Bakir, A., Burton, G. A. & Janssen, C. R. Microplastic as a Vector for Chemicals in the Aquatic Environment: Critical Review and Model-Supported Reinterpretation of Empirical Studies. *Environ. Sci. Technol.* **50**, 3315–3326 (2016).
50. Hermabessiere, L., Dehaut, A., Paul-Pont, I., Lacroix, C., Jezquel, R., Soudant, P. & Duflos, G. Occurrence and effects of plastic additives on marine environments and organisms: A review. *Chemosphere* **182**, 781–793 (2017).

51. Hahladakis, J. N., Velis, C. A., Weber, R., Iacovidou, E. & Purnell, P. An overview of chemical additives present in plastics: Migration, release, fate and environmental impact during their use, disposal and recycling. *J. Hazard. Mater.* **344**, 179–199 (2018).
52. Flint, S., Markle, T., Thompson, S. & Wallace, E. Bisphenol A exposure, effects, and policy: A wildlife perspective. *J. Environ. Manage.* **104**, 19–34 (2012).
53. Chen, D., Kannan, K., Tan, H., Zheng Z., Feng, Y. L., Wu, Y. & Widelka, M. Bisphenol Analogues Other Than BPA: Environmental Occurrence, Human Exposure, and Toxicity-A Review. *Environ. Sci. Technol.* **50**, 5438–5453 (2016).
54. Qiu, W., Zhang, H., Hu, J., Zhang, T., Xu, H., Wong, M., Xu, B. & Zheng C. The occurrence, potential toxicity, and toxicity mechanism of bisphenol S, a substitute of bisphenol A: A critical review of recent progress. *Ecotoxicol. Environ. Saf.* **173**, 192–202 (2019).
55. Vandenberg, L. N., Hauser, R., Marcus, M., Olea, N. & Welshons, W. V. Human exposure to bisphenol A (BPA). *Reprod. Toxicol.* **24**, 139–177 (2007).
56. Santangeli, S., Maradonna, F., Gioacchini, G., Cobellis, G., Piccinetti, C. C., Dalla Valle, L. & Carnevali, O. BPA-Induced Deregulation of Epigenetic Patterns: Effects On Female Zebrafish Reproduction. *Sci. Rep.* **6**, 21982 (2016).
57. Wu, L.-H. *et al.* Occurrence of bisphenol S in the environment and implications for human exposure: A short review. *Sci. Total Environ.* **615**, 87–98 (2018).
58. Rochester, J. R. Bisphenol A and human health: a review of the literature. *Reprod. Toxicol.* **42**, 132-55 (2013).
59. Cobellis, L., Colacurci, N., Trabucco, E., Carpentiero, C. & Grumetto, L. Measurement of bisphenol A and bisphenol B levels in human blood sera from healthy and endometriotic women. *Biomed. Chromatogr.* **23**, 1186-90 (2009).
60. Carnevali, O., Notarstefano, V., Olivotto, I., Graziano, M., Gallo, P., Di Marco Pisciotano, I., Vaccari, L., Mandich, A., Giorgini, E. & Maradonna, F. Dietary administration of EDC mixtures: A focus on fish lipid metabolism. *Aquat. Toxicol.* **185**, 95-104 (2017).
61. Choi, Y. J., Lee, L. S. Aerobic Soil Biodegradation of Bisphenol (BPA). Alternatives Bisphenol S and Bisphenol AF Compared to BPA. *Environ. Sci. Technol.* **51**, 13698-13704 (2017).

62. Russo, G., Barbato, F., Cardone, E., Fattore, M., Albrizio, S. & Grumetto, L. Bisphenol A and Bisphenol S release in milk under household conditions from baby bottles marketed in Italy. *J. Environ. Sci. Health. B.* **53**, 116-120 (2018).
63. Héliès-Toussaint, C., Peyre, L., Costanzo, C., Chagnon, M. C. & Rahmani, R. Is bisphenol S a safe substitute for bisphenol A in terms of metabolic function? An in vitro study. *Toxicol. Appl. Pharmacol.* **280**, 224-35 (2014).
64. Rosenmai, A. K., Dybdahl, M., Pedersen, M., van Vugt-Lussenburg A. B. M., Wedebye, E. B., Taxvig, C. & Vinggaard, A. M. Are structural analogues to bisphenol a safe alternatives? *Toxicol. Sci.* **139**, 35-47 (2014).
65. Qiu, W., Shao, H., Lei, P., Zheng, C., Qiu, C., Yang, M. & Zheng Y. Immunotoxicity of bisphenol S and F are similar to that of bisphenol A during zebrafish early development. *Chemosphere.* **194**, 1-8 (2018).
66. Guo, H., Li, H., Liang, N., Chen, F., Liao, S., Zhang, D., Wu, M. & Pan, B. Structural benefits of bisphenol S and its analogs resulting in their high sorption on carbon nanotubes and graphite. *Environ. Sci. Pollut. Res. Int.* **23**, 8976-84 (2016).
67. Fang, Z., Gao, Y., Wu, X., Xu, X., Sarmah, A. K., Bolan, N., Gao, B., Shaheen, S. M., Rinklebe, J., Ok, J. S., Xu, S. & Wang, H. A critical review on remediation of bisphenol S (BPS) contaminated water: Efficacy and mechanisms, *Crit. Rev. Env. Sci. Tec.*, **50**, 476-522 (2020).
68. Eladak, S., Grisin, T., Moison, D., Guerquin, M. J., N'Tumba-Byn, T., Pozzi-Gaudin, S., Benachi, A., Livera, G., Rouiller-Fabre, V. & Habert, R. A new chapter in the bisphenol A story: bisphenol S and bisphenol F are not safe alternatives to this compound. *Fertil. Steril.* **103**, 11-21 (2015).
69. Rochester, J. R. & Bolden, A. L. Bisphenol S and F: A Systematic Review and Comparison of the Hormonal Activity of Bisphenol A Substitutes. *Environ. Health Perspect.* **123**, 643-50 (2015).
70. Qiu, W., Zhao, Y., Yang, M., Farajzadeh, M., Pan, C. & Wayne, N. L. Actions of Bisphenol A and Bisphenol S on the Reproductive Neuroendocrine System During Early Development in Zebrafish. *Endocrinol.* **157**, 636-47 (2016).
71. Kinch, C. D., Ibhazehiebo, K., Jeong, J.-H., Habibi, H. R. & Kurrasch, D. M. Low-dose exposure to bisphenol A and replacement bisphenol S induces precocious hypothalamic neurogenesis in embryonic zebrafish. *PNAS*, **112**, 1475-1480 (2015).

72. Grignard, E., Lapenna, S. & Bremer, S. Weak estrogenic transcriptional activities of Bisphenol A and Bisphenol S. *Toxicol. In Vitro* **26**, 727-31 (2012).
73. Ben-Jonathan, N. & Hugo, E. R. Bisphenols Come in Different Flavors: Is "S" Better Than "A"? *Endocrin.* **157**, 1321-3 (2016).
74. Zhou, R. *et al.* Abnormal synaptic plasticity in basolateral amygdala may account for hyperactivity and attention-deficit in male rat exposed perinatally to low-dose bisphenol-A. *Neuropharmacology* **60**, 789–798 (2011).
75. Wang, W., Ru, S., Wang, L., Wei, S., Zhang, J., Qin, J., Liu, R. & Zhang, X. Bisphenol S exposure alters behavioral parameters in adult zebrafish and offspring. *Sci. Total. Environ* **741**, 140448 (2020).
76. Hermabessiere, L., Dehaut, A., Paul-Pont, I., Lacroix, C., Jezequel, R., Soudant, P. & Duflos, G. Occurrence and effects of plastic additives on marine environments and organisms: A review. *Chemosphere.* **182**, 781-793 (2017).
77. Cózar, A., Echevarría, F., González-Gordillo, J. I., Irigoien, X., Úbeda, B., Hernández-León, S., Palma, A. T., Navarro, S., García-de-Lomas, J., Ruiz, A., Fernández-de-Puelles, M., L. & Duarte, C. M. Plastic debris in the open ocean. *Pro. Natl. Acad. Sci.* **111**, 10239-10244 (2014).
78. Eriksen, M., Lebreton, L. C., Carson, H. S., Thiel, M., Moore, C. J., Borerro, J. C., Galgani, F., Ryan, P.G. & Reisser, J. Plastic pollution in the world's oceans: more than 5 trillion plastic pieces weighing over 250,000 tons afloat at sea. *PloS One* **9**, e111913 (2014).
79. Van Sebille, E., Wilcox, C., Lebreton, L., Maximenko, N., Hardesty, B. D., Van Franeker, J. A., Eriksen, M., Siegel, D., Galgani, F. & Law, K.L. A global inventory of small floating plastic debris. *Environ. Res. Lett.* **10**, 124006. Available on <http://dx.doi.org/10.1088/1748-9326/10/12/124006> (Accessed 21 March 2021) (2014).
80. Zhao, C. Xie, P., Yong, T., Wang, H., Chung, A. C. K. & Cai, Z. MALDI-MS Imaging Reveals Asymmetric Spatial Distribution of Lipid Metabolites from Bisphenol S-Induced Nephrotoxicity. *Anal. Chem.* **90**, 3196–3204 (2018).
81. Sparvero, L. J., Amoscato, A. A., Dixon, C. E., Long, J. B., Kochanek, P. M., Pitt, B. R., Bayir, H. & Kagan, V. E. Mapping of phospholipids by MALDI imaging (MALDI-MSI): realities and expectations. *Chem. Phys. Lipids* **165**, 545-62 (2012).

82. Fitzner, D., Bader, J. M., Penkert, H., Bergner, C. G., Su, M., Weil, M.-T., Surma, M. A., Mann, M., Klose, C. & Simons, M. Cell-Type- and Brain-Region-Resolved Mouse Brain Lipidome. *Cell Reports* **32**, 108132 (2020).
83. Liu, W., Nie, H., Liang, D., Bai, Y. & Liu, H. Phospholipid imaging of zebrafish exposed to fipronil using atmospheric pressure matrix-assisted laser desorption ionization mass spectrometry. *J. Talanta* **209**, 120357 (2020).
84. Koizumi, S., Yamamoto, S., Hayasaka, T., Konishi, Y., Yamaguchi-Okada, M., Goto-Inoue, N., Sugiura, Y., Setou, M. & Namba, H. Imaging mass spectrometry revealed the production of lyso-phosphatidylcholine in the injured ischemic rat brain. *Neuroscience*. **16**, 168, 219-25 (2016).
85. Hankin, J. A., Farias, S. E., Barkley, R. M., Heidenreich, K., Frey, L. C., Hamazaki, K., Kim, H.-Y. & Murphy, C. M. MALDI Mass Spectrometric Imaging of Lipids in Rat Brain Injury Models. *J. Am. Soc. Mass Spectrom.* **22**, 1014 (2011).
86. Römpp, A., Guenther, S., Schober, Y., Schulz, O., Takats, Z., Kummer, W. & Spengler, B. Histology by Mass Spectrometry: Label-Free Tissue Characterization Obtained from High-Accuracy Bioanalytical Imaging. *Angew. Chem. Int. Ed.* **49**, 3834-3838 (2010).
87. Berry, K. A., Hankin, J. A., Barkley R. M., Spraggins, J. M., Caprioli, R. M. & Murphy, R. C. MALDI imaging of lipid biochemistry in tissues by mass spectrometry. *Chem. Rev.* **111**, 6491-512 (2012).
88. Cornett, D. S., Reyzer, M. L., Chaurand, P. & Caprioli, R. M. MALDI imaging mass spectrometry: molecular snapshots of biochemical systems. *Nat. Methods*. **4**, 828-33 (2007).
89. Murphy, R. C., Fiedler, J. & Hevko, J. Analysis of Nonvolatile Lipids by Mass Spectrometry. *Chem. Rev.* **101**, 479-526 (2001).
90. Wang, C., Wang, M. & Han, X. Applications of mass spectrometry for cellular lipid analysis. *Mol. Biosyst.* **11**, 698-713 (2015).
91. Römpp, A. & Spengler, B. Mass spectrometry imaging with high resolution in mass and space. *Histochem. Cell Biol.* **139**, 759-83 (2013).
92. Kompauer, M., Heiles, S. & Spengler, B. Atmospheric pressure MALDI mass spectrometry imaging of tissues and cells at 1.4- μm lateral resolution. *Nat. Methods*. **14**, 90-96 (2017).
93. Schober, Y., Guenther, S., Spengler, B. & Römpp, A. Single Cell Matrix-Assisted Laser Desorption/Ionization Mass Spectrometry Imaging. *Anal. Chem.* **84**, 6293–6297 (2012).

94. Gessel, M. M., Norris, J. L. & Caprioli, R. M. MALDI imaging mass spectrometry: spatial molecular analysis to enable a new age of discovery. *J. Proteomics*. **107**, 71-82 (2014).
95. Stutts, W. L., Knuth, M. M., Ekelöf, M., Mahapatra, D., Kullman, S. W. & Muddiman, D. C. Methods for Cryosectioning and Mass Spectrometry Imaging of Whole-Body Zebrafish. *J. Am. Soc. Mass. Spectrom.* **31**, 768-772 (2020).
96. Ferain, A., De Saeyer, N., Larondelle, Y., Rees, J.-F., Debier, C. & De Schamphelaere, K. A. C. Body lipid composition modulates acute cadmium toxicity in *Daphnia magna* adults and juveniles. *Chemosphere* **205**, 328–338 (2018).

4. Synopsis

Thesis Topic

In this thesis, I applied intracellular *in vivo* recording in an individually identifiable central neuron – the teleost Mauthner neuron – to determine the impact of different anthropogenic chemicals on the adult vertebrate brain. First, I present how recording in the Mauthner neuron can quickly and systematically help filling the gap that currently exists between legislation and informed decision-making on anaesthetic use in ectothermic vertebrates. Second, using this model system, I reveal the alarming and uncompensated impact of exposure to the plasticizer bisphenol A and S, on basically every neuronal property, thereby calling for the rapid replacement of both plasticizers. In the third project, I address an additional and different topic: Here my focus is not on functional effects of anthropogenic chemicals but on their effect on the composition of animals, specifically on their lipid composition. To address this question, I use MALDI MSI on two model systems, the zebrafish and the water flea. I demonstrate the capacity of MALDI MSI, an imaging technique capable of combining molecular identification with highly resolved histology even down to subcellular resolution, providing histology-linked lipid pattern as an ideal basis to future evaluate molecular changes caused by anthropogenic chemicals in key aquatic organisms.

Chapter 1

In chapter 1, I used intracellular *in vivo* recording in the Mauthner neuron of goldfish (*Carassius auratus*) to assess the concentration-dependant impact of four anaesthetic agents on the central nervous system. These agents are commonly used in teleost fish despite the lack of information that would be needed for their responsible and informed application. I show that using the intracellular recordings quickly provide comprehensive data on several neuronal key functions, including the generating of resting and action potentials and sensory information processing, which confirmed the power of the Mauthner neuron as a new model to assay the impact of anaesthetic agents.

Anaesthetic agents were applied at different concentrations, analogous to published values for anaesthesia in fish and thereby served to obtain concentration effect curves. This enables the demanded targeted application of anaesthetics in fish, which can be used as a first guide for scientists, veterinarians and aquaculture specialist and, in addition, meets current legislative

demands to apply anaesthetic agents for any intervention that could be stressful not only in higher but also in lower vertebrates. In this context, informed-decision making was already possible in higher vertebrates due to the high amount of available data, which could be carefully obtained over years. For fish and other ectothermic vertebrates, time is now pressing to obtain equally comprehensive data. The speed of the new assay meets this challenge, providing quick and reliable comprehensive data. Summarizing, this study successfully demonstrates the first application of the Mauthner neuron to efficiently evaluate the effect of anthropogenic chemicals, such as the anaesthetic agents, on the mature vertebrate brain.

Chapter 2

In chapter 2, I used recording in the Mauthner neuron to reveal clear and alarming effects of the plasticizer BPA and its presumably safe substitute BPS, on nearly all aspects of neuronal function in the mature vertebrate brain. These findings thereby enlarge the spectrum of adverse effects for these plasticizers. Prior studies demonstrated that they act as estrogen-disrupting chemicals, and recent studies additionally demonstrated their impact on the developing juvenile brain. I present here the alarming fact that the neuronal effects of BPA and BPS are not restricted to developing brains and highlight the additional danger for human health, because offsetting balances in the brain are often the cause for severe neurological disorders. The sensitivity and speed of the established assay could therefore make it a powerful part of a battery of similarly sensitive assays to evaluate the next-generation plasticizers, before they become also ubiquitous and dangerous for animal and human health.

I first assayed effects of plasticizer exposition on neuronal function including the generation and characteristics of the action potential, the impact on neuronal backfiring and acoustic and visual processing after one month of exposure to low (10 µg/L) and high (1 mg/L) environmentally relevant concentrations. I could show that already low concentrations of the bisphenols cause strong effects on all aspects of neuronal function and that BPA and BPS, at low and high concentrations, have similar effects. Further, I could demonstrate that the observed strong neuronal effects do not establish quickly after short exposure (1 hour). Finally, I compared effects of both bisphenols to effects obtained after EE2 (ethinyl-estradiol) exposure and revealed similar effects on neuronal function, indicating that observed effects could be – at least partly – due to the activation of estrogen receptors. In summary, these findings clearly present the power of the Mauthner neuron as a powerful tool providing rapidly comprehensive data to evaluate the impact of anthropogenic substances on several neuronal key functions.

Chapter 3

Lipids are key components of cellular membranes and are essential for major physiological processes. Changes caused by anthropogenic chemicals can disrupt the physiology of animals and are often observed to occur during the development of diseases. Considering the various functions of lipids, structural methods linking histological features and lipid signatures at various scales are crucial to understand to which extent the lipid composition and thereby the animal's function is affected by anthropogenic chemicals. Matrix-assisted laser desorption/ionization (MALDI) mass spectrometry imaging (MSI) is such a structural method offering the possibility to link molecular information with spatial distribution of lipids in thin tissue sections. In chapter 3, I used MALDI MSI analysis to visualize histology-linked lipid pattern in zebrafish and *Daphnia magna* providing an ideal basis assaying spatial molecular changes in the presence of anthropogenic chemicals in further studies.

I first investigated the lipid content and distribution in body sections of zebrafish. Prior to my investigations, gross anatomical structures, like the brain, the eye or the gills, could roughly be localized using mass spectrometry imaging. In the current study, with the presented workflow I was able to not only localize but also to clearly differentiate single organs from the surrounding tissue. In addition, I present a fine analysis of those structures, visualizing characteristics features, e.g. different eye layers or brain regions, by their differing lipid content. Second, I improved tissue sectioning and matrix application to image, for the first time, even neuronal structures like the axon and the soma of the Mauthner neuron within whole vertebrate brain sections and thereby demonstrated the successful combination of MALDI MSI analysis with spatially highly resolved histology in aquatic tissue. Finally, I presented for the first time a MALDI MSI workflow for maintaining tissue integrity in non-preserved samples of *Daphnia magna* to visualize lipid pattern in the entire body and the brood chamber inside the carapace. This study should pave the path for future investigations of the impact of different anthropogenic substances on molecular level in aquatic organisms.

5. Publications and Manuscripts

- (1) Machnik, P., **Schirmer, E.**, Glück, L. and Schuster, S. Recordings in an integrating central neuron provide a quick way for identifying appropriate anaesthetic use in fish. *Sci Rep* **8**, 17541 (2018).
- (2) **Schirmer, E.**, Schuster, S. and Machnik, P. Bisphenols exert detrimental effects on neuronal signaling in mature vertebrate brains. *Commun Biol* **4**, 465 (2021).
- (3) **Schirmer, E.**, Ritschar, S., Laforsch, C., Schuster, S. and Römpp, A. Histology-linked MALDI mass spectrometry imaging workflow for *Danio rerio* and *Daphnia magna* (2021).

Manuscript is submitted to Scientific Reports.

- (4) Ritschar, S., **Schirmer, E.**, Hufnagl, B., Löder, M. G. J., Römpp, A. & Laforsch, C. Classification of target tissues of *Eisenia fetida* using sequential multimodal chemical analysis and machine learning. *Histochem Cell Biol* (2021).

Manuscript is not part of this doctoral thesis.

6. Own contributions to joined publications and manuscripts

- (1) Machnik, P., **Schirmer, E.**, Glück, L. and Schuster, S. Recordings in an integrating central neuron provide a quick way for identifying appropriate anaesthetic use in fish. *Sci Rep* **8**, 17541 (2018).

I performed and analyzed experiments in cooperation with Peter Machnik and Laura Glück. Peter Machnik and Stefan Schuster wrote the paper.

- (2) **Schirmer, E.**, Schuster, S. and Machnik, P. Bisphenols exert detrimental effects on neuronal signaling in mature vertebrate brains. *Commun Biol* **4**, 465 (2021).

I designed experimental procedures in agreement with Peter Machnik and Stefan Schuster. In cooperation with Peter Machnik, I performed and analyzed experiments. I wrote the manuscript together with Peter Machnik and Stefan Schuster.

- (3) **Schirmer, E.**, Ritschar, S., Laforsch, C., Schuster, S. and Römpp, A. Histology-linked MALDI mass spectrometry imaging workflow for *Danio rerio* and *Daphnia magna* (2021).

Manuscript is submitted to Scientific Reports.

I designed experimental procedures in agreement with Andreas Römpp, Christian Laforsch and Stefan Schuster. Sample preparation of *Daphnia magna* was performed by Sven Ritschar and I prepared zebrafish samples. I performed and analyzed experiments. Sven Ritschar, Christian Laforsch, Stefan Schuster, Andreas Römpp and I wrote the manuscript.

7. Chapter 1

7.1 Recordings in an integrating central neuron provide a quick way for identifying appropriate anaesthetic use in fish

Peter Machnik, Elisabeth Schirmer, Laura Glück and Stefan Schuster

Abstract

In animal husbandry, livestock industry and research facilities, anaesthetic agents are frequently used to moderate stressful intervention. For mammals and birds, procedures have been established to fine-tune anaesthesia according to the intervention. In ectothermic vertebrates, however, and despite changes in legislation and growing evidence on their cognitive abilities, the presently available information is insufficient to make similarly informed decisions. Here we suggest a straightforward way for rapidly filling this gap. By recording from a command neuron in the brain of fish whose crucial role requires it to integrate and process information from all sensory systems and to relay it to motor output pathways, the specific effects of candidate anaesthesia on central processing of sensory information can directly and efficiently be probed. Our approach allows a rapid and reliable way of deciding if and at which concentration a given anaesthetic affects the central nervous system and sensory processing. We employ our method to four anaesthetics commonly used in fish and demonstrate that our method quickly and with small numbers of animals provides the critical data for informed decisions on anaesthetic use.

Introduction

In many countries, legislation no longer distinguishes between 'higher' and 'lower' vertebrates, but requires for all vertebrates that anaesthetics are used in all interventions that could be stressful¹⁻⁵. However, anaesthetic agents differ largely in their anaesthetising and side effects. Hence, even with equal legal treatment of all vertebrates, detailed evidence is needed to select the appropriate anaesthesia for a particular intervention. Such information is available in birds and mammals. Based on the sensory system or structures of the central nervous system on which they act, a carefully designed mix of anaesthetic agents can be chosen for any given intervention, taking even potential side effects into account⁶. For fish and other ectothermic vertebrates, however, we are presently lacking information about the effects of potential anaesthetic agents on sensory systems and sensory processing. This massively limits the possibilities to make similar informed decisions on anaesthesia so that there currently is a serious gap between legislative demands and the data required to fulfil them. Time is pressing, because anaesthetisation, particularly of fish, is extensively used, both in research facilities, where the zebrafish *Danio rerio* has become one of the most potent and widely used vertebrate model systems⁷⁻⁹, but also in the economically extremely important aquaculture industry¹⁰. According to the FAO, fish production increases year after year, reaching an annual volume of more than 170 million tonnes now¹¹. With the continuous increase of fish production, anaesthetic quantities used in fish and the need of effective anaesthesia also grows continuously. Worldwide numbers are not available, but, for instance, in Norway state authorities track the used quantities of pharmaceuticals applied to fish. Despite responsible use, numbers indicate an exponential increase of anaesthetic quantities in aquaculture industry¹². Given the steadily accumulating evidence on higher cognitive functions in fish¹³⁻¹⁹, given that legislation already demands it in a growing number of states and given the time needed for drug companies and legislation to establish new anaesthetics, it is clear that we do not have equally long time as we took in mammals and birds to establish appropriate data for ectothermic vertebrates that can be used in legal decision making^{20,21}. It is therefore important to establish ways in which useful and yet reliable information can be obtained quickly both on potential novel anaesthetics and on the anaesthetics that are presently in use. Apart from their potential to make handling easier and to reduce stress, the effect of various anaesthetics on specific sensory systems particularly needs to be known for various concentrations to facilitate their aimed application for reducing suffering most efficiently.

Here we demonstrate that recording from the so-called Mauthner neurons, a pair of large identified neurons in the hindbrain of fish (and some amphibians)²² is ideally suited to address this challenging issue. The key is that their natural function requires these neurons to integrate information from all sensory systems and to rapidly issue a motor command that would allow the fish to rapidly escape from potential danger (Fig. 1a). We show that this system is ideally suited to determine quickly the effect of a given anaesthetic on various sensory systems, on central processing and motor output. Here we employed this system to provide a first suggestion of the use of four anaesthetics that could effectively be applied in fish and potentially some other ectothermic vertebrates. Two of them are benzocaine and the benzocaine derivative MS-222, which is currently the most commonly used anaesthetic in ectothermic animals^{2,21,23,24}. The other two are 2-phenoxyethanol (2-PE) and Aqui-S, with the latter one widely used in aquaculture facilities²⁰. Our findings thereby can be used as a first guide to scientists, veterinarians and aquaculture specialists until further pursuing our approach leads, in the coming years, to a finer picture with more options.

Results

Assaying the effect of anaesthetics on neuronal functionality

The Mauthner neuron can easily be localised (Fig. 1b, c), identified (Fig. 1d) and accessed *in vivo* for intracellular recording using well-established techniques and criteria²⁵. After having placed an electrode for recording the membrane potential of one of the two Mauthner neurons, examining the impact of anaesthetic agents on the animal's central processing can be started. We first tested the effect of our selection of agents, applied in reasonably administrable concentration (see Methods), on neuronal functionality. For that we activated the Mauthner neuron by stimulating the spinal cord electrically (Fig. 1d). This allows to easily assay both the resting potential and characteristics of the action potential (i.e. its delay, amplitude, half-maximal duration) as measures for how anaesthetics act at the cellular level in neurons (Fig. 2a). We first applied anaesthetic concentrations commonly used in teleost fish: 0.2 to 0.6 ml L⁻¹ 2-PE, 20 to 100 mg L⁻¹ MS-222 and benzocaine and 10 to 20 mg L⁻¹ Aqui-S, respectively^{4,21,23,26–29}. To determine the anaesthetic impact of each agent, we ran concentration effect curves by changing the anaesthetic concentration while recording from the Mauthner cell. However, none of the applied concentrations of 2-PE or Aqui-S significantly affected any cellular property of the Mauthner neuron (Fig. 2b–e; repeated measures ANOVA: $r^2 \leq 0.48$, $P \geq 0.07$ in all plots). In contrast, the two benzocaine derivatives (MS-222 and benzocaine) increased the delay from spinal cord stimulation to the action potential in the Mauthner neuron in a concentration-dependent way (repeated measures ANOVA: $r^2 \geq 0.89$, $P \leq 0.01$), and decreased the amplitude of the action potential (repeated measures ANOVA: $r^2 \geq 0.69$, $P \leq 0.01$). The resting potential and the half-maximal duration of the action potential were not affected by MS-222 or by benzocaine anaesthesia (repeated measures ANOVA: $r^2 \leq 0.16$, $P \geq 0.51$). Furthermore, we found no significant difference between the effects detected in the animals anaesthetised with MS-222 and those in the animals anaesthetised with benzocaine (paired *t* test: $P \geq 0.18$). This indicates that both benzocaine derivatives similarly affected neuronal properties.

Next, we asked whether the differences in how the anaesthetics affected cellular properties were simply due to different effective concentration levels or indicate inherent differences between the agents. We therefore increased the concentration further for 2-PE and for benzocaine, applying concentrations up to 1.0 ml L⁻¹ of 2-PE and up to 150 mg L⁻¹ of benzocaine. Both concentrations are substantially higher than needed for establishing surgical anaesthesia^{20,28}. The findings fully confirmed that 2-PE does not affect cellular properties of the Mauthner

neuron even at high concentrations. This is shown exemplarily for the amplitude of the action potential in Fig. 2f (linear regression analysis: $r^2 = 0.03$, $P = 0.37$), but also held for all other measures (delay, half-maximal duration, resting potential; linear regression analysis: $r^2 \leq 0.06$, $P \geq 0.23$ in all plots). In contrast, benzocaine at a concentration of 150 mg L^{-1} (i.e. at 2.5 times the surgical concentration²⁸) terminated in 3 of 3 animals tested the capacity of the neuron to fire an action potential (Fig. 2g). Benzocaine and 2-PE thus provide examples of anaesthetics that either do not affect the functionality of neurons (2-PE) or reduce it in a concentration-dependent fashion (benzocaine) and with an effect already at concentrations applied in surgery or handling.

Assaying the effects on hearing and acoustic processing

Both benzocaine and MS-222 reduced the amplitude of acoustically induced PSPs in a concentration-dependent fashion (Fig. 3c; repeated measures ANOVA: $r^2 \geq 0.66$, $P \leq 0.01$). However, even high concentrations did not completely block acoustic PSPs (Fig. 3c). In the animals anaesthetised with 20 mg L^{-1} MS-222, the amplitude of acoustically induced PSPs was $8.7 \pm 0.4 \text{ mV}$. Increasing the MS-222 concentration to 100 mg L^{-1} , only decreased the amplitude to $7.7 \pm 0.6 \text{ mV}$. In animals anaesthetised with benzocaine, the amplitude of acoustically induced PSPs was $14.8 \pm 1.4 \text{ mV}$ for 20 mg L^{-1} benzocaine and $12.9 \pm 1.9 \text{ mV}$ for 100 mg L^{-1} . Despite the substantial increase in concentration both anaesthetics only moderately reduced PSP amplitude (by less than 15%). Even when benzocaine was applied at the concentration that prevented the firing of action potentials (150 mg L^{-1} ; Fig. 2g), it did surprisingly not block the acoustically induced PSPs in the Mauthner neuron, but only reduced its amplitude to $9.8 \pm 0.8 \text{ mV}$. This is still 66% of the amplitude measured under anaesthesia established by applying only 20 mg L^{-1} benzocaine. While MS-222 and benzocaine thus had only a mild effect on the amplitude, they even had no detectable effect at all on the delay of the acoustically induced PSPs (Fig. 3b; repeated measures ANOVA: $r^2 \leq 0.42$, $P \geq 0.11$).

Also both 2-PE and Aqui-S did not affect delay and amplitude of acoustically induced PSPs (Fig. 3b, c; repeated measures ANOVA: $r^2 \leq 0.38$, $P \geq 0.14$). PSPs measured under differently deep anaesthesia are shown in Fig. 3d. In summary, none of the four anaesthetics blocked hearing and auditory processing even at very high concentrations.

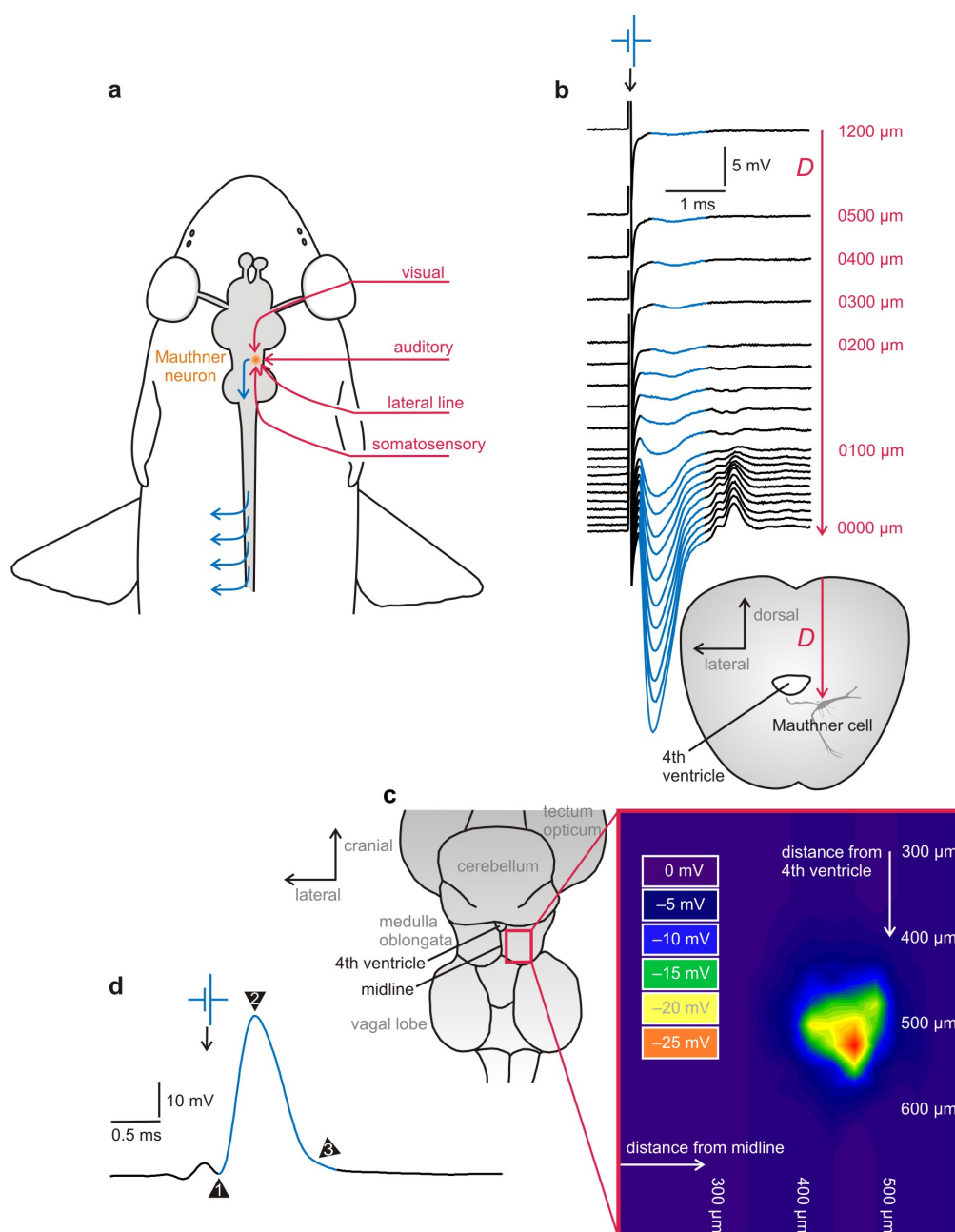


Fig. 1. Brief overview of major features that make the Mauthner cell an interesting experimental system to elucidate the differential actions of anaesthetics. (a) Multisensory integration and motor output: Sketch of a teleost fish with central nervous system (grey), the right one of its two Mauthner neurons (orange spot) in the hindbrain, sensory input to the Mauthner neuron (red) and its motor output (blue). When input is suprathreshold, one of the two Mauthner neurons fires one action potential and this will cause body bending by activating trunk muscles on the contralateral side. (b–d) The Mauthner neuron is an identified neuron that is easy to find and to record from. Though buried deeply in the hindbrain, the Mauthner cell soma can be found for *in vivo* recording on the basis of an all-or-none field potential that emerges from an associated structure in direct vicinity, the axon cap, when the Mauthner axon is activated by stimuli applied to the spinal cord. To illustrate this important feature, the known increase of this field potential during a direct approach from the medullary surface to the centre of the axon cap is shown for goldfish. *D* indicates the distance between the recording electrode and the centre of the axon cap at respective measuring position. (c) A map of the field potential amplitude at the depth of the goldfish Mauthner cell – about 1.2 mm under the surface of the medulla, with distance from major medullary landmarks (4th ventricle and midline) indicated (208 sampling points; right hemisphere; distance between points between 25 and 100 μm depending on steepness of change in field potential). (d) At the field potential maximum, advancing the electrode slightly further will allow recording from the Mauthner neuron. Its identity can be confirmed by several unique characteristics of its action potential, such as its short latency after spinal cord stimuli (1; arrowhead) and the absence of both overshoot (2) and undershoot (3).

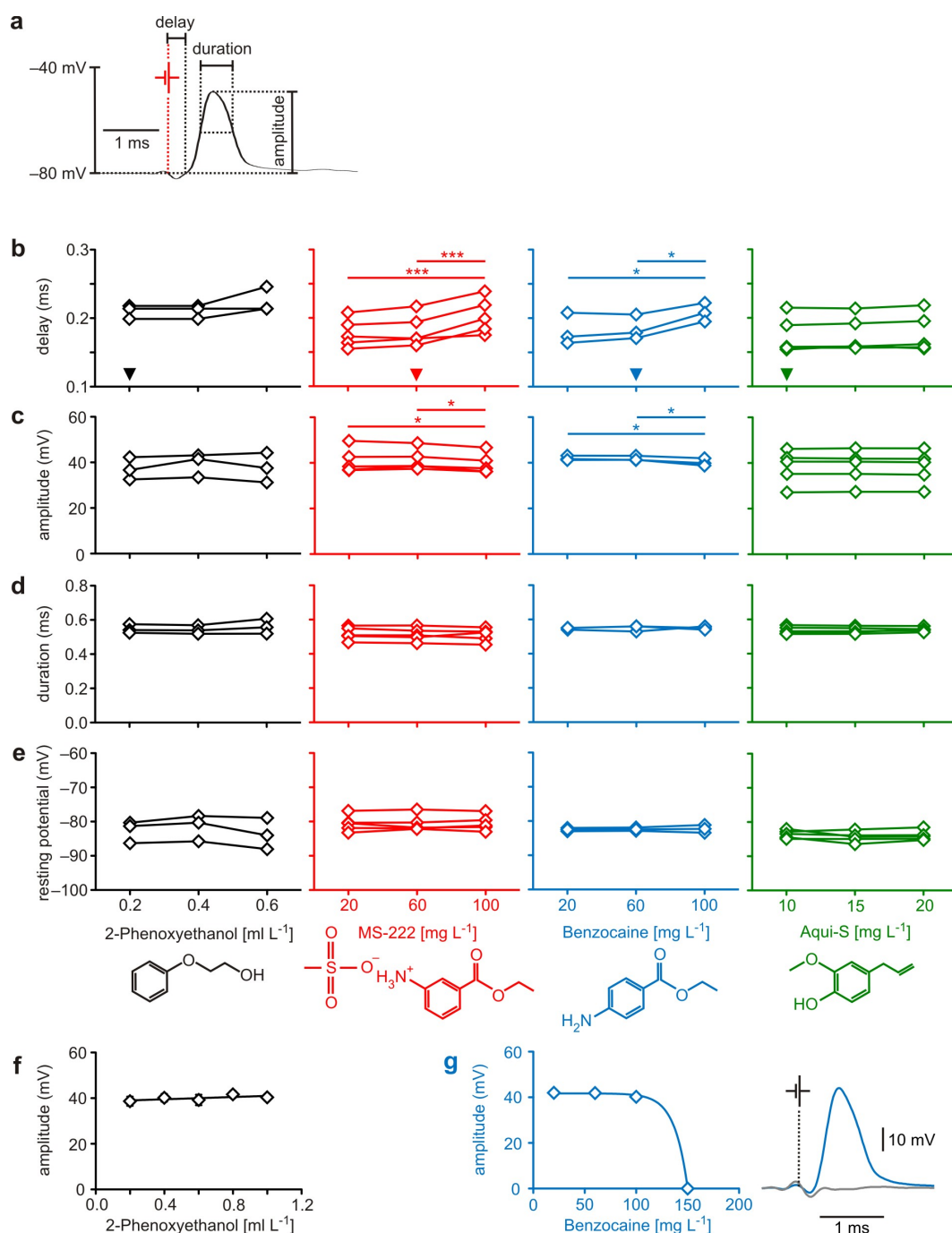


Fig. 2. The anaesthetics benzocaine, MS-222, 2-PE and Aquei-S act differently on the Mauthner cell. (a) To assess potential differences in how the anaesthetics could affect the functionality of neurons in the central nervous system of fish, we determined the resting potential of the Mauthner neuron and properties of its action potential. (b) Both benzocaine (blue) and its derivate MS-222 (red) reduced conduction speed (i.e. increased delay) in a concentration-dependent fashion. Arrowheads in the graphs indicate the anaesthetic concentration needed for achieving surgical anaesthesia, respectively, referring to Neiffer and Stamper (2009). (c) At concentrations above 60 mg L⁻¹ benzocaine and MS-222 caused a reduction in the amplitude of the action potential. (d, e) For concentrations up to 100 mg L⁻¹ benzocaine and MS-222 did not affect the resting potential and the duration of the action potential. However, increasing benzocaine concentration above 100 mg L⁻¹ blocked the functionality of the neuron (g). In 3 of 3 animals tested, no more action potentials were fired at the concentration of 150 mg L⁻¹, as illustrated by recordings taken in the same fish at benzocaine concentrations of 20 mg L⁻¹ (blue) and of 150 mg L⁻¹ (grey). In contrast, the two anaesthetics 2-PE and Aquei-S neither affected the resting potential of the Mauthner neuron (e) nor its action potential (b–d). (f) Even increasing 2-PE concentration to 1 ml L⁻¹ (5 times the concentration needed for establishing surgical anaesthesia) did not affect functionality. MS-222 and Aquei-S: *N* = 5 fish each; 2-PE and benzocaine: *N* = 3 fish each; * indicates *P* < 0.05; *** indicates *P* ≤ 0.001; significant differences between groups are indicated by horizontal lines with the level of significance indicated by asterisk(s).

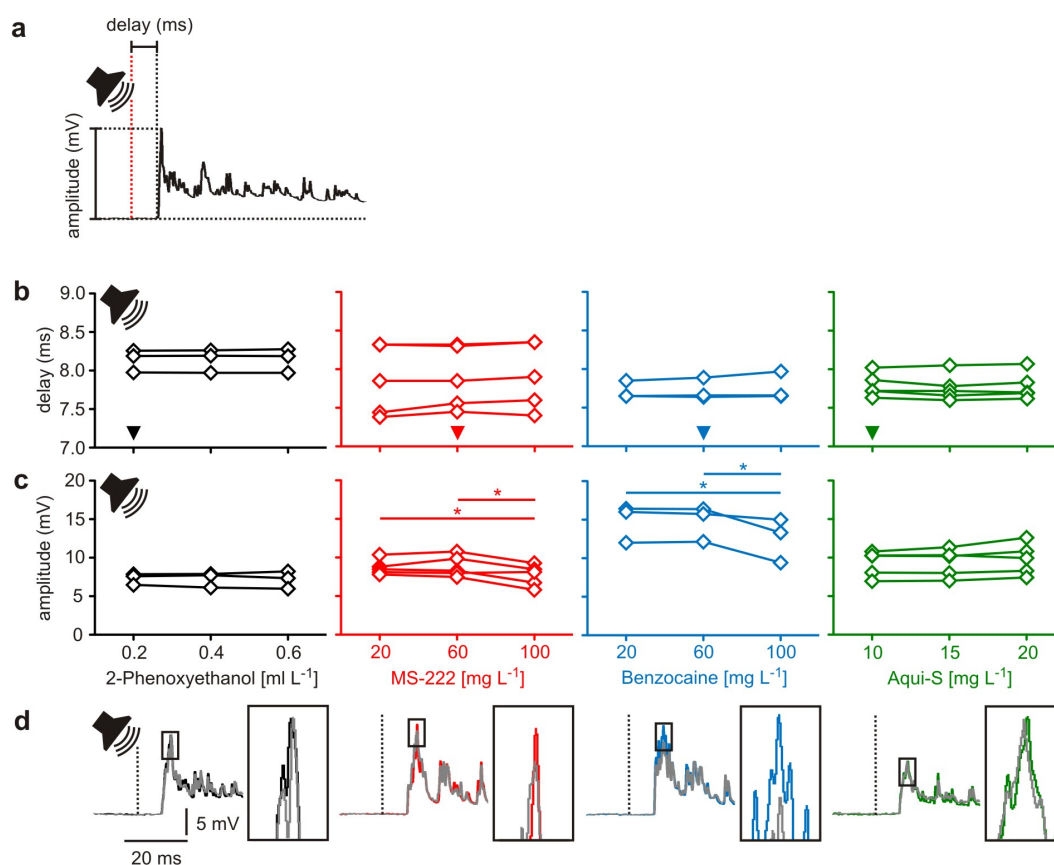


Fig. 3. The effect of anaesthetics on hearing and auditory processing. (a) Acoustic stimulation elicits postsynaptic potentials (PSPs) in the Mauthner neuron, whose delay and amplitude provide an easy way to examine the effect of anaesthetics on hearing and auditory processing. (b, c) 2-PE and Aqui-S had no effect on delay and amplitude of the acoustically induced PSPs. However, MS-222 and benzocaine, when applied at concentrations above the surgical level of 60 mg L⁻¹, significantly reduced the amplitude of acoustically induced PSPs. MS-222 and Aqui-S: $N = 5$ each; 2-PE and benzocaine: $N = 3$ each. * indicates $P < 0.05$. Significant differences between groups indicated by horizontal lines. The respective anaesthetic concentration needed for achieving surgical anaesthesia is indicated in the graphs of (b) by an arrowhead for better orientation. (d) Representative examples of PSPs measured in the same animal under anaesthesia with the lowest (coloured PSP) and the highest concentration (grey PSP) used, as indicated.

Assaying the effects on vision and visual processing

Recording PSPs in the Mauthner neuron in response to visual stimuli allows to assay the effects of the four anaesthetics on vision and visual processing. Our measurements clearly show that benzocaine and its widely used derivate MS-222 block vision and/or visual processing in a concentration-dependent fashion (Fig. 4d). Fig. 4b shows the effect of these agents on the delay of the light flash-induced PSPs in the Mauthner neuron (repeated measures ANOVA: $r^2 \geq 0.89$, $P \leq 0.01$). Measured in the same animals, delay rose from 28.4 ± 1.1 ms under anaesthesia established by the application of 20 mg L⁻¹ MS-222 to 33.0 ± 1.2 ms when anaesthetic

concentration was increased to 100 mg L⁻¹. In animals anaesthetised with benzocaine, delay was 30.5 ± 1.5 ms after the application of 20 mg L⁻¹ benzocaine and 38.4 ± 3.0 ms for the concentration of 100 mg L⁻¹. The amplitude of the visually induced PSP was affected even more impressively. It decreased drastically with increasing levels of both MS-222 and benzocaine (Fig. 4c; repeated measures ANOVA: $r^2 \geq 0.98$, $P \leq 0.0004$). Increasing the anaesthetic concentration from 20 mg L⁻¹ to 60 mg L⁻¹ decreased the amplitude of visually induced PSP substantially, from 5.6 ± 0.4 mV to less than 1.0 mV. 100 mg L⁻¹ further reduced the amplitude to less than 0.5 mV. In other words, animals anaesthetised with benzocaine or the benzocaine derivate MS-222 perform as if they were virtually blind for concentrations ≥ 60 mg L⁻¹. This is compatible with reports on the impact of MS-222 on retinal function taken from *in vitro* measurements³⁰⁻³². We would like to stress that our approach not only readily detects the effect, but also allows to conclude that MS-222 acts specifically on sensory function. The latter follows from a comparison of the effect of MS-222 on the auditory and the visually evoked responses in the Mauthner neuron. The absence of a correlated effect on both types of PSPs (correlation analysis on data of Figs. 3c and 4c: $P = 0.46$) suggests that the effect is largely due to its effect on vision and not on central processing. This also held true for the effect of benzocaine.

In contrast to MS-222 and benzocaine, 2-PE did not block visually induced PSPs (Fig. 4d). The application of 2-PE only slightly increased the delay of visually induced PSPs for concentrations higher than 0.4 ml L⁻¹ (Fig. 4b; repeated measures ANOVA: $r^2 = 0.90$, $P = 0.009$), and did not affect the PSP amplitude (Fig. 4c; repeated measures ANOVA: $r^2 = 0.63$, $P = 0.13$) at surgical concentrations. Also, the widely used anaesthetic Aqui-S does not always block vision. However, its effect on vision was remarkably variable (Fig. 4c). In 2 of the 5 experimental animals vision was fully intact at surgical levels. In contrast, Aqui-S, applied at the same concentration, effectively blocked visual PSPs in 3 of the 5 experimental animals (PSP amplitude < 0.5 mV). Note that all animals were checked before experiments (see Methods) for sensory induced responses and were clearly not blind. Furthermore, experiments were interspersed with experiments in which 2-PE was used for anaesthetisation and in which vision was unaffected, so that the variation in the effects could not be attributed to any parameters that might have changed in the setup between measurements in which Aqui-S had a strong effect and in which it had no effect on the visually induced PSPs. Aqui-S therefore appears to be highly variable in its effect on vision.

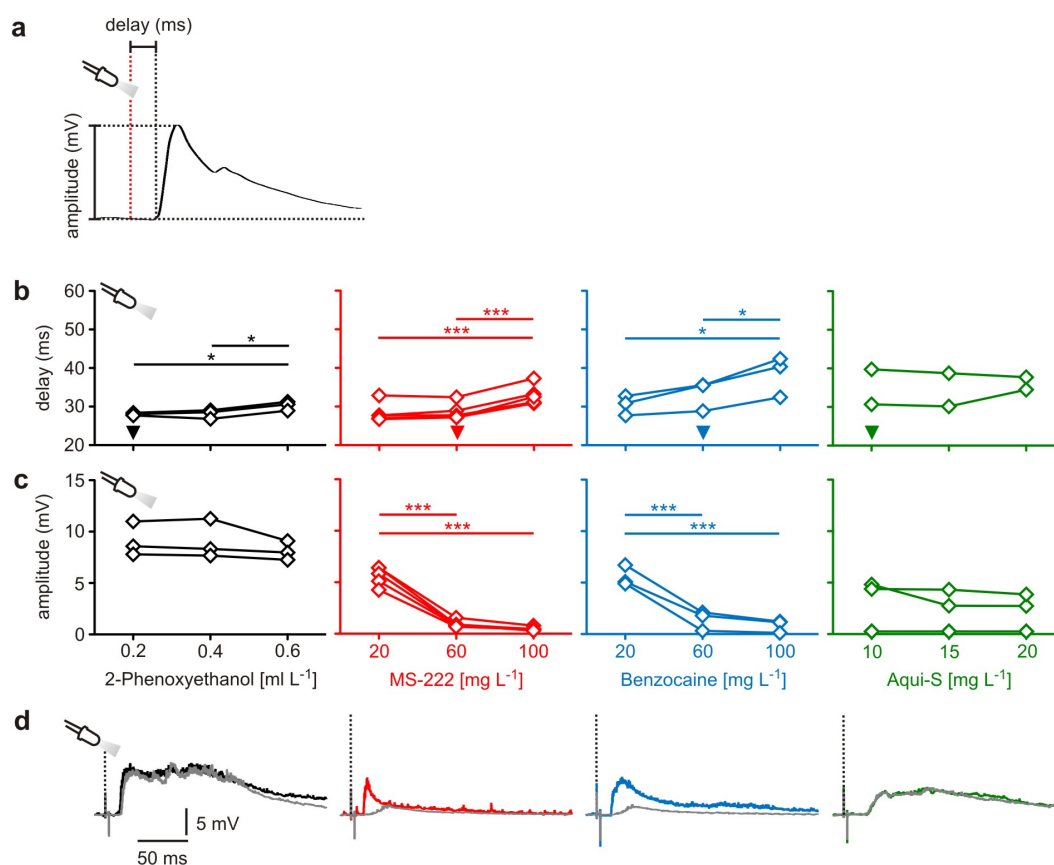


Fig. 4. The effect of anaesthetics on vision and visual processing. (a) Even simple visual stimuli, such as light flashes, elicit postsynaptic potentials (PSPs) in the Mauthner neuron. Their delay and amplitude provide a convenient measure of how anaesthetics affect vision and visual processing. (b, c) 2-PE did not reduce the amplitude of visually induced PSPs (repeated measures ANOVA: $r^2 = 0.63$, $P = 0.13$), but concentrations above 0.4 ml L^{-1} (i.e. concentrations 2 to 3 times above surgical concentration level) slightly increased their delay (repeated measures ANOVA: $r^2 = 0.90$, $P = 0.009$). In contrast, MS-222 and benzocaine strongly affected PSP amplitude and delay and PSPs were almost undetectable above the surgical concentration of 60 mg L^{-1} . In 2 of 5 experimental animals any Aqui-S concentration showed no effect on the visually induced PSPs, whereas in 3 further experimental animals Aqui-S reduced the amplitude of visually induced PSPs to zero. MS-222 and Aqui-S: $N = 5$ fish each; 2-PE and benzocaine: $N = 3$ fish each. * indicates $P < 0.05$; ** indicates $P \leq 0.01$; *** indicates $P \leq 0.001$. Significant differences between groups indicated by horizontal lines. Arrowheads indicate the anaesthetic concentration needed for achieving surgical anaesthesia in the graphs of (b), respectively, for better orientation. (d) Representative examples of PSPs measured in the same animal under anaesthesia with the lowest (coloured PSP) and the highest concentration (grey PSP) tested in the experiments.

Our approach allows significant statements based on small samples

As a critical check of the practical usefulness of our approach we asked how many experimental animals are required to meaningfully assess the effect of an agent or pharmaceutical actually. To critically assess this decisive question, we took measurements in additional three groups of three animals each. The additional three groups were tested for the effect of 2-PE for anaesthetisation at concentrations in the range from 0.2 to 0.6 ml L^{-1} as described above (Figs. 2b–e, 3b–c, 4b–c), so that we had four groups with a total of $N = 12$ experimental animals. To directly assess the variations between the groups of three animals, Figs. 5 and 6 show the results of a characterisation of the three additional groups. We compared the conclusions made in the

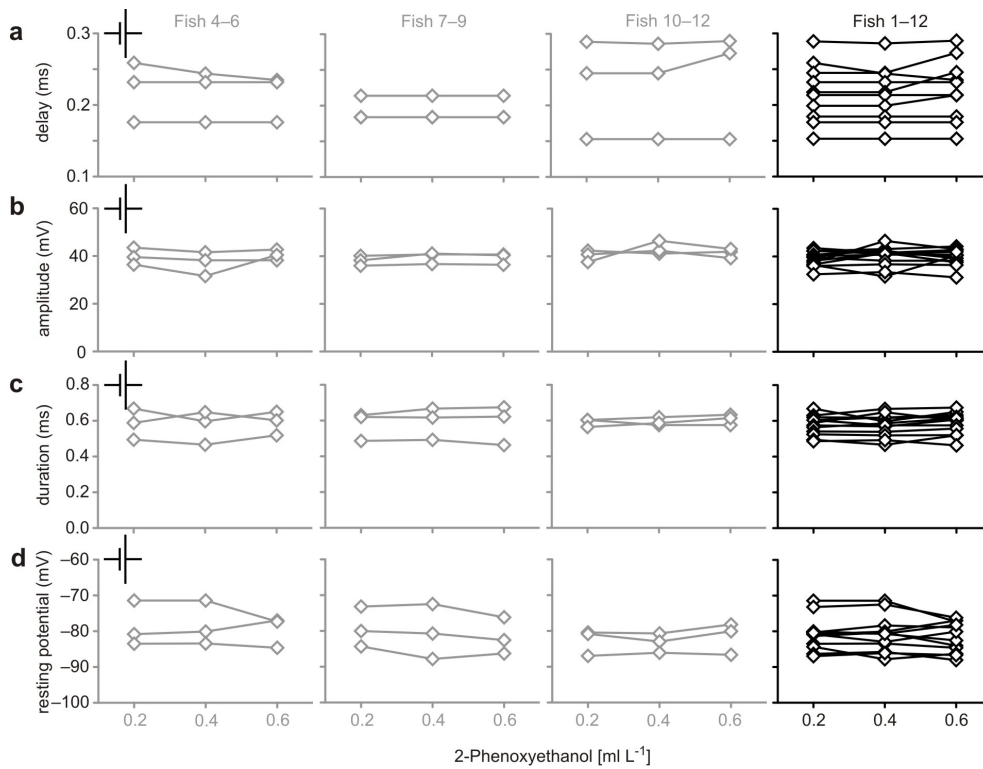


Fig. 5. Evidence suggesting that small numbers of animals are sufficient to characterise effects of anaesthetics on neuronal functionality. (a–c) shows data such as presented for $N = 3$ fish in Fig. 2b–e, but for three additional groups, also of $N = 3$ fish each, (d) shows the results obtained when the $N = 12$ fish had been pooled. 2-PE was used as anaesthetic.

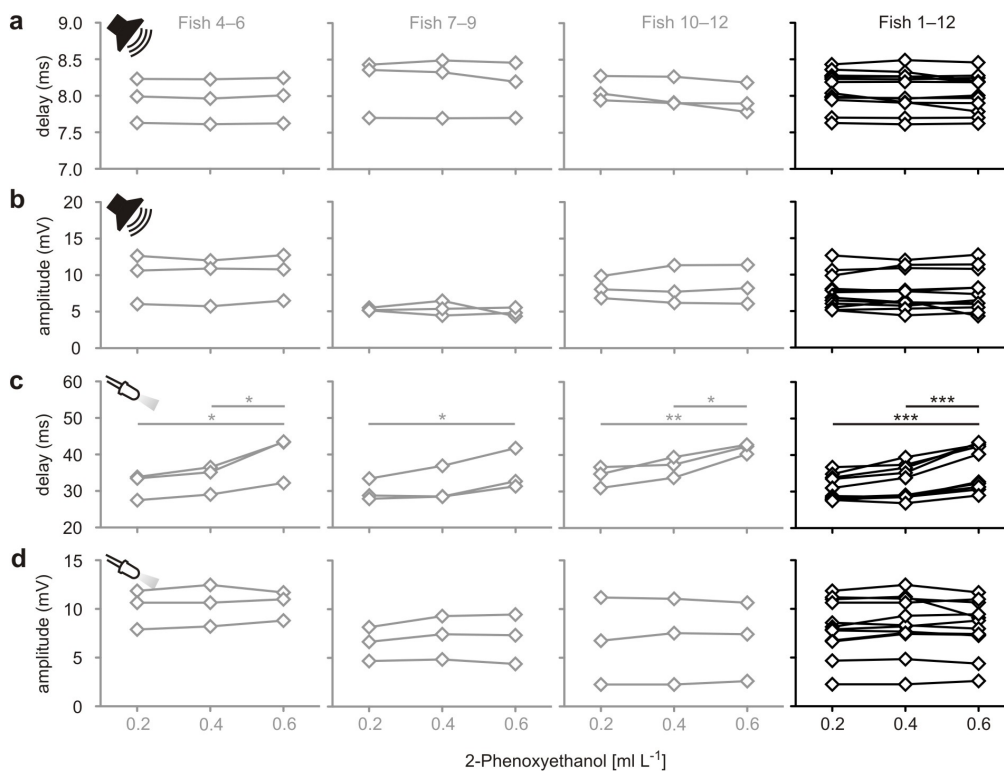


Fig. 6. Evidence suggesting that small numbers of animals are sufficient to determine the effect of anaesthetics on sensory function. Analyses as in Figs. 3 and 4, but with three additional groups, each of $N = 3$ fish. 2-PE was used as anaesthetic.

Table 1. Practical guidelines for anaesthetic use based on our findings in goldfish

Anaesthetic agent	Surgical conc.*	Functionality of CNS neurons		Handling in the presence of		Scientific study of	
		Affected	Vanished	Noise	Light	Hearing	Vision
2-PE (ml L ⁻¹)	0.2	no	no	no	no	yes	< 0.6
MS-222 (mg L ⁻¹)	60	> 60	n.d.	no	≥ 60	<100	no
Benzocaine (mg L ⁻¹)	60	> 60	> 100	no	≥ 60	<100	no
Aqui-S (mg L ⁻¹)	10	no	no	no	no	yes	no

* required concentration according to Neiffer and Stamper (2009); n.d. = not determined

small-sample groups among each other, but also with the conclusions basing on the measurements of the pooled group ($N = 12$). It is striking that none of the small-sample groups gave an effect that differed from that obtained for the large group. In none of the small sample groups or the pooled group we detected a direct effect of 2-PE on the Mauthner neuron (repeated measures ANOVA: $r^2 \leq 0.63$, $P \geq 0.14$ in all plots). Similarly, in no group did we detect an effect of 2-PE on the delay of acoustically induced PSPs and on the amplitude of both acoustically and visually induced PSPs (repeated measures ANOVA: $r^2 \leq 0.71$, $P \geq 0.09$ in all plots). Furthermore, all four small-sample groups revealed the concentration effect of 2-PE on the delay of the visually induced PSPs (repeated measures ANOVA: $r^2 \geq 0.86$, $P \leq 0.02$) just as in the pooled group (repeated measures ANOVA: $r^2 = 0.78$, $P < 0.001$).

Discussion

The goal of the current study was to explore how useful recordings of anti- and orthodromically stimulated Mauthner neurons would be to quickly obtain urgently needed reliable information on the various effects anaesthesia can have on sensory and neuronal function in fish. We demonstrate the power of our approach by studying the effect of four anaesthetics that are commonly used in ectothermic vertebrates: MS-222, benzocaine, 2-phenoxyethanol and Aquis-S. By monitoring neuronal functionality and visual and acoustic inputs to these command neurons^{22,33-35}, we showed that recording in the Mauthner neuron allows to not only detect differential effects of the anaesthetics, but even successfully narrows down its site of action. Our approach allows a quick way of determining, which concentrations are needed for the desired effect. We show that small numbers of animals are sufficient and so our method is likely to quickly widen the spectrum of anaesthetics for fish and potentially other 'lower' vertebrates for the required more targeted application in experimentation, treatment and aquaculture. Moreover, our findings already provide a basis for a recommendation which of the anaesthetics to use for different purposes and at which concentration (Table 1).

Our approach exploits the function and accessibility of a pair of identified neurons in the hindbrain of most fish species and in many amphibians, that can be identified from one animal to the next. The so-called Mauthner neurons form the centre of a network, that is crucial to elicit a life-saving escape behaviour in response to a threat, such as a suddenly approaching predator. To achieve this, the Mauthner neurons integrate and process information forwarded from all of the animal's sensory systems (Fig. 1a) to properly assess the necessity for driving an escape response²². This property makes the Mauthner neuron an ideal substrate for efficiently obtaining the differential effects agents have on central nervous processing and sensory function in fish. We show that important conclusions can already be obtained from small numbers of animals, a highly desirable property from an ethical point of view³⁶ and needed to speed up data acquisition. Measurements taken from three fish were sufficient for determining the concentration dependence and general action of our sample of anaesthetics on neuronal and sensory function (Figs. 5, 6) and could not be improved by using larger samples of 12 fish. Even small effects could be reliably detected in the small groups of three fish, such as the concentration dependency of the delay of visually induced PSPs for 2-PE application (Fig. 4b). Our findings strongly underline the importance of having detailed information available on anaesthetic effects in fish. We show that even the agents currently used to anaesthetise and to calm fish substantially differ in their effects. This is perhaps most striking in benzocaine and

Aqui-S, two widely and indiscriminately used anaesthetics for fish. Even when benzocaine is given at a concentration that blocks firing of the Mauthner neuron, sound can still elicit sizeable PSPs in the same cell. Similarly, when benzocaine is given at a concentration that blocks visually induced PSPs, then activation of the neuron is still possible as well as sound induced PSPs. In the case of Aqui-S, an agent that is widely used in aquaculture facilities, we discovered that a remarkable degree of unpredictability exists selectively for visually induced responses, but not for acoustically induced responses and neuronal function. Hence, Aqui-S is a potent agent for handling and for reducing stress in fish, but not for blocking vision or for the scientific study of visual functions (Tab. 1). Our findings also underline the importance of using other anaesthetics besides benzocaine derivatives like MS-222, the most commonly used anaesthetic in scientific work. It cannot be used, for instance, in studies on visual function, in which it should be substituted with 2-PE (Tab. 1). In studies on hearing all anaesthetics of our sample would be equally well suited. This means, however, also that none of them is capable of reducing strain of fish in particularly noisy environments. Presently our suggestions that we have condensed in Table 1 base, of course, on experiments performed in goldfish. In absence of any other data, it would still be useful to operate on the basis of Table 1, even for other ectothermic vertebrates for which we lack any data. Of course, it is also possible to quickly widen the approach introduced here to other species and to use it to widen the spectrum of useful agents for targeted applications in fish.

In conclusion, we demonstrated here how recordings in the Mauthner neuron can quickly and systematically help filling the gap that currently exists between legislation and informed decision-making on anaesthesia in ectothermic vertebrates. By scanning the effects of further candidate agents, and by exploring their effects in a few more key species of fish, our approach will in the coming years contribute to achieving a reasonable and targeted anaesthesia in fish and will be of value for other ectothermic vertebrates, for which any information is presently lacking.

Methods

Experimental animals

We used $N = 25$ goldfish (*Carassius auratus* (Linnaeus, 1758), Cypriniformes) of either sex with standard lengths from 7 to 9 cm. The fish were obtained commercially from an authorised specialist retailer (Aquarium Glaser GmbH, Rodgau, Germany). Before used in experiment, fish were kept for at least 12 weeks. In this period, they were maintained in a group at 20°C and 12:12h light/dark photoperiod in a tank (250 x 50 x 50 (cm)) filled with fresh water (water conductivity: 300 $\mu\text{S cm}^{-1}$; pH 7.5; total hardness of water: 7.7°dH; $\text{NH}_4^+ < 10 \mu\text{g L}^{-1}$; $\text{NO}_2^- < 5 \mu\text{g L}^{-1}$; $\text{NO}_3^- < 5 \text{mg L}^{-1}$). Water of the same quality was used in the electrophysiological recording chamber. Fish were fed with common fish food (sera goldy; sera GmbH, Heinsberg, Germany) and defrosted red mosquito larvae. Animal care procedures, surgical procedures and experimental procedures were in accordance with all relevant guidelines and regulations of the German animal protection law and explicitly approved by state councils (Regierung von Unterfranken, Würzburg, Germany). Before selecting fish for an experiment, we checked that they respond to visual and acoustic stimuli: they had to show escape responses both to rapid hand movements in front of the aquarium and to knocking on the aquarium.

Anaesthesia

We tested the effect of four anaesthetic agents commonly used in fish: (i) 2-phenoxyethanol (2-PE; 1-hydroxy-2-phenoxyethane; Sigma-Aldrich, Steinheim, Germany), (ii) ethyl-3-aminobenzoate methanesulfonate (also known as tricaine, TMS or MS-222; Sigma-Aldrich, Steinheim, Germany), (iii) benzocaine (Sigma-Aldrich, Steinheim, Germany; solved 1:10 in 95% ethanol), and (iv) Aqui-S (Scanvacc, Hvam, Norway). The use of one of these anaesthetics in a given experiment was selected at random to ensure that any differences could not be caused by unintended changes in the experimental setup or by undetected changes in the animals' state. Each of the experimental fish was solely exposed to one of the anaesthetic agents to exclude potential interactions between the anaesthetics. Anaesthetic concentration levels, particularly surgical concentrations, were chosen based on appropriate references^{4,21,23,26–29}. For the appropriate use of Aqui-S, an anaesthetic widely used in aquaculture facilities, we additionally used information provided by Aqui-S New Zealand Ltd (<http://www.aqui-s.com/aqui-s-products/aqui-s> (2018)). Concentration levels ranged from 0.2 to 1.0 ml L⁻¹ for 2-PE, 20 to 100 mg L⁻¹ for MS-222, 20 to 150 mg L⁻¹ for benzocaine, and 10 to 20 mg L⁻¹ for Aqui-S. 20 mg L⁻¹ of the anaesthetics MS-222 and benzocaine cause slight anaesthetisation in fish (stage II

anaesthesia^{1,20}), whereas all other applied anaesthetic concentrations cause at least surgical anaesthetisation (stage III anaesthesia)²¹. Before starting any surgical intervention, fish were surgically anaesthetised (stage III anaesthesia^{1,20}) by application of either 0.4 ml L⁻¹ 2-PE, 60 mg L⁻¹ MS-222 or benzocaine or 20 mg L⁻¹ Aqui-S for 15 min. We generally confirmed the sufficiency of the anaesthetisation after total loss of equilibrium by carefully exerting pressure to the fish's caudal peduncle. In responsive fish, this kind of touch reliably triggers an escape response and subsequent swimming behaviour. When this stimulation (and subsequent handling) yielded no response, then the fish was positioned in the electrophysiological recording chamber and artificial respiration was established with aerated water flowing via a tube through the mouth and out over the gills at a flow rate of 80 ml min⁻¹. Respiration water thereby was delivered to the fish from a reservoir (respiration water tank) using a suitably adjusted pump (EHEIM universal 300; EHEIM GmbH & Co. KG, Deizisau, Germany; regular power: 300 L h⁻¹, adjusted to 4.8 L h⁻¹). To maintain anaesthesia, the respiration water always contained the same anaesthetic as used for establishing anaesthesia. We started experiments randomly either with the lowest concentration used in the respective experiment or with the highest one. To examine anaesthetic concentration effects, we then changed the concentration level within a particular animal, while simultaneously recording intracellularly from the Mauthner neuron. To increase the concentration level during the experiment, we added additional anaesthetic to the respiration water. To quickly establish a uniform mixture of respiration water and anaesthetic, we used a circulation pump (EHEIM universal 600; EHEIM GmbH & Co. KG, Deizisau, Germany; power: 600 L h⁻¹) in the respiration water tank. To reduce the anaesthetic concentration, we added additional water of the same quality and temperature to the respiration water tank. After changing the anaesthetic concentration level, we always gave an acclimatisation period of 15 min before the next measurements were taken. This interval was chosen to be significantly beyond the estimated time (< 6 min) needed by the used anaesthetics to impact on the animal's physiology by simple add-on to the water surrounding the fish^{23,27}.

Surgical procedure

To access the Mauthner cells, we exposed the hindbrain by opening the skull from above using a bone rongeur. Additionally, we exposed a piece of the spinal column (about 5 mm length) in the region of the trunk from the side. The large axons of the Mauthner neurons run down the complete spinal cord and can be activated by applying electrical pulses to the spinal cord.

Activation of both Mauthner cells causes typical twitching of the experimental animal. Note that none of the used anaesthetics applied in surgical concentration (Tab. 1) ceased the massive muscle activation after firing the Mauthner neurons. After testing the correct positioning of the homemade bipolar stimulation electrode forwarding electrical pulses to the spinal cord, we therefore had to immobilise the experimental animal for intracellular *in vivo* recording by injecting d-tubocurarine (1 $\mu\text{g g}^{-1}$ body weight; Sigma-Aldrich, Steinheim, Germany).

After finishing recording, the experimental animal was sacrificed immediately and without recovery from anaesthesia by mechanically destroying the brain.

Experimental procedure

We used a bridge-mode amplifier (BA-01X; npi electronic GmbH, Tamm, Germany) in current clamp mode for intracellular recordings with sharp electrodes. Recording electrodes (4-7 M Ω) were pulled from 3 mm-glass capillaries (G-3; Narishige Scientific Instrument Lab, Tokyo, Japan) by using a vertical electrode puller (PE-22; Narishige International Limited, London, UK) and filled with 5 M potassium acetate. A motorised micromanipulator (MP-285; Sutter Instrument, Novato, CA, USA) was used to position and to move the recording electrode. The reference electrode was positioned in muscle tissue. Recordings were filtered (Hum Bug Noise Eliminator; Quest Scientific, North Vancouver, BC, Canada) and digitised (A/D converter Micro1401; Cambridge Electronic Design Limited, Cambridge, UK) at 50 kHz. For further processing and analysis we used the acquisition software package Spike2 (version 6; Cambridge Electronic Design Limited, Cambridge, UK). After localisation and identification of one of the two Mauthner cells by using well-established techniques^{22,25,37}, we determined the resting potential of the Mauthner cell, properties related to the Mauthner action potential (delay, action potential amplitude and its half-maximal duration) and properties related to acoustically and visually induced PSPs³⁷, respectively. Delay was taken as the time from onset of the stimulus to the first deflection of the membrane potential away from resting potential. For amplitude we determined the difference between the resting potential and the maximum of the action potential. To elicit an action potential in the Mauthner cell, we stimulated the spinal cord electrically (pulse amplitude: up to 65 V, as required, but regularly between 8 and 12 V; pulse duration: 10 μs ; stimulation rate: 2 Hz). Electric pulses thereby were delivered by a constant-voltage isolated stimulator (DS2A2 – Mk.II; Digitimer Ltd., Hertfordshire, UK). For acoustic stimulation, we used a multifunctional active loudspeaker (The box pro Achat 115 MA; Thomann GmbH, Burgebrach, Germany). The loudspeaker generated a short acoustical

broadband pulse (duration 1 ms; frequency distribution from 25 to 1000 Hz; peak amplitude at 300 Hz) with a sound pressure level (SPL) of 145 dB *re* 1 μ Pa. We measured SPL under water at the position of the fish in the recording chamber with a hydrophone (Type 8106; Brüel & Kjær, Nærum, Denmark). Visual stimuli were 7 ms-light flashes delivered by a light emitting diode (LED) (RS Components GmbH, Mörenfelden-Walldorf, Germany) directly positioned in front of the ipsilateral eye. The LED peak radiation at about 569 nm was 700 μ W m⁻² nm⁻¹ and the width at 100 μ W m⁻² nm⁻¹ was 56 nm (range: 543 to 599 nm).

Statistical analysis

Statistical tests were run by using the software package GraphPad Prism 5.0f (GraphPad Software, Inc., La Jolla, CA, USA) and performed two-tailed with $\alpha = 0.05$. We tested deviation from normal distribution using the Shapiro-Wilk test. We tested departure from linearity for 2-PE and benzocaine concentration level effects by using a runs test. If the runs test revealed no significant deviation from linearity, we performed a linear regression analysis, otherwise we searched for a better corresponding non-linear fit. To factor out interindividual differences, we changed anaesthetic concentration within particular experimental animals and then used repeated measures design for statistical analysis (e.g. paired *t* test, repeated measures ANOVA). To compare the impact of MS-222 and benzocaine on neuronal functionality, we also used repeated measures design. Here, we used anaesthetic concentration for pairing. Averages are given as mean \pm standard error of mean (s.e.m.). The heat map (Fig. 1c) was constructed in SigmaPlot 11.0 (Systat, Inc., Erkrath, Germany). *n* labels the number of analysed values; the number of analysed experimental animals is labelled *N*.

References

1. Brown, L. A. Anaesthesia and restraint in *Fish Medicine* (ed. Stoskopf, M. K.) 79–90 (Saunders, 1993).
2. Treves-Brown, K. M. *Applied Fish Pharmacology* (Kluwer Academic Publishers, 2000).
3. Broom, D. M. Cognitive ability and sentience: Which aquatic animals should be protected? *Dis. Aquat. Org.* **75**, 99–108 (2007).
4. Ross, L. G. & Ross, B. *Anaesthetic And Sedative Techniques For Aquatic Animals* (Wiley-VCH, 2008).
5. Browman, H. I. et al. Welfare of aquatic animals: where things are, where they are going, and what it means for research, aquaculture, recreational angling, and commercial fishing. *ICES J. Mar. Sci.*: <https://doi.org/10.1093/icesjms/fsy067> (2018).
6. Katzung, B. G., Masters, S. B. & Trevor, A. J. *Basic & Clinical Pharmacology, 12th edition* (McGraw-Hill, 2012).
7. Dooley K. & Zon, L. I. Zebrafish: a model system for the study of human disease. *Curr. Op. Gen. Dev.* **3**, 252–256 (2000).
8. Grunwald, D. J. & Eisen, J. S. Headwaters of the zebrafish – emerge of a new model vertebrate. *Nature Rev. Gen.* **3**, 717–724 (2002).
9. Lieschke, G. J. & Currie P. D. Animal models of human disease: zebrafish swim into view. *Nature Rev. Gen.* **8**, 353–367 (2007).
10. Conte, F. S. Stress and the welfare of cultured fish. *Appl. Anim. Behav. Sci.* **86**, 205–223 (2004).
11. Food and Agriculture Organization of the United Nations via *statistica.com* (<https://www.statista.com/statistics/272311/world-fish-production-by-fishing-and-aquaculture-since-2004/>)
12. Burridge, L., Weis, J. S., Cabello, F., Pizarro, J. & Bostick, K. Chemical use in salmon aquaculture: A review of current practices and possible environmental effects. *Aquaculture* **306**, 7–23 (2010).
13. Bshary, R., Wickler, W. & Fricke, H. Fish cognition: a primate’s eye view. *Anim. Cogn.* **5**, 1–13 (2002).

14. Sneddon, L. U. The evidence for pain in fish: the use of morphine as an analgesic. *Appl. Anim. Behav. Sci.* **83**, 153–162 (2003).
15. Sneddon, L. U. Pain in aquatic animals. *J. Exp. Biol.* **218**, 967–976 (2015).
16. Brown, C., Laland, K. & Krause, J. (eds.) *Fish cognition and behavior* (Wiley-Blackwell, 2011).
17. Bshary, R. & Brown, C. Fish cognition. *Curr. Biol.* **24**, R947–R950 (2014).
18. Sneddon, L. U., Elwood, R. W., Adamo, S. A. & Leach, M. C. Defining and assessing animal pain. *Anim. Behav.* **97**, 201–212 (2014).
19. Sneddon, L. U. et al. Fish sentience denial: muddying the waters. *Anim. Sent.* **115** (2018).
20. Coyle, S. D., Durborow, R. M. & Tidwell, J. H. Anesthetics in aquaculture. *Southern Regional Aquaculture Center (SRAC)* **3900**, 1–6 (2004).
21. Zahl, I. H., Samuelsen, O. & Kiessling, A. Anaesthesia of farmed fish: implications for welfare. *Fish Physiol. Biochem.* **38**, 201–218 (2012).
22. Sillar, K. T., Picton, L. D. & Heitler, W. J. Fish Escape: the Mauthner System in *The Neuroethology of Predation and Escape* (eds. Sillar, K. T., Picton, L. D. & Heitler, W. J.) 212–243 (Wiley Blackwell, 2016).
23. Ackerman, P. A., Morgan J. D. & Iwama, G. K. *Anaesthetics*. http://www.ccac.ca/Documents/Standards/Guidelines/Add_PDFs/Fish_Anesthetics.pdf. Accessed (01.12.2017) (2007).
24. Martins, T., Valentim A. M., Pereira, N. & Antunes, L. M. Anaesthesia and analgesia in laboratory adult zebrafish: a question of refinement. *Lab. Anim.* **50(6)**, 476–488 (2016).
25. Furshpan, E. J. & Furukawa, T. Intracellular and extracellular responses of the several regions of the Mauthner cell of goldfish. *J. Neurophysiol.* **25**, 732–771 (1962).
26. Iwama, G. K. & Ackerman, P. A. Anaesthetics in *Biochemistry And Molecular Biology Of Fishes*, vol. 3. (eds. Hochachka, P. W. & Mommsen, T. P.) 1–15 (Elsevier, 1994).
27. Weyl, O., Kaiser, H. & Hecht, T. On the efficacy and mode of action of 2-phenoxyethanol as an anaesthetic for goldfish, *Carassius auratus* (L.), at different temperatures and concentrations. *Aquaculture Res.* **27**, 757–764 (1996).

28. Neiffer, D. L. & Stamper, M. A. Fish sedation, anesthesia, analgesia, and euthanasia: considerations, methods, and types of drugs. *ILAR J.* **50**, 343–360 (2009).
29. Carter, K. M., Woodley, C. M. & Brown, R. S. A review of tricaine methanesulfonate for anesthesia of fish. *Rev. Fish Bio. Fisheries* **21**, 51–59 (2011).
30. Hoffman, R. T. & Basinger, S. F. The effect of MS-222 on rhodopsin regeneration in the frog. *Vision Res.* **17**, 335–336 (1977).
31. Rapp, L. M. & Basinger, S. F. The effect of local anaesthetics on retinal function. *Vision Res.* **22**, 1097–1103 (1982).
32. Bernstein, P. S., Digre, K. B. & Creel, D. J. Retinal toxicity associated with occupational exposure to the fish anesthetic MS-222. *Amer. J. Ophthalmol.* **124**, 834–843 (1997).
33. Zottoli, S. J. Correlation of the startle reflex and Mauthner cell auditory responses in unrestrained goldfish. *J. Exp. Biol.* **66**, 243–254 (1977).
34. Rock, M. K., Hackett, J. T. & Brown, D. L. Does the Mauthner cell conform to the criteria of the command neuron concept? *Brain Res.* **204**, 21–27 (1981).
35. Brownstone, R. M. & Chopek, J. W. Reticulospinal systems for tuning motor commands. *Front. Neural Circ.* **12:30**, doi: 10.3389/fncir.2018.00030 (2018).
36. Russell, W. M. S. & Burch, R. L. *The Principles of Humane Experimental Techniques* (Methuen and Co. Ltd., 1959).
37. Machnik, P., Leupolz, K., Feyl, S., Schulze, W. & Schuster S. The Mauthner cell in a fish with top-performance and yet flexibly-tuned C-starts II. Physiology. *J. Exp. Biol.:* <https://doi.org/10.1242/jeb.175588> (2018).

Acknowledgements

The current study was supported by a Reinhart Koselleck-project (to S.S.) of the Deutsche Forschungsgemeinschaft (German Research Foundation). We thank Antje Halwas for excellent technical support and Kathrin Leupolz, Alexander Hecker, Georg Welzel and Wolfram Schulze for helpful discussions and comments on the figures. Additionally, it is a pleasure to thank our reviewers for many helpful comments.

Author contribution

P.M. and S.S. designed and supervised experimental procedure; P.M., E.S. and L.G. performed and analysed experiments; P.M. and S.S. wrote the manuscript.

8. Chapter 2

8.1 Bisphenols exert detrimental effects on neuronal signaling in mature vertebrate brains

Elisabeth Schirmer, Stefan Schuster and Peter Machnik

Abstract

Bisphenols are important plasticizers currently in use and are released at rates of hundreds of tons each year into the biosphere¹⁻³. However, for any bisphenol it is completely unknown if and how it affects the intact adult brain⁴⁻⁶, whose powerful homeostatic mechanisms could potentially compensate any effects bisphenols might have on isolated neurons. Here we analyzed the effects of one month of exposition to BPA or BPS on an identified neuron in the vertebrate brain, using intracellular in vivo recordings in the uniquely suited Mauthner neuron in goldfish. Our findings demonstrate an alarming and uncompensated in vivo impact of both BPA and BPS – at environmentally relevant concentrations – on essential communication functions of neurons in mature vertebrate brains and call for the rapid development of alternative plasticizers. The speed and resolution of the assay we present here could thereby be instrumental to accelerate the early testing phase of next-generation plasticizers.

Introduction

Plasticizers are essential ingredients to plastic production^{7,8}. However, upon degradation of plastic products these additives are released into the environment in large quantity, making plasticizer contamination a serious environmental issue and potential risk for our health^{1,9–12}. For example, 8 million tons of the plasticizer bisphenol A (BPA; 2,2-bis-(4-hydroxyphenyl)-propane; CAS Registry No. 80-05-7) are produced worldwide each year and 100 tons per year are released into the biosphere^{2,3,13,14}, making BPA ubiquitously present in the environment from surface water to breast milk¹. Initially considered harmless, its various effects on hormonal balance, reproduction and development in vertebrates^{6,10,12,15,16} have led to its replacement – particularly in baby products – by other bisphenols, most notably bisphenol S (BPS; 4,4'-sulfonyldiphenol; CAS Registry No. 80-09-1)^{4,5}, which is presently available in the EU at rates of 10.000 tons per year¹⁷. Evidence, however, is mounting that also BPS might not be unproblematic^{1,4,18–24}. Its almost 100-fold higher solubility in water compared to BPA makes BPS now readily detectable in aqueous environments^{25,26}. Studies in fish models, however, indicate that exposition not only to BPA, but also to BPS results in developmental deformities, impaired and abnormal behavior^{27–30}.

Here we demonstrate an alarming effect of bisphenols that has, to our knowledge, never been described before: We describe here clear and alarming effects of both BPA and its substitute BPS on neuronal functionality in the mature vertebrate brain despite the powerful homeostatic mechanisms that act *in vivo*^{31,32} and that could in principle compensate for any effects seen *in vitro*^{33,34}. Our findings make it very likely that bisphenols also affect the adult human brain and can, among other aspects, change the delicate balance between excitation and inhibition, which is seen as the basis of several neuronal disorders^{6,35,36}. Our findings call for new approaches to speed up the development and efficient pre-testing of alternative plasticizers. Specifically, the assay that we describe here can rapidly and accurately provide comprehensive information on effects on the mature brain and should therefore be part of a battery of efficient tests in the development of future plasticizers.

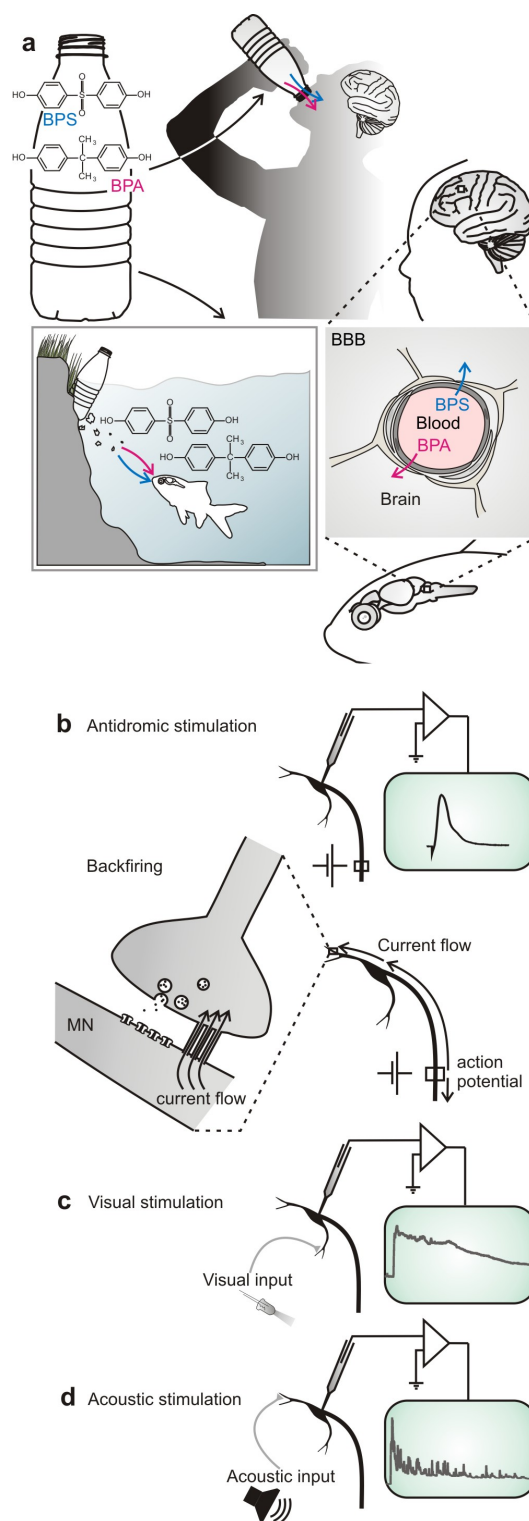


Fig. 1 Studying the in vivo effect of bisphenols on neural functionality in the mature CNS of a vertebrate. **a** Bisphenols are additives in plastic products. As plastic degrades these substances are released into the environment and are then able to pass the blood-brain barrier (BBB). Bisphenol A (BPA), the most widely used plasticizer, is released at millions of tons per year and has devastating effects, for instance during ontogeny. Its substitute bisphenol S (BPS) also appears problematic, but for both bisphenols any effect on the mature brain is unknown. **b–d** In vivo intracellular recordings in the central nervous system using the identified Mauthner neuron of the goldfish provide a comprehensive and rapid assay of fundamental aspects of the action of bisphenols in the intact adult brain: The effect on ion channels, chemical and electric synaptic transmission can be studied by antidromically stimulating the axon and monitoring backfiring by currents that spread to the presynaptic sites (**b**). The effect on visual (**c**) and acoustic (**d**) processing as well as transmission and integration at the dendrite can be studied by recording postsynaptic potentials after sensory stimulation

Results

Assaying neural function *in vivo*

To study the effect of exposure to bisphenols on the adult vertebrate brain (Fig. 1a), the Mauthner neuron of fish and some amphibians is an ideal substrate. It is one of the very few neurons in the vertebrate CNS that can be identified individually from one animal to the next and that is readily accessible to intracellular *in vivo* recording³⁷. Therefore, it has been a major source of insight into fundamental mechanisms of synaptic communication in the vertebrate CNS³⁸. The two Mauthner neurons are essential for triggering the vital escape in response to suddenly approaching predators^{39,40}. This requires the Mauthner neuron to integrate information from all sensory systems. Hence, intracellular recordings from the Mauthner neuron can rapidly and highly sensitively assay a number of key aspects of neuronal and circuit function. In our tests we elicited action potentials in the Mauthner neurons antidromically (Fig. 1b), i.e. by stimulating their large axons (see Methods), and quantitatively analyzed several of its characteristics. Additionally, we presented sensory stimuli to activate visual (Fig. 1c) and acoustic (Fig. 1d) processing and recorded postsynaptic potentials (PSPs) to analyze the integration of sensory information in the Mauthner neuron.

Effects on the action potential

We discovered that even at environmentally relevant concentration of $10 \mu\text{g L}^{-1}$ one month of exposure to BPA or BPS massively reduced the maximal initial slope of the action potential (Fig. 2a) *in vivo*. In the controls (exposed to the solvent DMSO) the maximal initial slope was $2.13 \pm 0.33 \text{ V ms}^{-1}$ ($N = 13$ independent animal samples; $n = 9$ to 31 measurements per fish). $10 \mu\text{g L}^{-1}$ BPA reduced it to $0.68 \pm 0.44 \text{ V ms}^{-1}$ ($N = 12$ independent animal samples; $76 \leq n \leq 114$; one-way ANOVA: $F = 17.55$; $R^2 = 0.5899$; $P < 0.0001$; Dunnett test: mean diff.: 1.39; confidence interval of diff.: 0.95 to 1.82; $P < 0.0001$) and 1 mg L^{-1} to $1.19 \pm 0.22 \text{ V ms}^{-1}$ ($N = 12$ independent animal samples; $17 \leq n \leq 19$; Dunnett test: mean diff.: 0.89; confidence interval of diff.: 0.46 to 1.33; $P < 0.0001$). Exposure to $10 \mu\text{g L}^{-1}$ BPS reduced the maximal initial slope of the action potential to $1.20 \pm 0.47 \text{ V ms}^{-1}$ ($N = 11$ independent animal samples; $86 \leq n \leq 104$; Dunnett test: mean diff.: 0.80; confidence interval of diff.: 0.35 to 1.24; $P < 0.0001$) and 1 mg L^{-1} to $1.93 \pm 0.62 \text{ V ms}^{-1}$ ($N = 11$ independent animal samples; $20 \leq n \leq 159$; Dunnett test: mean diff.: 0.48; confidence interval of diff.: 0.03 to 0.92; $P = 0.032$). Because we also noticed effects on the time course of the action potential, we analyzed the time-integrated action potential, taking the area I_1 for the first ms after onset (see Fig. 2a). Interestingly, here only the

higher plasticizer concentration showed an effect: In controls, I_1 was 23.8 ± 3.1 mV*ms ($N = 13$ independent animal samples; $9 \leq n \leq 31$). 1 mg L^{-1} BPA reduced the integrated action potential in the first ms of its duration to 20.5 ± 3.1 mV*ms ($N = 12$ independent animal samples; $17 \leq n \leq 19$; one-way ANOVA: $F = 6.249$; $R^2 = 0.3387$; $P < 0.0001$; Dunnett test: mean diff.: 3.45; confidence interval of diff.: 0.82 to 6.08; $P = 0.0055$). With 1 mg L^{-1} BPS, I_1 was 19.4 ± 2.9 mV*ms ($N = 11$ independent animal samples; $20 \leq n \leq 159$; Dunnett test: mean diff.: 4.09; confidence interval of diff.: 1.40 to 6.78; $P = 0.001$).

BPA increases neuronal backfiring

The action potential of the Mauthner neuron can backfire to presynaptic sites through electrical synapses (Fig. 1b). These are part of the mixed 'club-ending' synapses that convey acoustic input onto the lateral dendrite of the Mauthner neuron. The resulting depolarization of the presynaptic site can then again cause transmitter release, giving rise to a delayed potential (DP) that lags the action potential by about 1 ms^{41} . If this also backfires, even a second DP can be generated. The DPs are therefore a valuable tool for assessing how bisphenols affect electrical synapses and presynaptic transmitter release. Fig. 2b illustrates two exemplary DPs. They typically followed 0.86 ± 0.06 ms (amplitude 10.3 ± 3.8 mV; $N = 5$ independent animal samples; $n = 9$ to 31 measurements per fish; first DP) and 1.44 ± 0.05 ms (amplitude 4.9 ± 1.9 mV; $N = 4$ independent animal samples; $n = 9$ to 31; second DP) after onset of the action potential (Supplementary Fig. 1b). In the control group a pair of DPs occurred consistently in 31% (4 of 13) of the fish, a single DP in 38% (5 of 13). Consistent with the notion that the 2nd DP is caused by transmitter release due to the presynaptic spreading of the 1st DP, we found that the amplitude of the 2nd DP correlates with the amplitude of the first (Supplementary Fig. 1c; $N = 20$ independent animal samples; $9 \leq n \leq 114$; Spearman correlation: $P = 0.01$) and was absent when the first one was absent. In contrast, we found no correlation between the amplitude of the 1st DP and the amplitude of the action potential (Supplementary Fig. 1c; $N = 33$ independent animal samples; $9 \leq n \leq 114$; Spearman correlation: $P = 0.45$). Strikingly, one month of exposition to BPA strongly affected backfiring *in vivo* through mixed electrical and chemical synapses. While both BPA and BPS did not affect the amplitudes of the DPs (Supplementary Fig. 1d; one-way ANOVA: $F \leq 1.539$; $R^2 \leq 0.1751$; $P \geq 0.217$), specifically BPA (but not BPS) dramatically increased the occurrence of DPs: In the group of fish exposed to 1 mg L^{-1} BPA as

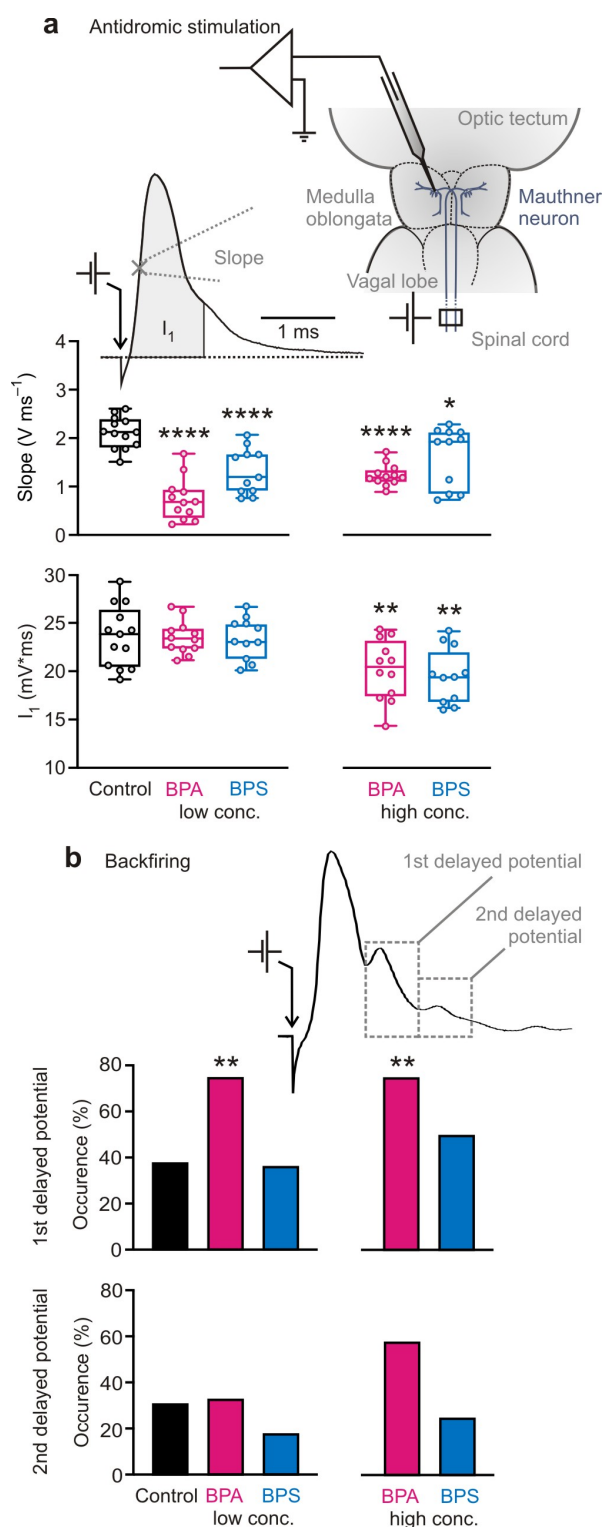


Fig. 2 BPA and BPS both affect central neurons. **a** BPA and BPS both affected the action potential in the Mauthner neuron. In high and low concentration, they significantly decreased the slope of the action potential. In high concentration, they additionally reduced the area I_1 . The sketch indicates the experimental setting for antidromic stimulation and intracellular recording from the Mauthner soma. The exemplary action potential from a control fish illustrates the interval in which slope and I_1 were determined. **b** Changes in the occurrence of delayed potentials (DPs) due to backfiring (see Fig. 1b) after bisphenol exposition indicate an impact on synaptic transmission in the CNS. BPA (but not BPS) increased the occurrence of DPs in exposed fish. Low conc. = $10\ \mu\text{g L}^{-1}$; high conc. = $1\ \text{mg L}^{-1}$; $N_{(\text{Control})} = 13$ independent samples; $N_{(10\ \mu\text{g L}^{-1}\ \text{BPA})} = 12$ independent samples; $N_{(1\ \text{mg L}^{-1}\ \text{BPA})} = 12$ independent samples; $N_{(10\ \mu\text{g L}^{-1}\ \text{BPS})} = 11$ independent samples; $N_{(1\ \text{mg L}^{-1}\ \text{BPS})} = 11$ independent samples; differently treated groups are indicated by colour; whiskers show the minimum and the maximum value, respectively; significant differences between groups and control are indicated by asterisk(s); * indicates $P < 0.05$; ** indicates $P \leq 0.01$; **** indicates $P \leq 0.0001$.

well as in that exposed to $10 \mu\text{g L}^{-1}$ BPA the first delayed potential occurred in 75% (9 of 12) (Wilcoxon test for difference from control: $P = 0.009$). An additional second DP occurred in 58% (7 of 12) of fish exposed to 1 mg L^{-1} BPA (Wilcoxon test for difference from control: $P = 0.086$) and in 33% (4 of 12) of fish exposed to $10 \mu\text{g L}^{-1}$ BPA (Wilcoxon test for difference from control: $P = 0.13$). BPA thus strongly increased neuronal backfiring. In light of the findings below, this is a likely consequence of increased transmission at the glutamatergic mixed synapses and increased spreading of the action potential to presynaptic sites.

Bisphenols affect acoustic processing

One month of exposure to BPA or BPS had striking and uncompensated effects on the PSPs that were elicited by our broadband acoustic pulse. The experimental setting and an exemplary PSP of a control animal are shown in Figure 3a,b. Strikingly, the bisphenols affected basically all aspects of the acoustic PSP. BPA and BPS both increased the amplitude, the temporal integral and its longtime decay. Maximum amplitude of the PSPs was increased from $7.1 \pm 1.4 \text{ mV}$ ($N = 13$ independent animal samples; between $n = 8$ to 29 measurements per fish) in the controls to $11.2 \pm 3.0 \text{ mV}$ ($N = 11$ independent animal samples; $16 \leq n \leq 49$) with $10 \mu\text{g L}^{-1}$ BPS and to $10.4 \pm 2.3 \text{ mV}$ ($N = 11$ independent animal samples; $9 \leq n \leq 46$) with 1 mg L^{-1} . $10 \mu\text{g L}^{-1}$ BPA increased the maximum amplitude to $10.2 \pm 2.1 \text{ mV}$ ($N = 12$ independent animal samples; $10 \leq n \leq 52$) and 1 mg L^{-1} to $11.4 \pm 1.9 \text{ mV}$ ($N = 12$ independent animal samples; $11 \leq n \leq 23$; Fig. 3c; one-way ANOVA: $F = 6.994$; $R^2 = 0.3569$; $P < 0.0001$; Dunnett test: $P \leq 0.0032$). To assay the concentration of the changes in membrane potential, we considered the temporal integral in four consecutive intervals, 50 ms each (Fig. 3b; integrals I_1 to I_4). This analysis showed a clear increase of the first integral (Fig. 3c; one-way ANOVA: $F = 6.479$; $R^2 = 0.3396$; $P < 0.0001$) from $117.5 \pm 32.1 \text{ mV*ms}$ ($N = 13$ independent animal samples; $8 \leq n \leq 29$) in the controls to $173.6 \pm 32.6 \text{ mV*ms}$ ($N = 11$ independent animal samples; $16 \leq n \leq 49$) with $10 \mu\text{g L}^{-1}$ BPS (Dunnett test: mean diff.: -53.74 ; confidence interval of diff.: -91.16 to -16.32 ; $P = 0.002$) and to $188.9 \pm 47.2 \text{ mV*ms}$ ($N = 11$ independent animal samples; $9 \leq n \leq 46$) with 1 mg L^{-1} BPS (Dunnett test: mean diff.: -67.47 ; confidence interval of diff.: -104.9 to -30.05 ; $P < 0.0001$). BPA significantly increased I_1 in high (Dunnett test: mean diff.: -63.64 ; confidence interval of diff.: -100.20 to -27.07 ; $P = 0.0001$), but not in low concentration (Dunnett test: mean diff.: -25.96 ; confidence interval of diff.: -62.53 to 10.61 ; $P = 0.2516$). In fish exposed to 1 mg L^{-1} BPA, I_1 was $176.4 \pm 35.8 \text{ mV*ms}$ ($N = 12$ independent animal samples; $11 \leq n \leq 23$). For the acoustic PSPs caused by our stimulus, the time integrals decayed

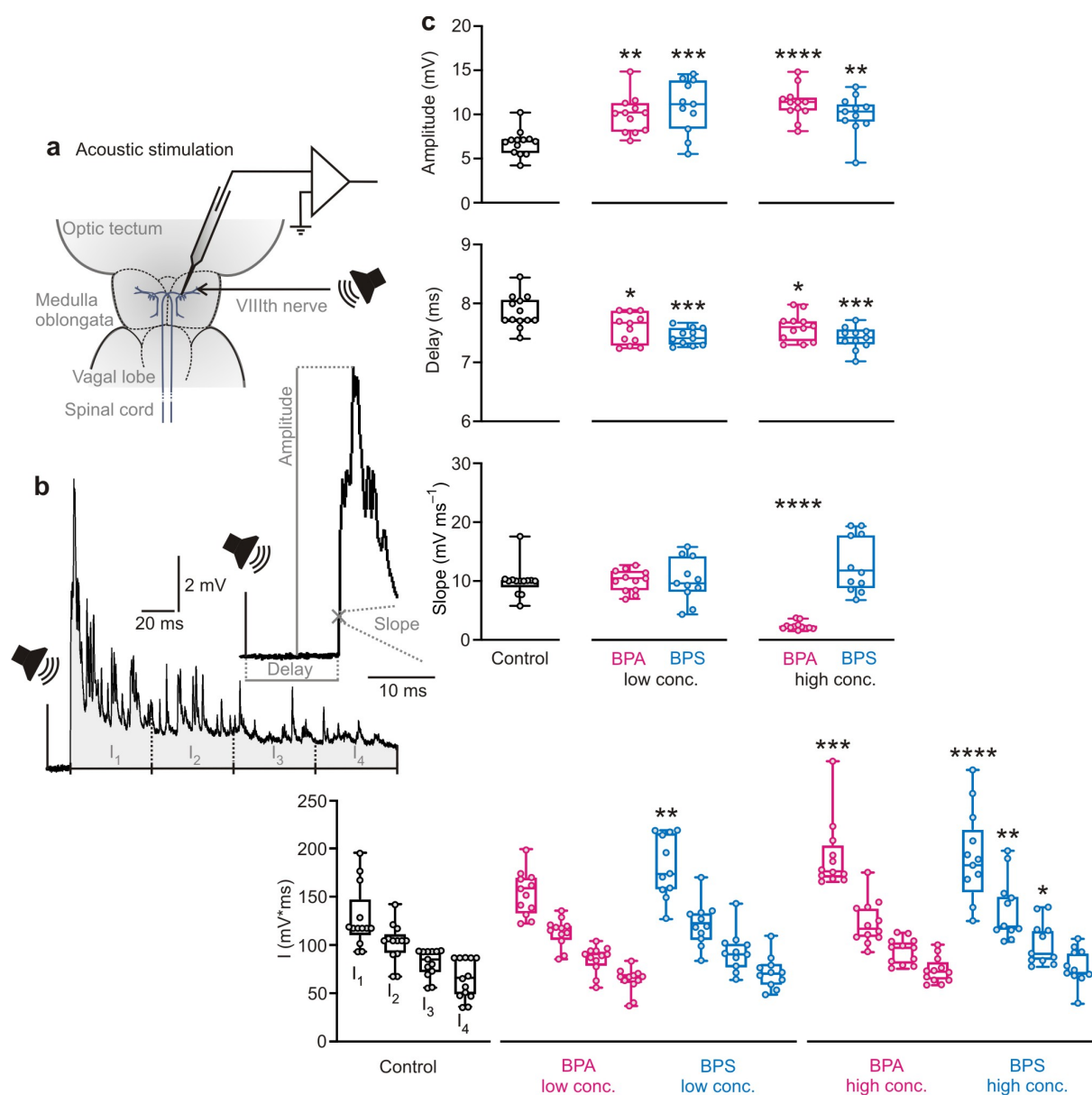


Fig. 3 Both BPA and BPS affect auditory processing. **a** Sketch of experimental setting for acoustic stimulation and **b** an exemplary acoustically induced postsynaptic potential (PSP) from a control fish with illustration of how measurements were taken. **c** Both concentrations of BPA increased the PSP amplitude and decreased delay of the PSP relative to stimulus onset. Additionally, the high BPA concentration increased area I_1 and decreased the slope of the PSP. BPS exposition also increased the amplitude of the acoustically induced PSP and I_1 . The high BPS concentration also increased the areas I_2 and I_3 . Additionally, exposition to BPS shortened the delay. Low conc. = $10 \mu\text{g L}^{-1}$; high conc. = 1 mg L^{-1} ; $N_{(\text{Control})} = 13$ independent samples; $N_{(10 \mu\text{g L}^{-1} \text{ BPA})} = 12$ independent samples; $N_{(1 \text{ mg L}^{-1} \text{ BPA})} = 12$ independent samples; $N_{(10 \mu\text{g L}^{-1} \text{ BPS})} = 11$ independent samples; $N_{(1 \text{ mg L}^{-1} \text{ BPS})} = 11$ independent samples; differently treated groups are indicated by colour; whiskers show the minimum and the maximum value, respectively; significant differences between groups and control are indicated by asterisk(s); * indicates $P < 0.05$; ** indicates $P \leq 0.01$; *** indicates $P \leq 0.001$; **** indicates $P \leq 0.0001$.

exponentially ($y = y_0 * \exp(-k * x)$) (goodness of fit: $r^2 \geq 0.54$), but with larger rate constants in bisphenol-exposed fish ($k_{\text{control}} = 0.22$; $k_{\text{BPS}} \geq 0.31$; $k_{\text{BPA}} \geq 0.30$). The increase of rate of decay from I_1 to I_4 thereby was significant in fish exposed to 1 mg L^{-1} BPA (Fig. 3c; one-way ANOVA: $F = 3.357$; $R^2 = 0.1991$; $P = 0.0159$; Dunnett test: mean diff.: 0.117; confidence

interval of diff.: 0.030 to 0.203; $P = 0.0047$) and those exposed to $10 \mu\text{g L}^{-1}$ BPS (Dunnett test: mean diff.: 0.095; confidence interval of diff.: 0.004 to 0.186; $P = 0.0371$). BPA and BPS significantly reduced the delay of the PSP relative to stimulus onset (Fig. 3c; one-way ANOVA: $F = 6.426$; $R^2 = 0.3377$; $P < 0.0001$; Dunnett test: $P \leq 0.0399$). Delay was 7.71 ± 0.28 ms ($N = 13$ independent animal samples; $8 \leq n \leq 29$) in controls. $10 \mu\text{g L}^{-1}$ BPA reduced it to 7.62 ± 0.26 ms ($N = 12$ independent animal samples; $10 \leq n \leq 52$) and 1 mg L^{-1} BPA to 7.60 ± 0.23 ms ($N = 12$ independent animal samples; $11 \leq n \leq 23$). $10 \mu\text{g L}^{-1}$ BPS reduced the delay to 7.41 ± 0.14 ms ($N = 11$ independent animal samples; $16 \leq n \leq 49$) and 1 mg L^{-1} BPS to 7.42 ± 0.19 ms ($N = 11$ independent animal samples; $9 \leq n \leq 46$). Finally, 1 mg L^{-1} BPA significantly reduced the maximal initial slope of the PSP from $10.0 \pm 2.7 \text{ mV ms}^{-1}$ ($N = 13$ independent animal samples; $8 \leq n \leq 29$) in the control group to $2.0 \pm 0.7 \text{ mV ms}^{-1}$ ($N = 12$ independent animal samples; $11 \leq n \leq 23$) (one-way ANOVA: $F = 16.62$; $R^2 = 0.5689$; $P < 0.0001$; Dunnett test: mean diff.: 7.72; confidence interval of diff.: 4.55 to 10.90; $P < 0.0001$).

In conclusion both bisphenols had striking effects on almost all functionally relevant aspects of the acoustic PSP. Most remarkably they increased the efficiency at which the acoustic stimulus excited the Mauthner neuron. Because at least BPS is thought to negatively affect sensory hair cells⁴², a decrease rather than an increase of the amplitude of acoustic PSPs would have been expected. Our findings therefore suggest important and unbalanced excitatory effects of BPA and BPS on (glutamatergic⁴¹) synaptic transmission in the CNS.

Bisphenols affect visual processing

The bisphenols not only affected acoustic circuits but had striking effects on the visual PSP. The experimental setting and an exemplary PSP are shown in Figure 4a,b. In contrast to their effect on the acoustic PSP, BPA and BPS strongly reduced the amplitude of the visual PSPs (Fig. 4c; one-way ANOVA: $F = 17.83$; $R^2 = 0.6058$; $P < 0.0001$; Dunnett test: $P \leq 0.0046$). In controls, PSP amplitude was 10.4 ± 1.8 mV ($N = 8$ independent animal samples; $n = 7$ to 21 measurements per fish). $10 \mu\text{g L}^{-1}$ BPA reduced it to 2.9 ± 1.5 mV ($N = 12$ independent animal samples; $8 \leq n \leq 27$) and 1 mg L^{-1} BPA to 6.3 ± 1.5 mV ($N = 12$ independent animal samples; $10 \leq n \leq 21$). In BPS exposed fish, PSP amplitude was 2.5 ± 2.4 mV ($N = 11$ independent animal samples; $7 \leq n \leq 31$) for $10 \mu\text{g L}^{-1}$ and 5.0 ± 3.4 mV ($N = 11$ independent animal samples; $11 \leq n \leq 25$) for 1 mg L^{-1} BPS. In addition, 1 mg L^{-1} BPA (but not the low concentration of BPA tested or BPS) also drastically reduced the maximal initial slope of the PSPs from $3.66 \pm 0.82 \text{ mV ms}^{-1}$ ($N = 8$ independent animal samples; $7 \leq n \leq 21$) to only $0.32 \pm 0.07 \text{ mV ms}^{-1}$ ($N = 12$

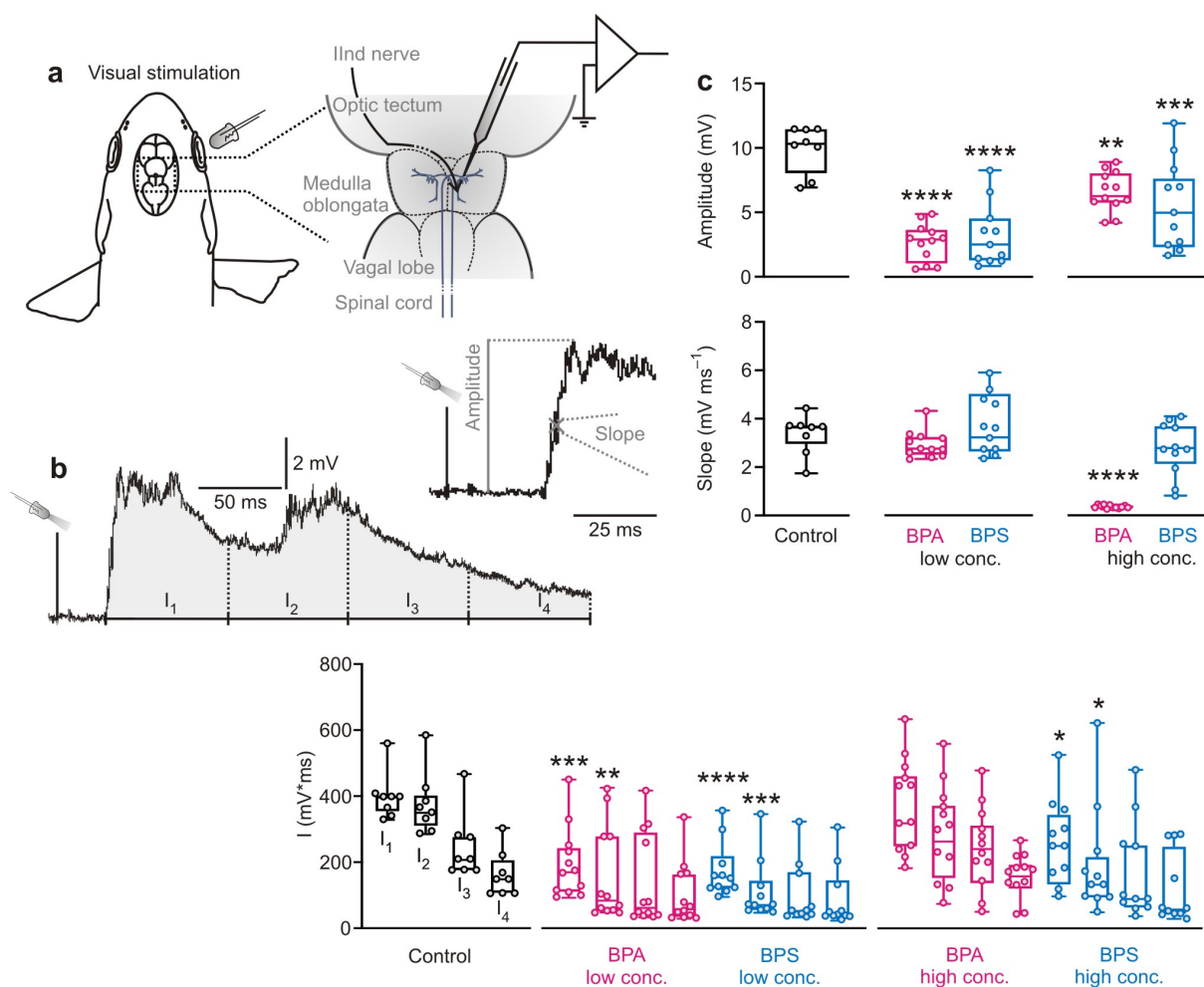


Fig. 4 Both BPA and BPS affect visual processing. **a** Sketch of experimental setting for visual stimulation to emphasize efficiency of the system: only stimulation needs to be changed, but recording is kept (cf. Fig. 2a and 3a). **b** shows an exemplary visually induced PSP from a control fish and how measurements were taken. **c** Both BPA and BPS affected the visually induced PSP. BPA and BPS significantly reduced its amplitude. BPA in high concentration (but not BPS) additionally reduced PSP slope. In contrast, after exposition to BPS and to low BPA concentration the beginning of the PSP (first 150 ms; I_1 and I_2) was reduced in area. Low conc. = $10 \mu\text{g L}^{-1}$; high conc. = 1 mg L^{-1} ; $N_{(\text{Control})} = 8$ independent samples; $N_{(10 \mu\text{g L}^{-1} \text{ BPA})} = 12$ independent samples; $N_{(1 \text{ mg L}^{-1} \text{ BPA})} = 12$ independent samples; $N_{(10 \mu\text{g L}^{-1} \text{ BPS})} = 11$ independent samples; $N_{(1 \text{ mg L}^{-1} \text{ BPS})} = 11$ independent samples; differently treated groups are indicated by colour; whiskers show the minimum and the maximum value, respectively; significant differences between groups and control are indicated by asterisk(s); * indicates $P < 0.05$; ** indicates $P \leq 0.01$; *** indicates $P \leq 0.001$; **** indicates $P \leq 0.0001$.

independent animal samples; $10 \leq n \leq 21$; one-way ANOVA: $F = 24.51$; $R^2 = 0.6788$; $P < 0.0001$; Dunnett test: mean diff.: 3.00; confidence interval of diff.: 2.04 to 3.96; $P < 0.0001$). BPA and BPS additionally affected the temporal integral of the PSPs (Fig. 4c; one-way ANOVA: $F = 11.43$; $R^2 = 0.4964$; $P < 0.0001$) with the first integral (of 75 ms duration) strongly decreased from $398.0 \pm 71.5 \text{ mV*ms}$ ($N = 8$ independent animal samples; $7 \leq n \leq 21$) in the control group to $169.5 \pm 107.8 \text{ mV*ms}$ with $10 \mu\text{g L}^{-1}$ BPA ($N = 12$ independent animal samples; $8 \leq n \leq 27$; Dunnett test: mean diff.: 205.4; confidence interval of diff.: 83.8 to 327.1; $P = 0.0003$), to $150.9 \pm 82.8 \text{ mV*ms}$ with $10 \mu\text{g L}^{-1}$ BPS ($N = 11$ independent animal samples;

$7 \leq n \leq 31$; Dunnett test: mean diff.: 227.1; confidence interval of diff.: 103.3 to 350.9; $P < 0.0001$) and to 250.0 ± 125.4 mV*ms with 1 mg L^{-1} BPS ($N = 11$ independent animal samples; $11 \leq n \leq 25$; Dunnett test: mean diff.: 134.3; confidence interval of diff.: 10.5 to 258.2; $P = 0.0293$).

Effects of EE2

For many of the varied non-neuronal effects of bisphenols their structural similarity with estrogens is crucial^{15,16,22}. A series of experiments was therefore aimed at exploring whether this might also apply, to some extent, to the strong neuronal effects we describe here. We therefore ran experiments just as with BPA and BPS (Figs. 2–4) and also with one month of exposure, but with fish exposed not to any bisphenols but to ethinyl estradiol (EE2) at a concentration of 1 mg L^{-1} . A full account of all results obtained in these experiments is given in Supplementary Table 1. Table 1 highlights all significant effects that we were able to detect with EE2 and compares their occurrence and direction with those we found after BPA and BPS exposition (at any concentration).

Substance	EE2	BPA	BPS
Effect on antidromically induced action potential			
Amplitude	↑		
Delay	↓		
Slope	↓	↓	↓
Area		↓	↓
1st DPs	↑	↑	
Effect on auditory induced PSPs			
Amplitude	↑	↑	↑
Delay		↓	↓
Slope		↓	
Area	↑	↑	↑
Effect on visually induced PSPs			
Amplitude	↓	↓	↓
Delay			
Slope		↓	
Area	↓	↓	↓

Based on data shown in Figs. 2-4 and Supplementary Table 1.
 ↓ Indicate a significant decrease in comparison to control and ↑ a significant increase; free fields represent values that have not changed significantly in comparison to control.

EE2 highly significantly increased action potential amplitude and shortened the delay after which an action potential followed after spinal cord stimulation, effects that we found neither with BPA nor BPS at any concentration. However, all other effects including their direction were strikingly similar as with the bisphenols. This might suggest that at least some of the neuronal effects of the bisphenols could also result from their similarity with estrogens.

Acute effects of BPA and BPS

One month of exposition to BPA or BPS at concentrations of $10 \mu\text{g L}^{-1}$ or 1mg L^{-1} , caused strong effects on all aspects of neuronal function. Our final series of experiments was therefore aimed at testing whether the effects required prolonged exposition or might at least partly be seen in acute experiments. In these, the tests shown in Figs. 2–4 were run for a total of 20 min in untreated fish, to establish baseline properties. Then either BPS ($N = 6$ independent animal samples) or BPA ($N = 7$ independent animal samples) was added so that the fish now faced a concentration of $10 \mu\text{g L}^{-1}$. After 10 min of incubation the 20 min stimulus program was run again. Subsequently the concentration of the respective bisphenol was increased to 1mg L^{-1} and an incubation of 10 min was allowed before the stimulus program was given. At the measurements at the higher concentration the fish had been exposed to bisphenol for a comparably brief time between 40 min (10 min at the high concentration plus 30 min at the lower concentration) and 60 min. The results of all three series (baseline, $10 \mu\text{g L}^{-1}$, 1mg L^{-1}) for both BPA and BPS are reported in detail in Supplementary Table 2. In none of the experiments did the acute exposition cause any significant deviations from baseline (RM one-way ANOVA: $F \leq 3.59$; $R^2 \leq 0.42$; $P \geq 0.07$). These findings therefore suggest that the strong neuronal effects seen after one month of exposure do not establish quickly after short exposure of only about one hour.

Discussion

Our *in vivo* recordings demonstrate strikingly strong and uncompensated effects of bisphenols on all aspects of neuronal function in the adult vertebrate brain, from the action potential, the balance between excitatory and inhibitory inputs to auditory and visual sensory circuits. Our findings have been obtained in a particularly accessible identified neuron in the mature vertebrate CNS, the Mauthner neuron of the goldfish. This neuron is particularly interesting for an analysis of whether effects of bisphenols could be buffered: Buffering should be particularly strong in this neuron, because its inputs and outputs are essential for driving life-saving escapes. Although the effects of bisphenols certainly vary between individual neurons and across species, our findings clearly establish that the effects of bisphenols on the nervous system are by no means restricted to developing brains. Rather, being exposed to either BPA or BPS at the environmentally relevant concentration^{2,43} of $10 \mu\text{g L}^{-1}$ for one month strongly affects neuronal function in the adult brain.

On the more optimistic side, our findings demonstrate that it is possible to quickly gain sensitive information on basic neuronal functions – from generation of the action potential, synaptic transmission to auditory and visual function – by using multisensory integration in identified neurons such as the Mauthner neuron as a powerful tool. Studying the postsynaptic potentials in response to acoustic or visual stimulation showed clear effects of both bisphenols on sensory systems and on central processing. Although it has been suggested that BPA damages sensory hair cells in fish and amphibia⁴², we find that BPA – surprisingly – increased the amplitude of acoustical PSPs and that BPS acted similarly. These effects could be explained by a strong effect of both BPA and BPS on excitatory synaptic transmission. However, our findings also demonstrate that not all synapses are equally potentiated: For instance, backfiring through the mixed synapses was strongly increased by BPA, but not affected by BPS. Furthermore, the visual PSPs were clearly reduced both after exposition to BPA or BPS, which would only for BPS be attributable to an effect on retinal function⁴⁴.

The strong effects we find here and the apparent lack of efficient buffering are alarming. The effects of bisphenols have previously been discussed mainly from a developmental point of view (causing the ban of BPA from baby products in some countries) or from its varied endocrinological effects. Now we face an additional danger whose effect on healthy humans and on patients with neurological deficits is difficult to foresee. Offsetting balances in brains is the basis of severe neurological disorders^{6,24,27,30,35,36} and so our findings must be taken very seriously. What is most needed, is an effort to develop a new generation of plasticizers

combined with an efficient but sufficiently broad and sensitive array of tests to quickly detect and sort out substances that bear large environmental and health risks^{5,11}. The tests we described here are particularly efficient and can quickly assay effects on neuronal functions. Together with similarly sensitive assays they could guide our way to the urgently needed next-generation plasticizers.

Methods

Animals and treatment. We used $N=98$ goldfish (*Carassius auratus*, Cypriniformes) of either sex with an average standard length of 69.5 ± 7.8 mm (range from 56.5 to 100 mm) and an average body weight of 10.3 ± 3.8 g (range from 6.7 to 20.8 g). The fish were obtained from an authorized specialist retailer (Aquarium Glaser GmbH, Rodgau, Germany). Prior start of the project fish were kept for at least 4 weeks in large glass tanks (250 x 50 x 50 (cm)) filled with fresh water (water conductivity: $300 \mu\text{S cm}^{-1}$; pH 7.5; total hardness of water: 7.7°dH ; $\text{NH}_4^+ < 10 \mu\text{g L}^{-1}$; $\text{NO}_2^- < 5 \mu\text{g L}^{-1}$; $\text{NO}_3^- < 5 \text{mg L}^{-1}$) at a water temperature of 20°C . Light/dark photoperiod was 12:12 h. Fish were fed once a day with common fish food (sera goldy; sera GmbH, Heinsberg, Germany). After this period of acclimatization and quarantine, fish were checked for disorders and for responsiveness to visual and acoustic stimuli. We only chose healthy and responsive fish for the experiment. They were divided randomly into experimental groups exposed either to bisphenol A (BPA; 4,4'-(propane-2,2-diyl)-diphenol), bisphenol S (BPS; 4,4'-sulfonyldiphenol) or to ethinyl estradiol (EE2; 17α -ethinyl-1,3,5(10)-oestratrien-3,17 β -diol). BPA and BPS were obtained in granular form from Sigma-Aldrich (Steinheim, Germany). EE2 was obtained in powder form from Merck KGaA (Darmstadt, Germany). For application, they were dissolved in dimethyl sulfoxide (DMSO), with a final DMSO concentration of 0.001% and added in required concentration to the water.

Two experimental groups (7 fish each) were used to test for acute effects of BPA and BPS. Fish of these groups were not exposed to plasticizer prior to experiment. However, during Mauthner neuron intracellular recording, we added plasticizer (BPA or BPS) so that the fish acutely faced either BPA or BPS. Thereby, we were able to collect robust data for two concentrations ($10 \mu\text{g L}^{-1}$ and 1mg L^{-1}) in $N=7$ fish of the BPA group and $N=6$ fish of the BPS group.

In six further groups (14 fish each), we tested for effects of BPA, BPS and EE2 after a month of exposition. Fish of these groups were, respectively, exposed either to $10 \mu\text{g L}^{-1}$ BPA, 1mg L^{-1} BPA, $10 \mu\text{g L}^{-1}$ BPS, 1mg L^{-1} BPS, 1mg L^{-1} EE2 or received only DMSO in the concentration used as dissolvent in the other groups. The latter group served as a control. By starting exposition at different times, experimental fish were exactly exposed to the respective chemical for 30 to 33 days. We were able to collect robust data in $N=13$ fish of the control group, $N=12$ fish of the $10 \mu\text{g L}^{-1}$ BPA group, $N=12$ fish of the 1mg L^{-1} BPA group, $N=11$ fish of the $10 \mu\text{g L}^{-1}$ BPS group, $N=11$ fish of the 1mg L^{-1} BPS group and $N=10$ fish of the 1mg L^{-1} EE2 group. Two fish exposed to EE2 died prior experiment in the third week of exposition. Animal care procedures, surgical procedures and experimental procedures were in

accordance with all relevant guidelines and regulations of the German animal protection law and explicitly approved by state councils (Regierung von Unterfranken, Würzburg, Germany).

Anesthesia and surgical procedure. Before starting surgery, the experimental fish was anaesthetized (2-phenoxyethanol in the concentration of 0.4 ml L^{-1}) for 15 min in the water it was used to. Anesthesia was maintained also during surgery and during recording and the protocol is known not to affect neuronal functionality nor the acoustical or the visual system of goldfish⁴⁵. To confirm sufficiency of anesthetization we carefully exerted pressure to the fish's caudal peduncle after the fish had lost equilibrium, which normally would trigger vigorous escapes. Only when this stimulation (and subsequent handling) yielded no response, the fish was positioned in the recording chamber and given artificial respiration with aerated, anesthetic loaded water flowing via a tube through the fish's mouth and out over the gills at a flow rate of 80 ml min^{-1} . Here, we also used water of the same quality as for housing. Respiration water was delivered to the fish from a reservoir using a suitably adjusted pump (EHEIM universal 300; EHEIM GmbH & Co. KG, Deizisau, Germany; regular power: 300 L h^{-1} , adjusted to 4.8 L h^{-1}).

Access to the Mauthner neurons was achieved by using a bone rongeur to open the skull from above in the area of the hindbrain. To expose the medulla oblongata containing the pair of Mauthner neurons, the cerebellum was lifted up with a piece of filter paper and fixed in place. To stimulate the axons of the two Mauthner neurons we additionally exposed a piece of the spinal column (about 5 mm in length) from the side in the region of the trunk (between 20 and 25 mm caudal from the position of the Mauthner somata) and confirmed suprathreshold stimulation of the Mauthner axons from the characteristic twitching of the experimental animal. To prepare for the intracellular *in vivo* recording the experimental animal was then immobilized by injecting d-tubocurarine ($1 \mu\text{g g}^{-1}$ body weight; Sigma-Aldrich, Steinheim, Germany) in the core muscles. After finishing measurements, the experimental animal was sacrificed immediately and without recovery from anesthesia by mechanically destroying the brain. Finally, a necropsy was performed to check for any unnoticed diseases of inner organs. This confirmed that all fish of this study were healthy.

Experimental procedure. For intracellular recordings, we used a bridge-mode amplifier (BA-01X; npi electronic GmbH, Tamm, Germany) in current clamp mode. Recording electrodes were pulled from 3 mm-glass capillaries (G-3; Narishige Scientific Instrument Lab, Tokyo,

Japan) using a vertical electrode puller (PE-22; Narishige International Limited, London, UK). Filled with 5 M potassium acetate, they had a resistance between 4 and 7 M Ω . For moving and positioning the recording electrode, we used a motorized micromanipulator (MP-285; Sutter Instrument, Novato, CA, USA). We used established techniques to determine recording position from extracellular space and to ensure recordings are always taken in the soma of the Mauthner neuron⁴⁶. The reference electrode was positioned in muscle tissue. Recordings were filtered (Hum Bug Noise Eliminator; Quest Scientific, North Vancouver, BC, Canada) and then digitized at the sample rate of 50 kHz using an A/D converter (Micro1401; Cambridge Electronic Design Limited, Cambridge, UK) and the acquisition software package Spike2 (version 6; Cambridge Electronic Design Limited, Cambridge, UK). For data analysis, we used custom-made software written in Python. After localization and identification of one of the two Mauthner neurons using well-established techniques^{37,46} and after establishing a stable intracellular recording of the Mauthner neuron we applied a set of stereotyped stimuli to elicit Mauthner neuron responses. A set of stimuli, as designed for the present study, contained repeated antidromic activation of the Mauthner neuron and repeated acoustic and visual stimulation of the fish. Each of the stereotyped stimuli was consecutively presented to the fish at least 40 times per set. In total, presentation took about 20 min. To ensure stable intracellular recording, we continuously monitored the resting potential of the Mauthner neuron. In all cases, deviations were far less than our criterion (5%). We used electrical pulses (pulse duration: 10 μ s; stimulation rate: 2 Hz) applied to the spinal cord to activate the Mauthner neuron antidromically. The electric pulses were delivered by a constant-voltage isolated stimulator (DS2A2 – Mk.II; Digitimer Ltd., Hertfordshire, UK). The desired pulse amplitude for antidromic stimulation was determined by first reducing amplitude until antidromic stimulation did not activate the Mauthner neuron anymore. Then amplitude was increased by 5 V above threshold. In the current study pulse amplitude for antidromic stimulation ranged from 15 to 40 V. Next, we tested the processing of sensory information in the Mauthner neuron. For acoustic stimulation, we used a multifunctional active loudspeaker (The box pro Achat 115 MA; Thomann GmbH, Burgebrach, Germany). The loudspeaker generated a short acoustical broadband pulse (duration: 1 ms; frequency distribution from 25 to 1000 Hz; peak amplitude at 300 Hz) with a sound pressure level (SPL) of 145 dB *re* 1 μ Pa. We measured SPL under water at the position of the fish in the recording chamber with a hydrophone (Type 8106; Brüel & Kjær, Nærum, Denmark). For visual stimulation, we used a light emitting diode (LED; RS Components GmbH, Mörenfelden-Walldorf, Germany), which was positioned directly in front of the ipsilateral eye. The light flash used for visual stimulation had a duration of 7 ms. LED

peak radiation at 569 nm was $700 \mu\text{W m}^{-2} \text{nm}^{-1}$ and the width at $100 \mu\text{W m}^{-2} \text{nm}^{-1}$ was 56 nm (range: 543 to 599 nm).

In experiments on the acute effect of plasticizers, each fish was given the set of stimuli three times. The first set of stimuli was presented 10 min after establishing intracellular Mauthner neuron recording and before adding any plasticizer and served to establish a baseline. Next, we added plasticizer (either BPA or BPS) to the water to reach a concentration of $10 \mu\text{g L}^{-1}$. After an incubation period of 10 min we recorded Mauthner neuron responses to our set of stimuli again. Then, we increased the concentration to 1mg L^{-1} , again gave 10 min for incubation before taking the final measurement. In total, all measurements were completed within 90 min of intracellular recording, and the maximum time any bisphenol could have acted in our acute experiments was 60 min. In fish exposed for a month to either BPA, BPS or EE2 we presented our set of stimuli 10 min after establishing intracellular Mauthner neuron recording only once. Per fish we needed 30 min of intracellular recording.

Statistics and Reproducibility. Statistical tests were run using the software package GraphPad Prism 8.2.1 (GraphPad Software, Inc., La Jolla, CA, USA) and performed two-tailed with $\alpha = 0.05$. Averages are reported as median \pm standard deviation. N denotes the number of independent animal samples, n the number of measurements per animal. When data from animals were pooled, we never used the measurement repetitions (n) taken from the individual animals, but a single averaged value for each animal. To determine whether there are acute effects of BPA and BPS, we used RM one-way ANOVAs. To determine whether there is an effect of one month exposure to BPA or BPS in comparison to the control group, we performed one-way ANOVAs and the Dunnett test for comparing each group with control. To determine whether there is an effect of one month exposure to EE2 in comparison to the control group, we performed unpaired t tests. Rate constants of exponential decay were compared using one-way ANOVA and Dunnett test. Differences in occurrence (in %) were compared using the Wilcoxon test with occurrence for control set as hypothetical value. To test whether there are correlations between action potential amplitude and DP amplitude and between DP amplitudes, we used Spearman tests. To test whether data is distributed normally, we used the Shapiro-Wilk test.

References

1. Chen, D. et al. Bisphenol analogues other than BPA: environmental occurrence, human exposure, and toxicity – a review. *Environ. Sci. Technol.* **50**, 5438–5453 (2016).
2. Wu, L.-H. et al. Occurrence of bisphenol S in the environment and implications for human exposure: a short review. *Sci. Total Environ.* **615**, 87–98 (2018).
3. Li, J. et al. Transformation of bisphenol AF and bisphenol S by permanganate in the absence/presence of iodide: kinetics and products. *Chemosphere* **217**, 402–410 (2019).
4. Glausiusz, J. The plastics puzzle. *Nature* **508**, 306–308 (2014).
5. Zimmerman, J. B. & Anastas, P. T. Toward substitution with no regrets. *Science* **347**, 1198–1199 (2015).
6. Tshala-Katumbay, D., Mwanza, J.-C., Rohlman, D. S., Maestre, G. & Oria, R. B. A global perspective on the influence of environmental exposures on the nervous system. *Nature* **527**, S187–S192 (2015).
7. Hermabessiere, L. et al. Occurrence and effects of plastic additives on marine environments and organisms: A review. *Chemosphere* **182**, 781–793 (2017).
8. Hahladakis, J. N., Velis, C. A., Weber, R., Iacovidou, E. & Purnell, P. An overview of chemical additives present in plastics: Migration, release, fate and environmental impact during their use, disposal and recycling. *J. Hazard. Mater.* **344**, 179–199 (2018).
9. Kaiser, J. Controversy continues after panel rules on bisphenol A. *Science* **317**, 884–885 (2007).
10. Borrell, B. The big test for bisphenol A. *Nature* **464**, 1122–1124 (2010).
11. Fagin, D. The learning curve. *Nature* **490**, 462–465 (2012).
12. Flint, S., Markle, T., Thompson, S. & Wallace, E. Bisphenol A exposure, effects, and policy: a wildlife perspective. *J. Environ. Manag.* **104**, 19–34 (2012).
13. Vandenberg, L. N. et al. Urinary, circulating, and tissue biomonitoring studies indicate widespread exposure to bisphenol A. *Environ. Health Persp.* **118**, 1055–1070 (2010).
14. Jiang, D., Chen, W.-Q., Zeng, X. & Tang L. Dynamic stocks and flows analysis of bisphenol A (BPA) in China: 2000–2014. *Environ. Sci. Technol.* **52**, 3706–3715 (2018).
15. Howdeshell, K. L., Hotchkiss, A. K., Thayer, K. A., Vandenberg, J. G. & vom Saal, F. S. Exposure to bisphenol A advances puberty. *Nature* **401**, 763–764 (1999).

16. Heindel, J. J., Newbold, R. & Schug, T. T. Endocrine disruptors and obesity. *Nat. Rev. Endocrinol.* **11**, 653–661 (2015).
17. Choi, Y. J. & Lee, L. S. Aerobic soil biodegradation of bisphenol (BPA) alternatives bisphenol S and bisphenol BPAF compared to BPA. *Environ. Sci. Technol.* **51**, 13698–13704 (2017).
18. Helies-Toussaint, C., Peyre, L., Costanzo, C., Chagnon, M. C. & Rahmani, R. Is bisphenol S a safe substitute for bisphenol A in terms of metabolic function? An in vitro study. *Toxicol. Appl. Pharmacol.* **280**, 224–235 (2014).
19. Rosenmai, A. K., Dybdahl, M., Pedersen, M., van Vugt-Lussenburg, B. M., Wedebye, E. B., Taxvig, C. & Vinggaard, A. M. Are structural analogues to bisphenol A safe alternatives? *Toxicol. Sci.* **139**, 35–47 (2014).
20. Kinch, C. D., Ibhazhiebo, K., Jeong, J.-H., Habibi, H. R. & Kurrasch, D. M. Low-dose exposure to bisphenol A and replacement bisphenol S induces precocious hypothalamic neurogenesis in embryonic zebrafish. *PNAS* **112**, 1475–1480 (2015).
21. Yamazaki, E., Yamashita, N., Taniyasu, S., Lam, J., Lam, P. K. S., Moon, H.-B., Jeong, Y., Kannan, P., Achyuthan, H., Munuswamy, N. & Kannan K. Bisphenol A and other bisphenol analogues including BPS and BPF in surface water samples from Japan, China, Korea and India. *Ecotox. Environ. Savety* **122**, 565–572 (2015).
22. Kolla, S., McSweeney, D. B., Pokharel, A. & Vandenberg, L. N. Bisphenol S alters development of the male mouse mammary gland and sensitizes it to a peripubertal estrogen challenge. *Toxicology* **424**, 152234 (2019).
23. Zhang, X., Li, C., Pan, J., Liu, R. & Cao, Z. Searching for a bisphenol A substitute: effects of bisphenols on catalase molecules and human red blood cells. *Sci. Total Environ.* **669**, 112–119 (2019).
24. Salahinejad, A. et al. Effects of chronic exposure to bisphenol-S on social behaviors in adult zebrafish: Disruption of the neuropeptide signaling pathways in the brain. *Environ. Pollut.* **262**, 113992 (2020).
25. Guo, H., Li, H., Liang, N., Chen, F., Liao S., Zhang, D., Wu, M. & Pan, B. Structural benefits of bisphenol S and its analogs resulting in their high sorption on carbon nanotubes and graphite. *Environ. Sci. Pollut. Res.* **23**, 8976–8984 (2016).

26. Fang, Z., Gao, Y., Wu, X., Xu, X., Sarmah, A. K., Bolan, N., Gao, N., Gao, B., Shaheen, S. M., Rinklebe, J., Ok, Y. S., Xu, S. & Wang, H. A critical review on remediation of bisphenol S (BPS) contaminated water: efficiency and mechanisms. *Crit. Rev. Environ. Sci Tech.* **50**, DOI: 10.1080/10643389.2019. 1629802 (2020).
27. Saili, K. S. et al. Neurodevelopmental low-dose bisphenol A exposure leads to early life-stage hyperactivity and learning deficits in adult zebrafish. *Toxicology* **291**, 83–92 (2012).
28. Gu, J. et al. Neurobehavioral effects of bisphenol S exposure in early life stages of zebrafish larvae (*Danio rerio*). *Chemosphere* **217**, 629–635 (2019).
29. Kim, S. S. et al. Neurochemical and behavioral analysis by acute exposure to bisphenol A in zebrafish larvae model. *Chemosphere* **239**, 124751 (2019).
30. Naderi, M., Salahinejad, A., Attaran, A., Chivers, D. P. & Niyogi, S. Chronic exposure to environmentally relevant concentrations of bisphenol S differently affects cognitive behaviors in adult female zebrafish. *Environ. Pollut.* **261**, 114060 (2020).
31. Davis, G. W. Homeostatic signaling and the stabilization of neural function. *Neuron* **80**, 718–728 (2013).
32. Keck, T., Keller, G. B., Jacobsen, R. I., Eysel, U. T., Bonhoeffer, T. & Hübener, M. Synaptic scaling and homeostatic plasticity in the mouse visual cortex in vivo. *Neuron* **80**, 327–334 (2013).
33. Zhou, R., Bai, Y., Yang, R., Zhu, Y., Chi, X., Li, L., Chen, L., Sokabe, M. & Chen, L. Abnormal synaptic plasticity in basolateral amygdala may account for hyperactivity and attention-deficit in male rat exposed perinatally to low-dose bisphenol-A. *Neuropharm.* **60**, 789–798 (2011).
34. Hu, F., Li, T., Gong, H., Chen, Z., Jin, Y. et al. Bisphenol A impairs synaptic plasticity by both pre- and postsynaptic mechanisms. *Adv. Sci.* **4**, 1600493 (2017).
35. Ramocki, M. B. & Zoghbi, H. Y. Failure of neuronal homeostasis results in common neuropsychiatric phenotypes. *Nature* **455**, 912–918 (2008).
36. Nelson, S. B. & Valakh, V. Excitatory/inhibitory balance and circuit homeostasis in autism spectrum disorders. *Neuron* **87**, 684–698 (2015).
37. Furshpan, E. J. & Furukawa, T. Intracellular and extracellular responses of the several regions of the Mauthner cell of goldfish. *J. Neurophysiol.* **25**, 732–771 (1962).

38. Korn, H. & Faber, D. S. The Mauthner cell half a century later: a neurobiological model for decision-making? *Neuron* **47**, 13–28 (2005).
39. Sillar, K. T., Picton, L. D. & Heitler, W. J. Fish Escape: the Mauthner System in *The Neuroethology of Predation and Escape* (eds Sillar, K. T., Picton, L. D. & Heitler, W. J.) 212–243 (Wiley Blackwell, 2016).
40. Hecker, A., Schulze, W., Oster, J., Richter, D. O. & Schuster, S. Removing a single neuron in a vertebrate brain forever abolishes an essential behavior. *PNAS* **117**, 3254–3260 (2020).
41. Pereda, A. E., Bell, T. D. & Faber, D. S. Retrograde synaptic communication via gap junctions coupling auditory afferents to the Mauthner cell. *J. Neurosci.* **15**, 5943–5955 (1995).
42. Hayashi, L., Sheth, M., Young, A., Kruger, M., Wayman, G. A. & Coffin, A. B. The effect of the aquatic contaminants bisphenol-A and PCB-95 on the zebrafish lateral line. *NeuroToxicology* **46**, 125–136 (2015).
43. Corrales, J., Kristofco, L. A., Steele, W. B., Yates, B. S., Breed, C. S., Williams, E. S. & Brooks, B. W. Global assessment of bisphenol A in the environment: review and analysis of its occurrence and bioaccumulation. *Dose-Response* **13**, 1–29 (2015).
44. Liu, W., Zhang, X. Wei, P., Tian, H., Wang, W. & Ru, S. Long-term exposure to bisphenol S damages the visual system and reduces the tracking capability of male zebrafish (*Danio rerio*). *J. Appl. Toxicol.* **38**, 248–258 (2018).
45. Machnik, P., Schirmer, E., Glück, L. & Schuster, S. Recordings in an integrating central neuron provide a quick way for identifying appropriate anaesthetic use in fish. *Sci. Rep.* **8**, 17541 (2018).
46. Machnik, P., Leupolz, K., Feyl, S., Schulze, S. & Schuster, S. The Mauthner cell in a fish with top-performance and yet flexibly tuned C-starts II. Physiology. *J. Exp. Biol.* **221**, <https://doi.org/10.1242/jeb.175588> (2018).
47. Furshpan, E. J. Electrical transmission at an excitatory synapse in a vertebrate brain. *Science* **144**, 878–880 (1964).

Acknowledgements

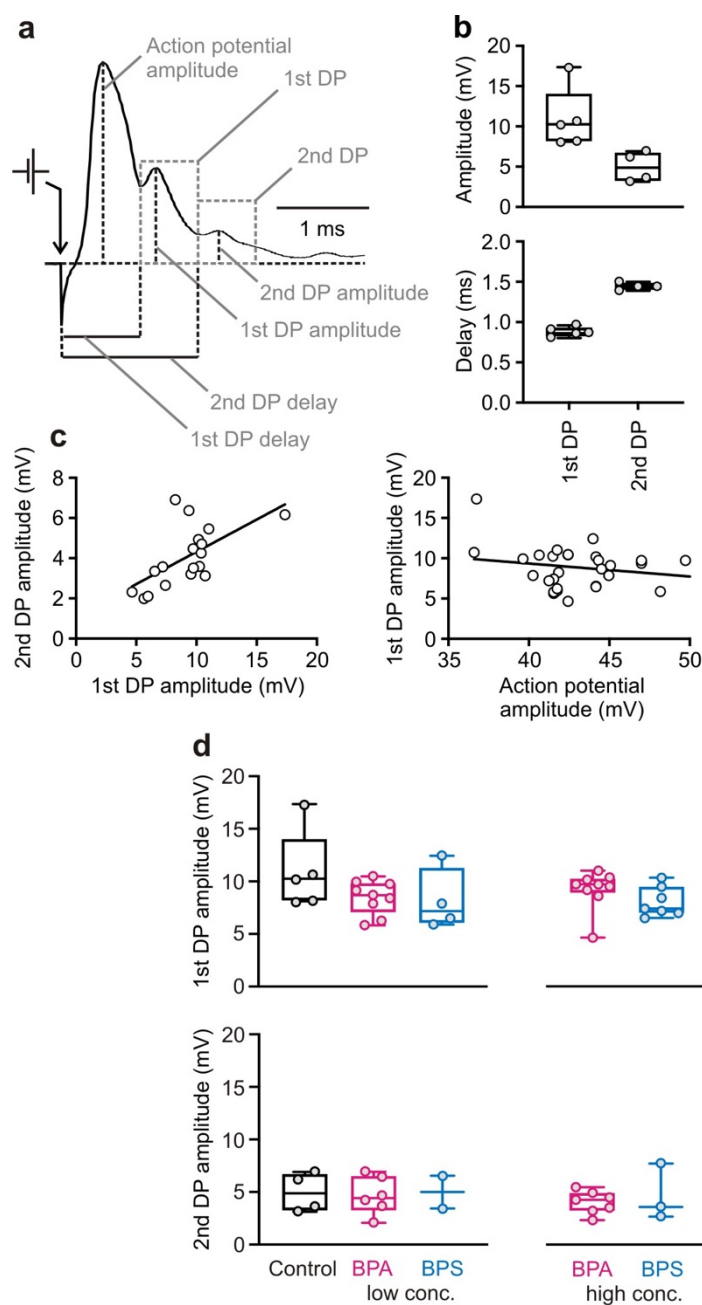
The study was funded by a Reinhart Koselleck-project (Schu1470/8) of the Deutsche Forschungsgemeinschaft (German Research Foundation). We would like to thank Dr. Wolfram Schulze for help and for writing software, Antje Halwas for excellent technical support and Mercedes Hildebrandt, Florian Gerstner, Elisa Mendez-Montilla, Nastaran Biazar and Carina Weigel for assistance in electrophysiological measurements and data analysis.

Author Contributions

E.S., S.S. and P.M. designed experimental procedures. E.S. and P.M. performed and analyzed experiments; E.S., S.S. and P.M. wrote the manuscript.

Additional Information

Supplementary Information



Supplementary Fig. 1 Effects of BPA and BPS on neuronal backfiring. **a** shows an exemplary action potential accompanied by delayed potentials (DPs) with illustration of how measurements were taken. **b** In controls, first DPs had on average an amplitude of 10.3 ± 3.8 mV ($N = 5$ independent samples; $n = 9$ to 31 measurements per fish) and followed 0.86 ± 0.06 ms after onset of the action potential. Second DPs had on average an amplitude of 4.9 ± 1.9 mV ($N = 4$ independent samples; $n = 9$ to 31) and followed 1.44 ± 0.05 ms after action potential onset. **(c)** The amplitude of the 2nd DP correlates with the amplitude of the first ($N = 20$ independent samples; $9 \leq n \leq 114$; Spearman correlation: $P = 0.01$), the amplitude of the 1st DP and the amplitude of the action potential do not correlate ($N = 33$ independent samples; $9 \leq n \leq 114$; Spearman correlation: $P = 0.45$). **(d)** Both BPA and BPS (in any concentration) did not affect the amplitude of the DPs (one-way ANOVA: $F \leq 1.54$; $R^2 \leq 0.18$; $P \geq 0.22$). Whiskers show the minimum and the maximum value, respectively.

Supplementary Table 1: Comparison of EE2 group and control				
	Median \pm SD		Unpaired t test	
	Control	EE2	t	P
Action potential				
Amplitude (mV)	41.4 \pm 4.9	44.7 \pm 2.7	2.453	0.0240
Delay (ms)	0.20 \pm 0.03	0.15 \pm 0.02	4.813	0.0001
Slope (V ms ⁻¹)	2.13 \pm 0.33	0.82 \pm 0.32	8.388	<0.0001
Area I ₁ (mV*ms)	23.8 \pm 3.1	23.1 \pm 1.1	0.339	0.7384
	<i>N</i> = 13	<i>N</i> = 10		
	9 $\leq n \leq$ 31	81 $\leq n \leq$ 110		
Acoustically induced PSP				
Amplitude (mV)	7.1 \pm 1.4	11.5 \pm 2.5	5.128	<0.0001
Delay (ms)	7.71 \pm 0.28	7.76 \pm 0.30	0.437	0.6664
Slope (mV ms ⁻¹)	10.01 \pm 2.66	10.76 \pm 3.26	0.899	0.3787
Area I ₁ (mV*ms)	117.5 \pm 32.1	160.4 \pm 38.4	2.543	0.0189
Area I ₂ (mV*ms)	104.7 \pm 20.2	111.6 \pm 21.7	1.427	0.1683
	<i>N</i> = 13	<i>N</i> = 10		
	8 $\leq n \leq$ 29	33 $\leq n \leq$ 56		
Visually induced PSP				
Amplitude (mV)	10.4 \pm 1.8	2.1 \pm 1.4	10.22	<0.0001
Delay (ms)	30.0 \pm 4.9	30.69 \pm 5.3	0.276	0.7865
Slope (mV ms ⁻¹)	3.66 \pm 0.82	2.52 \pm 0.69	1.926	0.0710
Area I ₁ (mV*ms)	398.0 \pm 71.5	131.4 \pm 47.6	10.33	<0.0001
Area I ₂ (mV*ms)	357.1 \pm 95.6	90.3 \pm 68.0	7.173	<0.0001
	<i>N</i> = 8	<i>N</i> = 10		
	7 $\leq n \leq$ 21	9 $\leq n \leq$ 26		
Bold type highlights significant results. <i>N</i> denotes the number of independent animal samples, <i>n</i> the number of measurements per animal.				

Supplementary Table 2: Data suggesting that the strong effects of BPA and BPS do not occur after short exposition of less than 1 hour.						
BPA	Median \pm SD			RM one-way ANOVA		
	0 $\mu\text{g L}^{-1}$	10 $\mu\text{g L}^{-1}$	1000 $\mu\text{g L}^{-1}$	F	R ²	P
Action potential						
Amplitude (mV)	43.9 \pm 5.6	42.8 \pm 3.8	42.6 \pm 4.7	1.55	0.21	0.25
Delay (ms)	0.22 \pm 0.03	0.21 \pm 0.02	0.22 \pm 0.02	1.16	0.16	0.35
Slope (V ms ⁻¹)	1.80 \pm 0.49	1.81 \pm 0.51	1.80 \pm 0.55	1.35	0.18	0.30
Area I ₁ (mV*ms)	21.7 \pm 2.9	21.6 \pm 2.2	21.8 \pm 2.2	1.18	0.16	0.34
Acoustically induced PSP						
Amplitude (mV)	9.0 \pm 2.5	9.1 \pm 2.5	8.6 \pm 2.6	3.35	0.40	0.09
Delay (ms)	7.50 \pm 0.11	7.52 \pm 0.12	7.49 \pm 0.12	0.22	0.04	0.81
Slope (mV ms ⁻¹)	9.23 \pm 2.55	8.53 \pm 2.45	8.95 \pm 2.17	3.59	0.42	0.07
Area I ₁ (mV*ms)	132.4 \pm 35.8	126.3 \pm 35.9	125.7 \pm 38.9	2.04	0.25	0.20
Area I ₂ (mV*ms)	109.7 \pm 26.1	102.8 \pm 26.5	100.0 \pm 30.8	3.30	0.35	0.11
Visually induced PSP						
Amplitude (mV)	8.5 \pm 4.2	8.8 \pm 2.9	7.1 \pm 2.6	0.93	0.16	0.43
Delay (ms)	28.28 \pm 4.59	29.24 \pm 4.84	29.48 \pm 4.47	2.90	0.33	0.09
Slope (mV ms ⁻¹)	2.85 \pm 2.28	3.14 \pm 2.06	2.95 \pm 2.12	1.58	0.24	0.25
Area I ₁ (mV*ms)	325.4 \pm 73.1	312.0 \pm 75.1	299.9 \pm 66.7	2.37	0.28	0.14
Area I ₂ (mV*ms)	190.8 \pm 147.4	190.7 \pm 98.4	189.0 \pm 65.1	2.20	0.31	0.16
BPS	Median \pm SD			RM one-way ANOVA		
	0 $\mu\text{g L}^{-1}$	10 $\mu\text{g L}^{-1}$	1000 $\mu\text{g L}^{-1}$	F	R ²	P
Action potential						
Amplitude (mV)	43.7 \pm 5.4	43.3 \pm 4.5	42.4 \pm 4.5	0.57	0.10	0.58
Delay (ms)	0.20 \pm 0.04	0.20 \pm 0.04	0.20 \pm 0.03	0.17	0.03	0.84
Slope (V ms ⁻¹)	1.95 \pm 0.36	1.99 \pm 0.29	1.99 \pm 0.25	0.48	0.09	0.63
Area I ₁ (mV*ms)	21.3 \pm 3.2	21.0 \pm 2.9	21.1 \pm 2.5	0.13	0.02	0.88
Acoustically induced PSP						
Amplitude (mV)	9.6 \pm 2.7	9.3 \pm 2.8	9.7 \pm 2.7	0.97	0.16	0.41
Delay (ms)	8.4 \pm 1.6	7.9 \pm 0.8	7.9 \pm 0.4	0.73	0.16	0.48

Slope (mV ms ⁻¹)	9.40 ± 3.80	9.03 ± 3.13	9.33 ± 3.04	2.29	0.31	0.15
Area I ₁ (mV*ms)	125.6 ± 44.2	122.3 ± 35.4	117.5 ± 31.8	0.49	0.09	0.62
Area I ₂ (mV*ms)	108.5 ± 23.7	108.8 ± 19.2	112.7 ± 22.1	0.15	0.03	0.86
Visually induced PSP						
Amplitude (mV)	8.1 ± 2.6	9.3 ± 2.2	8.7 ± 2.5	0.03	0.01	0.96
Delay (ms)	27.84 ± 2.61	28.20 ± 2.47	28.26 ± 1.74	0.09	0.01	0.92
Slope (mV ms ⁻¹)	3.29 ± 0.65	3.32 ± 0.64	3.26 ± 0.61	1.57	0.28	0.27
Area I ₁ (mV*ms)	319.1 ± 118.6	324.7 ± 104.5	330.1 ± 102.2	0.43	0.08	0.66
Area I ₂ (mV*ms)	247.9 ± 140.2	255.7 ± 155.2	290.0 ± 160.1	2.36	0.37	0.16

9. Chapter 3

9.1 Histology-linked MALDI mass spectrometry imaging workflow for *Danio rerio* and *Daphnia magna*

Elisabeth Schirmer, Sven Ritschar, Christian Laforsch, Stefan Schuster and Andreas Römpp

Abstract

Lipids play various essential roles in the function of animals. It is therefore crucial to understand to which extent animals can stabilize their lipid composition in the presence of external stressors, such as environmental chemicals. Here, we combine MALDI mass spectrometry imaging and spatially highly resolved histology, down to subcellular resolution, to examine if changes in the lipid content and distribution can be used as potential assay to detect effects of environmental chemicals. Specifically, we present a histology directed MALDI MSI workflow for two aquatic model organisms, the zebrafish *Danio rerio* and waterflea *Daphnia magna*. In zebrafish we demonstrate that a detailed mapping between histology and simultaneously determined lipid composition is possible at various scales, from extended structures such as the brain or gills down to subcellular structures such as a single axon in the central nervous system. For *D. magna* we present a MALDI MSI workflow, that demonstrably maintains tissue integrity during cryosectioning of non-preserved samples, and further provides a spatial resolution of lipids in the entire body and the brood chamber inside the carapace. In conclusion, the observed lipid signatures are an ideal basis to analyse changes caused by pollutants in two key aquatic model organisms.

Introduction

The pollution not only in marine but also in freshwater ecosystems rises due to increasing amount of chemicals in use today¹. On particular concern are lipophilic substances affecting the physiological homeostasis of aquatic organisms, mainly by disruption of the lipid content². Considering, that lipids are one of the fundamental compounds necessary for the tissue architecture and its function³ it is not surprising that changes in lipid pattern are often correlated with pathological processes^{4,5}. Hence, there is a need to understand how the lipid content and distribution reacts to chemical stressors. This requires not only the identification but also the localization of the referring compounds. Moreover, the lipid signature gained in normal healthy tissue could thereby function as a marker^{6,7} for comparison with pollutant-exposed tissue by detecting changes and the resulting physiological outcomes. MALDI mass spectrometry imaging is an analytical tool to compete with the challenging task of analyzing the molecular content of complex biological samples. This technique is capable of visualizing the distribution of lipids in thin tissue sections. Moreover, due to technological improvements like high-resolution mass spectrometers and increased spatial resolution^{8,9}, even challenging tasks like the investigation of single cells were successfully overcome^{10,11}. Compared to traditional biochemical methods including histochemistry or immunohistochemistry, MSI generates a similar, compound-specific distribution map¹². In contrast, MSI can detect a broad range of unknown compounds even without prior knowledge and is not limited to a specific number¹². MALDI MSI offers the possibility to obtain molecular and spatial resolution of a wide range of compounds in one tissue section, which can further be compared with anatomical features delivering a more detailed view^{13,14}. The advantage of a histology directed MSI workflow could be already demonstrated in mice brain tissue. Its complex morphology could be clearly visualized by different lipid distributions and paved the way for studies evaluating the outcomes of lipid changes in specific brain structures¹⁵. Furthermore, rodent models were used to demonstrate that some environmental contaminants (e.g. bisphenols) not only affect neuronal but also non-neuronal compartments⁶. However, information about the impact on the detailed spatial lipid distribution in aquatic organisms is still lacking (Fig. 1), although aquatic ecosystems are highly affected natural systems. Environmental chemicals are released by industry, agriculture and even household and can enter aquatic ecosystems in different ways. The zebrafish (*Danio rerio*) and the waterflea *Daphnia magna* are two widely used aquatic model organism in the field of environmental science and ecotoxicology^{16,17,18}. The use of *D. rerio* represents an excellent compromise between complexity and practical simplicity and further allows also conclusions for both, animal and human health¹⁹.

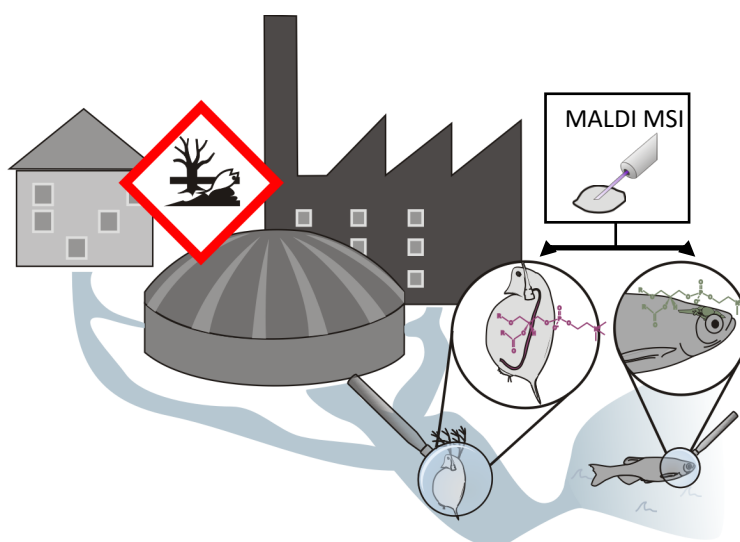


Figure 1. Lipid distribution within aquatic organisms can be affected by environmental pollution.

Chemical pollutants released into aquatic ecosystems mainly through industrial sewage or wastewater treatment can influence homeostatic processes in aquatic organisms such as *D. rerio* and *D. magna*, which manifests in the distribution of lipid species in tissue. MALDI MS imaging is an analytical technique capable of visualizing the distribution of lipids in thin tissue sections.

Beside its high availability, easy handling and husbandry, the small size offers the opportunity to investigate the lipid distribution in neuronal and non-neuronal compartments in one measurement. Further, *D. rerio* offers the unique possibility to examine the lipid distribution next to a central command neuron. This can be clearly identified due to its morphological characteristics as its soma and axon exceed in size compared to other neurons in the vertebrate central nervous system²⁰. Studies within this neuron already enabled the investigation of neuronal key functions under exposure of environmental contaminants⁴⁰ and its spatial localization within a tissue section could be further function to examine the spatial distribution of those contaminants, allowing further conclusion about the neuronal impact. The filter feeder *Daphnia* on the other hand is a key-stone species in the food web of nearly every lentic aquatic habitat, as it serves as a link between autotrophic algae and consumers of higher trophic levels, such as fish²¹. Due to its global distribution, easy cultivation and its clonal reproduction, the genus *Daphnia* is frequently used for research in environmental toxicology. Especially *D. magna* is a well-established organism for eco-toxicological testing (OECD, 2012) and was added by the American National Institute of Health (NIH) to their list of model organisms for biomedical research^{17,18}. *D. magna* provides a biological system with a high sensitivity for the detection of even weak effects to a wide range of pollutants on various levels reaching from life-history²² to physiology and molecular effects^{23,24}. For *Daphnia*, it is already described, that the lipidome is impacted by environmental factors like food quality²⁴ or pollutants²⁵. However,

to date it is not known how environmental stressors affect lipid composition and spatial distribution of lipids in different tissues.

Here, we used technological improvements in MALDI MSI to establish a histology directed sample preparation workflow for correlating lipid patterns with anatomical features of neuronal and non-neuronal compartments in two model organisms, *D. rerio* and *D. magna*. For *D. rerio*, we could thereby overcome limitations of solely localizing different compartments within tissue sections by adding a more detailed view for the analyzed regions. Additionally, we expanded our workflow from the fine analysis of organs to cellular resolution by localizing the command neuron. Cryosectioning of non-preserved *D. magna* individuals remained until now a challenging task due to the calcified exoskeleton²⁶. In our study, we show for the first time a suitable workflow inter alia for ensuring tissue integrity during cryosectioning for the visualization of the lipid distribution within different tissues of *D. magna* by MALDI MSI. The observed lipid pattern in *D. magna* and *D. rerio* may serve as marker for future analysis of changes in lipid signatures after exposure to environmental contaminants.

Results and Discussion

Adjusted histology-directed MALDI MSI workflow for *D. rerio* and *D. magna*.

MALDI MSI is a molecular imaging technique capable of identifying and localizing lipids within biological tissue¹³. Spatial resolution of the compounds visualizing precise structures of different compartments allows a deeper insight in the molecular network, its dynamic interaction and will in future function to analyze the reaction to chemical stressors like environmental chemicals. The clear differentiation of anatomical features within different tissue types thereby puts an emphasis on the sample preparation and handling to maintain equal lipid distribution in the tissue section *in vitro*, as it was *in vivo*.

Workflow for the precise analysis of (non)-neuronal compartments in D. rerio:

Fig. 2 a shows the histology directed MALDI MSI workflow for the precise analysis of neuronal and non-neuronal compartments in *D. rerio*. As this paper should function as basis for future studies evaluating the effect of environmental contaminants, focus was put on compartments contributing either as the main route of exposure (e.g. gills, eye) or being dependent on blood perfusion and transport to be potentially affected (e.g. brain, liver). Prior sample preparation we recommend the use of 2-phenoxyethanol for euthanizing, as it reduces stress response in the animal. This could otherwise in turn affect the lipid content, which may differ from normal conditions observed *in vivo*. To maintain the fine anatomical structures in the neuronal and non-neuronal anatomical compartments, tissue embedding using CMC was sufficient to clearly correlate lipid signatures with anatomical features in the sagittal prepared sections and will be discussed in detail below (Fig. 3). Matrix application for MALDI imaging experiments were carried out by applying para-nitroaniline (pNA) on the sample. The matrix was chosen for its superior performance in lipid imaging²⁷, especially in retinal tissue parts. MALDI MSI experiments for those sagittal cryosections were carried out at 25 μm step size.

Workflow for the spatial localization of a central command neuron in D. rerio:

In contrast to the sagittal fish sections, sample preparation for brain slices required a more precise and careful handling (Fig. 2 b). Maintaining the delicate neuronal structure of a command neuron within the brain section thereby required two essential fixation steps. Sucrose was used to prevent cell swelling during the freezing process. As this has to be done overnight the prior step of tissue fixation in paraformaldehyde was necessary. Euthanizing and embedding

was equal to the prior *D. rerio* workflow. In contrast, coronal brain sections were prepared due to the contralateral arrangement of the Mauthner axons within the central nervous system, allowing the precise detection of the Mauthner soma. Details will be discussed below (Fig. 4 b-d). The localization of the Mauthner soma was further confirmed by fluorescence microscopy (for details see methods section). Furthermore, to detect the small neuronal structures, high spatial resolution using a step size of 5 μm was necessary.

Workflow enabling the first spatial resolution of lipid patterns in thin-sections of D. magna:

In comparison to *D. rerio* as an important vertebrate model system, *D. magna* is a common invertebrate model organism for freshwater ecosystems and one of the most frequently used ones in aquatic toxicology^{28,29}. To our knowledge, we are the first to apply a sample preparation workflow examining the spatial lipid distribution in different tissue compartments in thin sections of *D. magna* (Fig. 2 c). Relating to maintain tissue integrity due to the bone structures in *D. rerio*, cryosectioning of *D. magna* is even more difficult. *D. magna* are small in size (about 1-2 mm) and have a carapace, consisting of two opposing integuments that encapsulate the body²¹. The carapace of *D. magna* consists of amorphous calcium carbonate, which contributes to its stability²⁶. During cryosectioning it often fractures, which results in a disruption body integrity. To overcome this challenge, whole body *D. magna* were embedded in 8 % gelatine. Thereby the body cavity within the carapace and appendices of the animal were filled, keeping the fragile thoracic legs from fractioning during cryosectioning (for details see Fig. 5). Sections of 18 μm sample thickness were prepared maintaining tissue integrity. Matrix application was carried out using pNA. MALDI MSI experiments showed a detailed spatial distribution of lipids in different compartments at 10 μm step size.

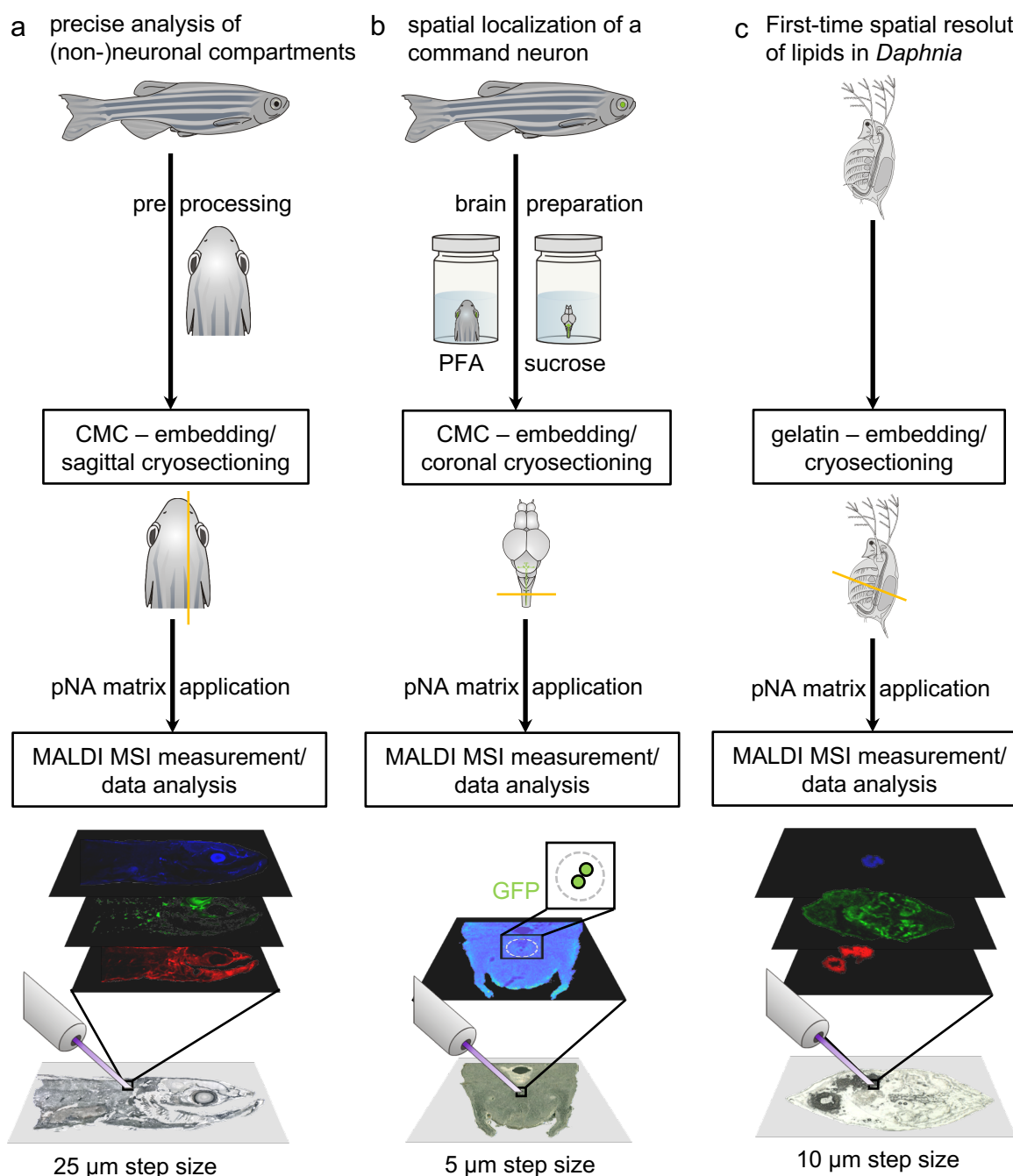


Figure 2. Histology-linked MALDI MSI workflow in *D. rerio* and *D. magna*. (a) Workflow for the precise analysis of lipid pattern visualizing anatomical features within neuronal and non-neuronal compartments. For sample preprocessing the adult zebrafish was cut cranial to the anal fin. The prepared sample was embedded in carboxymethylcellulose (CMC) and sagittal cryosections were prepared as indicated by the yellow line. Sections were covered with pNA matrix and MALDI MSI experiments were carried out in positive ion mode with 25 µm step size. Ion images were generated using the open source interface MSiReader. (b) Workflow for the spatial localization of a command neuron in brain sections. Adult zebrafish were cut cranial to the anal fin and fixated in PFA. After removal of the brain, it was fixated in sucrose. Prepared brain sample was embedded in CMC and coronal cryosections were prepared indicated by the yellow line. Brain sections (70 µm) were coated with pNA matrix and MALDI MSI measurements were carried out in positive ion mode with 5 µm step size. Prior matrix application the sections were investigated by fluorescence microscopy to ensure the presence of the soma of the command neuron. Data analysis was performed as described for the sagittal zebrafish sections. (c) Workflow revealing the spatial distribution of lipid pattern in sections of *D. magna*. The sample was directly embedded in gelatin solution and sections (18 µm) were prepared and coated with pNA matrix. MALDI MSI experiments (10 µm step size) were performed as described before.

Lipid signatures visualize detailed anatomical features in different compartments of *D. rerio*.

Understanding the contribution of lipids for tissue structure or function and their spatial connection is the basis to evaluate future changes occurring after exposure of chemical stressors. This required improved sample preparation strategies, which could be seen in Fig. 2. The results of the improved histology directed MALDI MSI workflow are shown in Fig. 3. We focused on visualizing the lipid distribution in characteristic structures of selected compartments that belong to the main routes for exposure (Fig. 3 a-d) and selected compartments being dependent on blood perfusion and transport to be potentially affected by environmental pollutants (Fig. 3 e-i). For the first time, we were not only able to distinguish between different compartments³⁰ but also show characteristic details of the compartments of interest. H&E staining results of the sections highlighting the regions of interest are shown in Fig. 3 a, e. The gills, the respiratory compartments of *D. rerio*, are one of the main routes for exposure of environmental contaminants. The fine analysis of the filaments structure could be visualized by the distribution of the lipid PC (O-32:0) [M+H]⁺ (m/z 720.5902; RMSE 1.3078 ppm, 24773 spectra) (Fig. 3 c). Furthermore, we could distinguish between different layers of the eye, including the retina and the lens. The distribution of PC (30:0) [M+K]⁺ (m/z 744.4940; RMSE 1.2396 ppm, 26056 spectra) (Fig. 3 d) thereby clearly distinguished between those two anatomical features. Fig. 3 b shows an RGB overlay of these two lipids in the section with PC (O-32:0) [M+H]⁺ given in red and PC (30:0) [M+K]⁺ given in green. Thereby the visualized lipid signature matches the anatomical features seen in the H&E stained section.

The eye is originally defined as a part of the central nervous system³¹. Thereby the retina and the optic nerve are an outgrowth of the developing vertebrate brain. This is of special interest, as we could show in the next sagittal section, which includes parts of the brain, that the lipid PC (40:6) [M+H]⁺ (m/z 834.6007; RMSE 1.1319 ppm, 57101 spectra) is distributed within the brain tissue but also within the retina (Fig. 3 i). As the *tectum opticum* receives mainly visual input, changes in the lipid signature due to environmental contaminants could thereby function as marker for the impact on the visual function. Beside the *tectum opticum* the lipid PC (40:6) [M+H]⁺ also visualizes parts of the cerebellum and the *telencephalon*. A more detailed view of the *tectum opticum* is given in Fig. 3 h by the distribution of PC (O-36:1) [M+K]⁺ (m/z 812.5930; RMSE 1.1146 ppm, 21713 spectra), which showed high intensity in this region. In contrast to the neuronal region, non-neuronal tissue of this section was again visualized by the distribution of PC (O-32:0) [M+H]⁺ (m/z 720.5902; RMSE 0.8647 ppm, 33686 spectra), as in the section before (Fig. 3 g). Additionally, the liver could be localized and the distribution of

the lipid PC 40:6 [M+H]⁺ matches the homogenous consistence of this organ (Fig. 3 i). Fig. 3 f shows an RGB overlay of the lipids highlighting compartments that can be affected through secondary exposure occurring due to blood perfusion and transport.

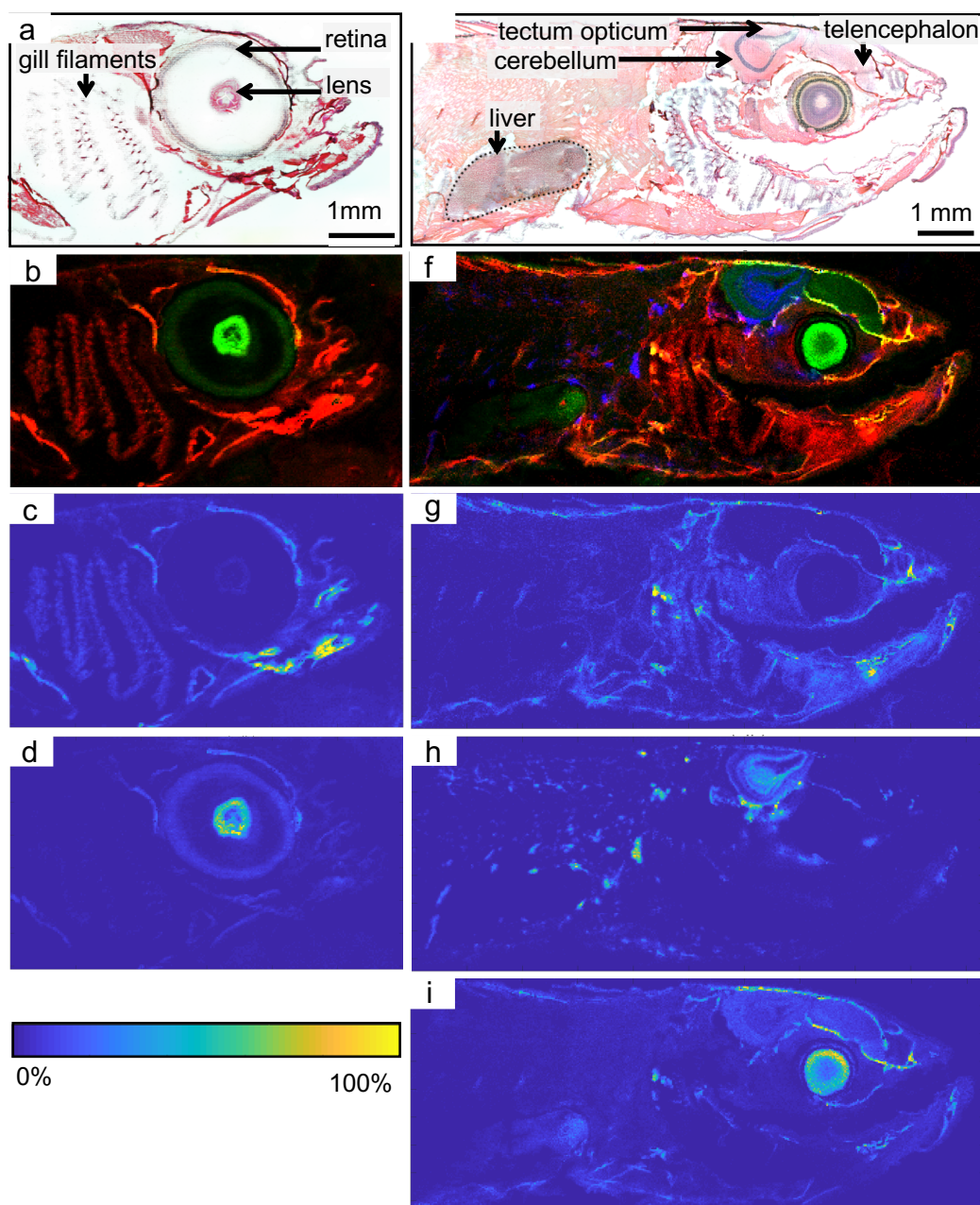


Figure 3. Lipid signatures visualizing anatomical features of neuronal and non-neuronal compartments. (a,e) H&E staining of the sagittal cryosections in adult zebrafish showing detailed structures within the gills' filaments, eye (retina, lens), brain (*telencephalon*, *tectum opticum*, *cerebellum*) and liver. (b) RGB Overlay of PC (O-32:0) [M+H]⁺ (red colored) and PC (30:0) [M+K]⁺ (green colored). (c-d), (g-i) Positive-ion MS images. (c) Ion image of PC (O-32:0) [M+H]⁺ showing high intensity in the region of the gills' filaments (white arrow). (d) Ion image of PC (30:0) [M+K]⁺ showing visualizing the lens and the retina of the eye (white arrows). (f) RGB Overlay of PC (O-32:0) [M+H]⁺ (red colored), PC (O-36:1) [M+K]⁺ (blue colored) and PC (40:6) [M+H]⁺ (green colored). (g) Ion image of PC (O-32:0) [M+H]⁺ showed distribution with high intensity in non-neuronal tissue, exemplarily shown for muscle tissue (white arrow). (h) Ion image of PC (O-36:1) [M+K]⁺, visualized the structural differentiation within the *tectum opticum* and parts of the *cerebellum*. (i) Ion image of PC (40:6) [M+H]⁺ showed a distribution within the brain and eye and presents the liver as relative homogenous tissue (white arrows).

The distribution of PC (O-32:0) [M+H]⁺ given in red, PC (O-36:1) [M+K]⁺ given in blue and PC (40:6) [M+H]⁺ given in green matches the anatomical features observed in the H&E staining (Fig. 3 f).

Spatial localization of a central command neuron in *D. rerio*.

After we succeeded in the finer spatial resolution of selected compartments of interest, we tried to further improve our workflow to localize a central command neuron within a tissue section. The soma of the neuron can be located in the *medulla oblongata* and its axons cross the midline and extend contralaterally down the spinal cord (Fig. 4 a). Coronal sections facilitate the sample preparation as one can follow the symmetric orientated axons upstream from the spinal cord (Fig. 4 b) to the point where they cross the midline (Fig. 4 c). Afterwards using a sample thickness of 70 μm, the next section includes parts of the soma (Fig. 4 d). Before the crossover, both axons converge (Fig. 4 b) and then align themselves atop each other (Fig. 4 c). This progression can be visualized by the distribution of PC (36:1) [M+H]⁺ (Fig. 4 b: m/z 788.6164; RMSE 0.8182 ppm, 42069 spectra; Fig. 4 c: RMSE 1.0264 ppm, 51363 spectra). In this context axonal membranes can be identified, because lipids are key components of cell membranes and further contribute in information transmission. In contrast, there is no lipid distribution within the axons as the axoplasm does not contain any lipids. The soma could be visualized by the distribution of the lipid PC (38:6) [M+H]⁺ (m/z 806.5694; RMSE 1.8184 ppm, 33076 spectra). As the MS image solely shows two round spots, the localization of the neuron was verified by fluorescence microscopy. This clearly shows, that the axon origin from the soma is at first thin. This is in comparison to the morphological structure of this command neuron, as the thicker part indicates the start of the myelination. The soma outgrowths, indicating the two main dendrites, are visualized by fluorescence microscopy but couldn't be visualized by any lipid distribution so far (Fig. 4 e). This workflow shows, for the first time in a vertebrate model organism, the spatial localization of a well identified command neuron. In electrophysiological studies this neuron is used to examine neuronal key functions as this neuron integrates information from all sensory system. Thereby it takes part in a network triggering life-saving behavior response. As many chemical stressors are lipophilic, it is likely that they affect the lipid structures next to the neuron, resulting in neurological effects.

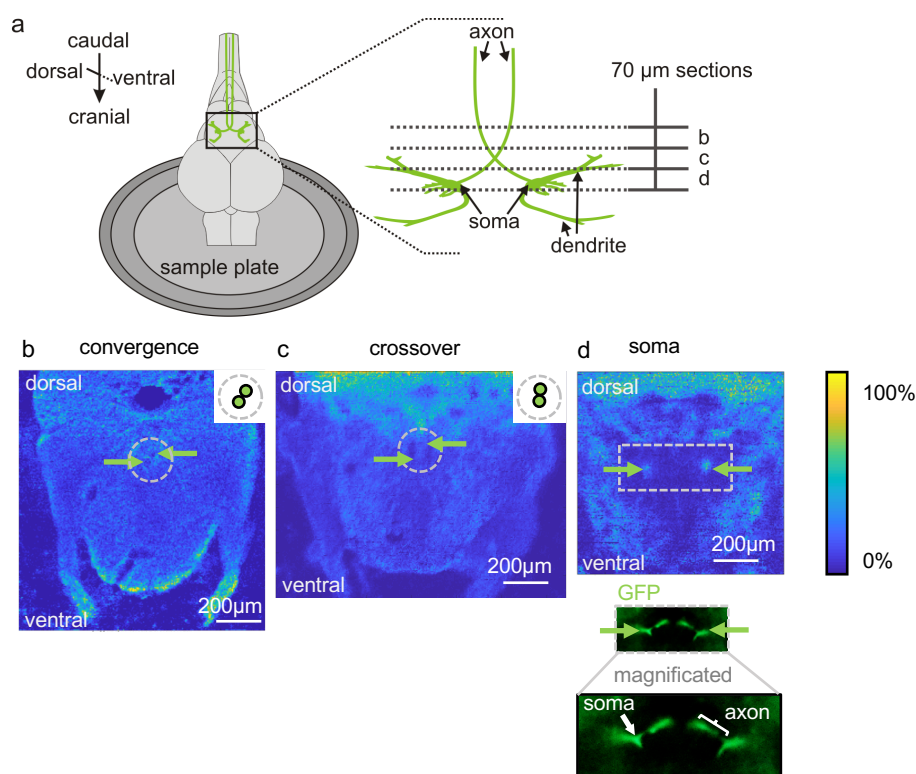


Figure 4. Spatial localization of a central command neuron within tissue sections of zebrafish using MALDI MSI. (a) Illustrated zebrafish brain is fixated on a sample plate, with the central command neurons (the pair of Mauthner neurons) colored in green. On the right side the Mauthner neurons are magnified and the serial sections (70 μm sample thickness) are presented by dotted lines. (b-d) Positive-ion MS images. (b-c) MSI image visualizing the axon arrangement before (b) and at (c) the crossover. Axons are labeled with green arrows and a schematic illustration of the axon region is shown on the right side of the MS image. PC (36:1) $[\text{M}+\text{H}]^+$ localizes the axon and its morphological orientation by visualizing the surrounding lipid distribution. (d) MS image of the Mauthner soma (labelled with green arrows), visualized by the distribution of PC (38:6) $[\text{M}+\text{H}]^+$. Orientation of the soma within the section is verified by the fluorescence image of GFP, which is expressed within the neuron.

First-time spatial resolution of lipids in tissue sections of *D. magna*.

The sample preparation workflow examining the lipid distribution within different compartments of *D. magna* by MALDI MSI was successfully developed for the first time. Anatomical features like the intestine, integuments and the thoracic legs as well as embryos within the brood pouch could be successfully obtained during cryosectioning. Anatomical presentation of whole *D. magna* is shown in Fig. 5a with the cutting plane indicated by a red line. The intestine could be visualized by the distribution of PC (36:0) $[\text{M}+\text{Na}]^+$ (m/z 812.6140; RMSE 1.2381 ppm, 20844 spectra) (Fig. 5 c). In contrast, structures characterized as embryos and eggs could be visualized by the distribution of the lipid HexCer (41:1;O2) $[\text{M}+2\text{Na}-\text{H}]^+$ (m/z 842.6456; RMSE 0.8426 ppm, 5173 spectra) (Fig. 5 d). Surrounding structures like the body wall and parts of the thoracic legs could be visualized due to the distribution of SM (38:1;O2) $[\text{M}+\text{Na}]^+$ (m/z 781.6194; RMSE 0.6500 ppm, 31188 spectra) (Fig. 5 e). An RGB

overlay of the three lipids within this section is shown in Fig. 5 b with HexCer (41:1;O₂) [M+2Na-H]⁺ colored in red, SM (38:1;O₂) [M+Na]⁺ colored in green and PC (36:0) [M+Na]⁺ colored in blue.

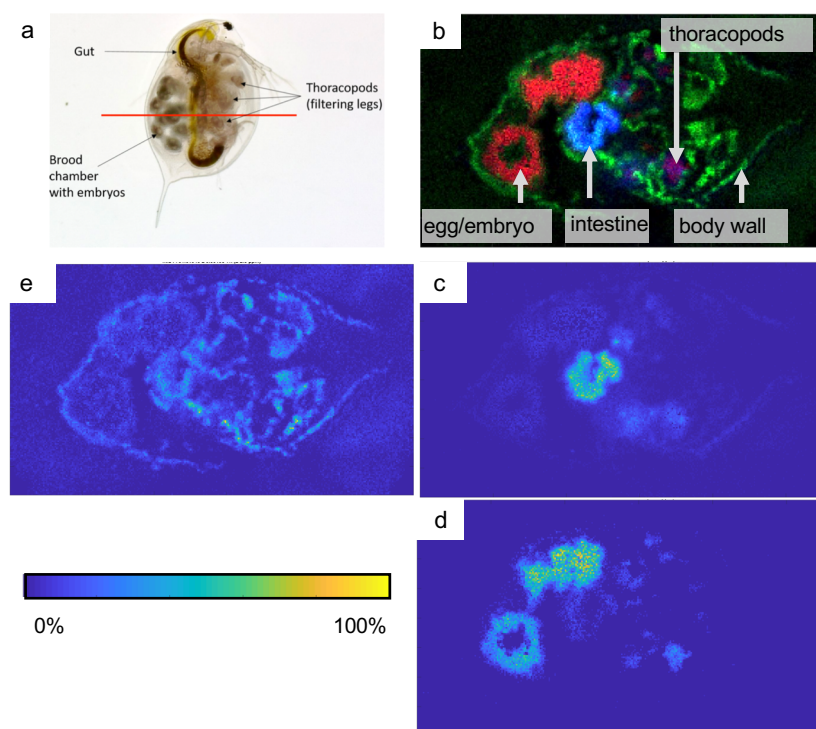


Figure 5. MALDI MSI workflow visualizing the lipid distribution in *D. magna*. (a) Light microscopic presentation of *D. magna*. (b) RGB Overlay of PC (36:0) (blue colored), HexCer (41:1;O₂) [M+2Na-H]⁺ (red colored) and SM (38:1;O₂) [M+Na]⁺ (green colored) visualizing different anatomical regions (thoracic legs, egg/embryo, intestine, body wall). (b-d) Positive-ion MS images. (c) Ion image of PC (36:0) [M+Na]⁺, highlighting the intestine region (labelled by a white arrow). (d) Ion image of HexCer (41:1;O₂) [M+2N-H]⁺, highlighting the lipid distribution within the egg/embryo (labelled by a white arrow). (e) Ion image of SM (38:1;O₂) [M+Na]⁺, showing the lipid distribution in the surrounding tissue, including body wall (labelled by a white arrow) and thoracic legs.

Analyzing the lipid distribution of daphnids can be of special interest regarding the assessment of environmental impact on organism level. For instance, Scanlan et al.,³² were able to show that various toxicants like e.g. octabromodiphenyl ether or tetrabromophthalate influence the glycosphingolipid biosynthesis, analyzed via NMR-based lipidomic profiling. MALDI-MSI might offer the possibility to map and thereby visualize the areas of impact of toxicants directly within a tissue section, adding another perspective for understanding the mechanism of action of substances of interest. The gut of *Daphnia* as well as the embryos carried by the animals pose one of the first contact zones with pollutants within these animals. Studies already showed the damage that can be inflicted to *Daphnia*s gut wall, as an example Heinlaan et al.³³, evidenced changes in the gut wall of *Daphnia* exposed to copper oxide nanoparticles with

transmission electron microscopy (TEM). This is especially interesting given the fact, that alterations of cell walls might also coincide with changes in lipid distribution or appearance.

Summarizing, the presented enabling the analysis of lipid distribution in different anatomical compartments in *D. magna* is promising for future spatial analysis of the lipidome of Daphnia.

Conclusion

The goal of the study was the implementation of a histology directed MALDI MSI workflow for the lipid analysis in two important aquatic model organisms, *D. rerio* and *D. magna*. In *D. rerio*, we were able to overcome previous limitations by demonstrating a fine structure analysis of selected compartments. This is of high importance as different anatomical parts of an organ can be affected in a different manner. Further, in regard to future studies including environmental contaminants, it is necessary to establish a workflow being able to visualize the different neuronal and non-neuronal compartments with clear borders. We succeeded in the fine analysis for fish samples, concentrating on compartments being the main route of exposure (e.g. eye, gills) and compartments relying on blood perfusion and transport to be affected (e.g. brain, liver). Thereby we could identify and localize lipids with high intensity in those compartments in one measurement using one tissue section. We further asked if it is possible to even extend this workflow by localizing even neuronal structures. Thereby we took advantage of *D. rerio*, as it consists of a central command neuron, which is the largest one in the central nervous system of vertebrates. The so-called Mauthner neuron is part of a network triggering life-saving behavior response, like the escape response due to a suddenly appearing predator²⁰. Thereby it integrates information from all sensory systems, which could be already used in electrophysiological studies to investigate several neuronal key functions. Further, this neuron was already used as a model system evaluating the effects of bisphenols⁴⁰, highly discussed environmental contaminants, on the mature vertebrate brain. Localizing this neuron with MALDI MSI within a tissue section could extend the gained knowledge by adding information about the distribution of bisphenols next to the neuron. Indeed, we were able to localize parts of the axon and the soma. The presented results function as part of the feasibility study and will be improved in future studies.

For *D. magna*, we were the first to show a suitable sample preparation workflow enabling the application of MALDI-MSI on *Daphnia* sections. Thereby, we could overcome challenges like maintaining tissue integrity during cryosectioning of non-preserved whole-mount samples of *Daphnia*. We further present the first spatial mapping of compartment specific lipids with a high spatial resolution.

Lipid pattern highlight characteristic structures of body compartments and are therefore an ideal basis for the analysis of molecular changes in aquatic organisms. With regards to this, the developed working procedures in this study might enable the analysis of e.g. the effects of environmental pollutants from a different, non-invasive, histochemical perspective.

Methods

Experimental Animals.

Adult zebrafish (*D. rerio*) lines used in this study were of the Bt line (wild type) and Casper-Tol-056 line (mutant type). The Casper-Tol-056 line was generated by crossing the pigmentless casper [mitfa^{w2/w2};mpv17^{a9/a9}]³⁴ strain with the Tol-056 enhancer³⁵ trap line, in which the Mauthner neurons, among others, express GFP. All fish used in this study were kept at the Chair of Animal Physiology at the University of Bayreuth. Juvenile fish were raised at 28 °C on a 12:12 h light/dark photoperiod in E3-medium (5 mM NaCl, 0.17 mM KCl, 0.33 mM CaCl₂, 0.33 mM MgSO₄ x 7H₂O, 10-5 % Methylene Blue in dH₂O). Adult fish were kept in groups of about 15 animals in commercial fish tanks (Stand-alone unit V60, Aqua Schwarz; Göttingen, Germany; size: 137 x 60 x 231 cm (width, depth, height)) at 28 °C. Water quality parameters were controlled daily (salt content: 0.1 g/L; pH 7.2; water conductivity: 400 µS). Adult fish were fed with commercial fish food (Tetramin: Tatra GmbH; Melle, Germany). Experiments were conducted with adult animals. Animal experiments were in accordance with the relevant guidelines and regulations of the German animal protection law and approved by state councils (Regierung von Unterfranken, Würzburg, Germany).

Adult female *D. magna* (clone: K34J) were cultivated in a climate chamber (20 °C + 1 °C) with a 15:9 h light/dark photoperiod at the Chair of Animal Ecology I at the University of Bayreuth. The daphnids were held on artificial M4 medium³⁶ and were fed daily with the green algae *Acutodesmus obliquus*.

Sample preparation for cryosectioning.

Euthanasia of all experimental fish was applied by an overdose of the anaesthetic agent 2-phenoxyethanol. Sectioning of embedded *D. rerio* and *D. magna* samples were performed on a cryomicrotome (CM 3050 S cryostat, Leica Microsystems; Nussloch, Germany). For the wild-type *D. rerio*, 20 µm sagittal sections were prepared at a chamber temperature of -15 °C. Coronal brain sections of Casper-Tol-056 *D. rerio* were prepared at -17 °C and 70 µm thickness. Whole-body sections of *D. magna* were prepared at -27 °C chamber temperature and a thickness of 18 µm.

Preparation of sections from wild-type D. rerio:

Animals were dissected cranial to the anal fin and immediately embedded in 3 % carboxymethyl cellulose (CMC; (Sigma-Aldrich, Taufkirchen, Germany)). The embedding

medium was prepared by dissolving 750 mg CMC (Sigma-Aldrich, Taufkirche, Germany) in pre-warmed 25 mL Milli-Q water and subsequently cooled to room temperature for further use. For embedding, the cryomold (Science Services, Munich, Germany) was filled with a thin uniform layer of embedding medium and stored at -20 °C. The prepared *D. rerio* was transferred onto the frozen CMC layer, completely coated by additional CMC medium and immediately stored at -80 °C until cryosectioning.

Preparation of brain sections from the Casper-Tol-056 line:

The skull of the fish was opened and the head placed overnight in 4 % paraformaldehyde (PFA) in PBS. Next day the brain was extracted from the skull and transferred to 30 % sucrose (Sigma-Aldrich, Taufkirche, Germany), diluted in 4 % PFA in PBS. After overnight incubation, the brain was embedded in 3 % CMC as it is described before and stored at -80 °C until cryosectioning.

Preparation of D. magna sections:

Gelatin embedding solution was prepared by dissolving 800 mg gelatin powder (VWR, Darmstadt, Germany) in 10 mL ultrapure water and the suspension was heated to 55 °C to dissolve the gelatin. The embedding medium was poured in a cryomold and given time to cool down to approximately room temperature. After cooling, a daphnid was placed in a glass bowl filled with embedding medium for approximately one minute so that the movement of the thoracic legs spread the embedding medium within the carapace and appendices of *D. magna*. Afterwards, the individual was placed in a cryomold filled with embedding medium and transferred to a brass plate cooled with dry ice. During the freezing process the daphnids were aligned with tweezers. Frozen samples were stored at -80 °C until cryosectioning.

Matrix application.

Prior to matrix application, *D. rerio* and *D. magna* sections were placed in a desiccator for 1 hour to avoid condensation on the sample surface. Matrix application was carried out using a semi-automatic pneumatic sprayer system built in house. All sections were coated with 4-nitroanilin matrix (pNA, $\geq 99\%$, Sigma Aldrich Chemie, Taufkirche, Germany) at 5 mg/mL in 3:1 acetone / water.

MALDI MSI measurements.

MALDI MSI measurements were performed on a QExactive™ HF Hybrid-Quadrupole-Orbitrap mass spectrometer (Thermo Fisher Scientific GmbH, Bremen, Germany), coupled to an AP-SMALDI5 source (TransMIT GmbH, Gießen, Germany) equipped with a $\lambda = 343$ nm solid state laser operating at a repetition rate of 100 Hz. Measurements were carried out in positive ion mode with a mass range of 600-1000 with one scanning event per pixel at a mass resolution of 240k @ m/z 200 full width at half maximum (FWHM). All measurements were performed with a fixed C-trap injection time of 500 ms. Step sizes were set to 25 μm for the sagittal wild-type zebrafish line sections, 10 μm for *D. magna* sections and 5 μm for the coronal Casper-Tol-056 *D. rerio* line sections. Tentatively identification of lipids from *D. rerio* sections was based on online data base search³⁷ and on tissue MS/MS of lipids with a precursor isolation window width of ± 0.2 m/z . Tentatively identification of lipids in *D. magna* sections was based on online data base search³⁷.

Data processing and image generation.

Conversion of proprietary Thermo RAW files to imzML was performed using the java based open access software ‘jimzML’ Converter³⁸. Ion images and RGB composite images were generated in the open source software MSiReader Version 1.0.³⁹ Images were generated using a bin width ± 2.5 ppm. Mass deviations across imaging datasets are given as the root mean square error (RMSE) of the Δm values in ppm of each individual spectrum containing the targeted ion within a ± 4 ppm window of the exact mass.

H&E staining.

D. rerio sections were used for H&E staining after MALDI MSI experiments. Prior staining, the matrix layer was removed with acetone. The sections were then rehydrated with decreasing ethanol concentrations (2 min in 100 %, 70 %, 40 %), rinsed in 100 % distilled water and stained with Mayers Hematoxylin Solution for 12 minutes, before sections were submerged in tab water and rinsed again in distilled water. 0.5 % acidified Eosin Y was used for counterstaining. Stained sections were fixated in xylol and mounted with Eukitt mounting medium and coverslips.

References

1. Know more about the effects of the chemicals we use in Europe - All news - ECHA. <https://echa.europa.eu/de/-/know-more-about-the-effects-of-the-chemicals-we-use-in-europe>.
2. Liu, W., Nie, H., Liang, D., Bai, Y. & Liu, H. Phospholipid imaging of zebrafish exposed to fipronil using atmospheric pressure matrix-assisted laser desorption ionization mass spectrometry. *Talanta* 209, 120357 (2020).
3. Sparvero, L. J. et al. Mapping of phospholipids by MALDI imaging (MALDI-MSI): realities and expectations. *Chem. Phys. Lipids* 165, 545–562 (2012).
4. Koizumi, S. et al. Imaging mass spectrometry revealed the production of lysophosphatidylcholine in the injured ischemic rat brain. *Neuroscience* 168, 219–225 (2010).
5. Ja, H. et al. MALDI mass spectrometric imaging of lipids in rat brain injury models. *J. Am. Soc. Mass Spectrom.* 22, 1014–1021 (2011).
6. Zhao, C. et al. MALDI-MS Imaging Reveals Asymmetric Spatial Distribution of Lipid Metabolites from Bisphenol S-Induced Nephrotoxicity. *Anal. Chem.* 90, 3196–3204 (2018).
7. Barbacci, D. C. et al. Mass Spectrometric Imaging of Ceramide Biomarkers Tracks Therapeutic Response in Traumatic Brain Injury. *ACS Chem. Neurosci.* 8, 2266–2274 (2017).
8. Römpp, A. & Spengler, B. Mass spectrometry imaging with high resolution in mass and space. *Histochem. Cell Biol.* 139, 759–783 (2013).
9. Kompauer, M., Heiles, S. & Spengler, B. Atmospheric pressure MALDI mass spectrometry imaging of tissues and cells at 1.4- μm lateral resolution. *Nat. Methods* 14, 90–96 (2017).
10. Schober, Y., Guenther, S., Spengler, B. & Römpp, A. Single Cell Matrix-Assisted Laser Desorption/Ionization Mass Spectrometry Imaging. *Anal. Chem.* 84, 6293–6297 (2012).
11. Veelen, P. A. van et al. Direct peptide profiling of single neurons by matrix-assisted laser desorption–ionization mass spectrometry. *Org. Mass Spectrom.* 28, 1542–1546 (1993).

12. Monroe, E. B. et al. SIMS and MALDI MS imaging of the spinal cord. *PROTEOMICS* 8, 3746–3754 (2008).
13. Römpf, A. et al. Histology by mass spectrometry: label-free tissue characterization obtained from high-accuracy bioanalytical imaging. *Angew. Chem. Int. Ed Engl.* 49, 3834–3838 (2010).
14. Chaurand, P., Cornett, D. S., Angel, P. M. & Caprioli, R. M. From whole-body sections down to cellular level, multiscale imaging of phospholipids by MALDI mass spectrometry. *Mol. Cell. Proteomics MCP* 10, O110.004259 (2011).
15. Fitzner, D. et al. Cell-Type- and Brain-Region-Resolved Mouse Brain Lipidome. *Cell Rep.* 32, 108132 (2020).
16. Bambino, K. & Chu, J. Chapter Nine - Zebrafish in Toxicology and Environmental Health. in *Current Topics in Developmental Biology* (ed. Sadler, K. C.) vol. 124 331–367 (Academic Press, 2017).
17. Seda, J. & Petrussek, A. *Daphnia* as a model organism in limnology and aquatic biology: Introductory remarks. *J. Limnol.* 70, 337–344 (2011).
18. Altshuler, I. et al. An Integrated Multi-Disciplinary Approach for Studying Multiple Stressors in Freshwater Ecosystems: *Daphnia* as a Model Organism. *Integr. Comp. Biol.* 51, 623–33 (2011).
19. Panula, P. et al. The comparative neuroanatomy and neurochemistry of zebrafish CNS systems of relevance to human neuropsychiatric diseases. *Neurobiol. Dis.* 40, 46–57 (2010).
20. Korn, H. & Faber, D. S. The Mauthner Cell Half a Century Later: A Neurobiological Model for Decision-Making? *Neuron* 47, 13–28 (2005).
21. Book Review: *Cladocera: The Genus Daphnia (including Daphniopsis)*. By John A. H. Benzie (Ed.) - Flößner - 2005 - *International Review of Hydrobiology* - Wiley Online Library. <https://onlinelibrary.wiley.com/doi/abs/10.1002/iroh.200590003>.
22. Muysen, B. T. A. & Janssen, C. R. Multigeneration zinc acclimation and tolerance in *Daphnia magna*: Implications for water-quality guidelines and ecological risk assessment. *Environ. Toxicol. Chem.* 20, 2053–2060 (2001).

23. Yang, J. H., Kim, H. J., Lee, S. M., Kim, B.-M. & Seo, Y. R. Cadmium-induced biomarkers discovery and comparative network analysis in *Daphnia magna*. *Mol. Cell. Toxicol.* 13, 327–336 (2017).
24. Blewett, T. A. et al. Sublethal and Reproductive Effects of Acute and Chronic Exposure to Flowback and Produced Water from Hydraulic Fracturing on the Water Flea *Daphnia magna*. *Environ. Sci. Technol.* 51, 3032–3039 (2017).
25. Ferain, A. et al. Body lipid composition modulates acute cadmium toxicity in *Daphnia magna* adults and juveniles. *CHEMOSPHERE* 205, 328–338 (2018).
26. Ritschar, S., Bangalore Narayana, V. K., Rabus, M. & Laforsch, C. Uncovering the chemistry behind inducible morphological defences in the crustacean *Daphnia magna* via micro-Raman spectroscopy. *Sci. Rep.* 10, 22408 (2020).
27. Steven, R. T., Race, A. M. & Bunch, J. para-Nitroaniline is a Promising Matrix for MALDI-MS Imaging on Intermediate Pressure MS Systems. *J. Am. Soc. Mass Spectrom.* 24, 801–804 (2013).
28. Barata, C., Baird, D. & Markich, S. Influence of genetic and environmental factors on the tolerance of *Daphnia magna* Straus to essential and non-essential metals. (1998) doi:10.1016/S0166-445X(98)00039-3.
29. Miner, B. E., De Meester, L., Pfrender, M. E., Lampert, W. & Hairston, N. G. Linking genes to communities and ecosystems: *Daphnia* as an ecogenomic model. *Proc. R. Soc. B Biol. Sci.* 279, 1873–1882 (2012).
30. Stutts, W. L. et al. Methods for Cryosectioning and Mass Spectrometry Imaging of Whole-Body Zebrafish. *J. Am. Soc. Mass Spectrom.* 31, 768–772 (2020).
31. Purves, D. et al. *The Retina*. *Neurosci.* 2nd Ed. (2001).
32. Scanlan, L. D. et al. Gene Transcription, Metabolite and Lipid Profiling in Eco-Indicator *Daphnia magna* Indicate Diverse Mechanisms of Toxicity by Legacy and Emerging Flame-Retardants. *Environ. Sci. Technol.* 49, 7400–7410 (2015).
33. Heinlaan, M. et al. Changes in the *Daphnia magna* midgut upon ingestion of copper oxide nanoparticles: A transmission electron microscopy study. *Water Res.* 45, 179–190 (2011).
34. White, R. M. et al. Transparent adult zebrafish as a tool for in vivo transplantation analysis. *Cell Stem Cell* 2, 183–189 (2008).

35. Nagayoshi, S. et al. Insertional mutagenesis by the Tol2 transposon-mediated enhancer trap approach generated mutations in two developmental genes: *tcf7* and *synembryn*-like. *Development* 135, 159–169 (2008).
36. Elendt, B.-P. Selenium deficiency in Crustacea. *Protoplasma* 154, 25–33 (1990).
37. Sud, M. et al. LMSD: LIPID MAPS structure database. *Nucleic Acids Res.* 35, D527-532 (2007).
38. Race, A. M., Styles, I. B. & Bunch, J. Inclusive sharing of mass spectrometry imaging data requires a converter for all. *J. Proteomics* 75, 5111–5112 (2012).
39. Robichaud, G., Garrard, K. P., Barry, J. A. & Muddiman, D. C. MSiReader: An Open-Source Interface to View and Analyze High Resolving Power MS Imaging Files on Matlab Platform. *J. Am. Soc. Mass Spectrom.* 24, 718–721 (2013).
40. Schirmer, E., Schuster, S. & Machnik, P. Bisphenols exert detrimental effects on neuronal signaling in mature vertebrate brains. <https://doi.org/10.1038/s42003-021-01966-w> (2021).

Acknowledgements

The current study was supported by the Deutsche Forschungsgemeinschaft (DFG, German Research Foundation), Project Number 391977956 – SFB 1357.

Author contributions

E.S., S.R., S.S., C.L. and A.R. designed and supervised experimental procedure; E.S. and S.R. performed and analyzed experiments. E.S., S.R., S.S. and A.R. wrote the manuscript.

10. Conference participations

Parts of this thesis were presented at the following international conferences:

Machnik, P., Schirmer, E., Glück, L. and Schuster, S. Recordings in an integrating neuron provide a quick way for achieving appropriate anaesthetic use in fish. 13th Göttingen Meeting of the German Neuroscience Society, 2019. (poster presentation)

Schirmer, E., Ritschar, S., Laforsch, S., Schuster, S. and Römpp, A. MALDI mass spectrometry imaging in aquatic model systems. OurCon, Saint-Malo, France, 2020. (poster presentation)

Schirmer, E., Ritschar, S., Laforsch, S., Schuster, S. and Römpp, A. MALDI mass spectrometry imaging in aquatic model systems. ASMS, 2020. (online poster presentation)

Schirmer, E., Ritschar, S., Laforsch, S., Schuster, S. and Römpp, A. MALDI mass spectrometry imaging in aquatic model systems. Micro2020, 2020. (online poster presentation)

11. Acknowledgements

The last four years were a hard time in which one develops, fails, rebuilds and gets to know oneself in a new way. These experiences have shaped and strengthened me, they positively surprised and encouraged me. First and foremost, I would like to express my gratitude to Prof. Dr. Stefan Schuster at the

You are allowed to be both – a masterpiece and a work in progress.

– Sophia Bush

Department of Animal Physiology, for shaking my hand four years ago on the last day of my master's thesis, because on that day you handed me the opportunity to decide and to grow. Since then, you encouraged and supported me in every way. You were a mentor, a team member and a friend and although there were good and tough times I just want to say – thank you.

Furthermore, I would like to express great thanks to Prof. Dr. Andreas Römpp at the Department of Bioanalytics and Food Chemistry. You gave me the chance to dive into an incredible interesting topic and handed me the opportunity to hold on to my dreams.

Next, I have a big smile on my face, while I want to thank my dear friend and colleague – Dr. Peter Machnik. There are many things to be grateful for, but I just want to say one thing: thank you for still being around – as a friend after all these years and surely even beyond.

I would have never dreamed of to have so many heart-warming and supportive people around me as I had the last years. A big thanks to my room colleagues Kathrin Leupolz, Sabine Blum, Jasmin Kniese and Axel Treu – each of you is incredible, made me laugh, had always handkerchiefs and we always supported each other to hold on. Beyond, I am grateful for all the time and conversations I had with Thomas Liebenstein, Dr. Alex Hecker, Dr. Georg Welzel, Martin Schulze, Dr. David Richter, Oliver Wittek, Bastian Jahreis, Matthias Ochs, Julia Kokesch-Himmelreich, Alan Race and Sven Ritschar and for all the hot chocolate and time I spend with Antje Halwas. A really big ‘thank you’ also belongs to Dr. Wolfram Schulze. You did not only rescue my laptop and my hard drives but it is what it is – you rescued my life. Moreover, a special thanks to Monika Painter and Gudrun Brauner, the heroes of administration.

I also want to thank PD Dr. Heinar Schmidt for all his helpful advices and that he encouraged me to stick to my principles.

Finally, without all the support of my beloved family, I would not have been that brave, purposeful and optimistic and it would not have been such a pleasure to finally end this chapter of life.

12. (Eidesstattliche) Versicherungen und Erklärungen

(§ 8 Satz 2 Nr. 3 PromO Fakultät)

Hiermit versichere ich eidesstattlich, dass ich die Arbeit selbstständig verfasst und keine anderen als die von mir angegebenen Quellen und Hilfsmittel benutzt habe (vgl. Art. 64 Abs. 1 Satz 6 BayHSchG).

(§ 8 Satz 2 Nr. 3 PromO Fakultät)

Hiermit erkläre ich, dass ich die Dissertation nicht bereits zur Erlangung eines akademischen Grades eingereicht habe und dass ich nicht bereits diese oder eine gleichartige Doktorprüfung endgültig nicht bestanden habe.

(§ 8 Satz 2 Nr. 4 PromO Fakultät)

Hiermit erkläre ich, dass ich Hilfe von gewerblichen Promotionsberatern bzw. –vermittlern oder ähnlichen Dienstleistern weder bisher in Anspruch genommen habe noch künftig in Anspruch nehmen werde.

(§ 8 Satz 2 Nr. 7 PromO Fakultät)

Hiermit erkläre ich mein Einverständnis, dass die elektronische Fassung der Dissertation unter Wahrung meiner Urheberrechte und des Datenschutzes einer gesonderten Überprüfung unterzogen werden kann.

(§ 8 Satz 2 Nr. 8 PromO Fakultät)

Hiermit erkläre ich mein Einverständnis, dass bei Verdacht wissenschaftlichen Fehlverhaltens Ermittlungen durch universitätsinterne Organe der wissenschaftlichen Selbstkontrolle stattfinden können.

.....

Ort, Datum, Unterschrift